Universität Zürich[UZH]

Geographisches Institut

Alpine red deer habitat selection during summer using a multi-temporal imaging spectroscopy approach: trade-off between food quality and quantity

ESS 511 Master's Thesis

Author: Antonia Breitling, 21-700-166

Supervised by: Prof. Dr. Maria J. Santos, Dr. Christian Rossi

Faculty representative: Prof. Dr. Maria J. Santos

23.04.2026

Universität Zürich[UZH]

ESS 511

Master Thesis

April 2026

Alpine red deer habitat selection during summer using a multi-temporal imaging spectroscopy approach: trade-off between food quality and quantity

Antonia Breitling

21-700-166

Supervised by:

Prof. Dr. Maria J. Santos

Dr. Christian Rossi

Faculty member:

Prof. Dr. Maria J. Santos

Remote Sensing Laboratories

Department of Geography

University of Zurich

Acknowledgements

First and foremost, I would like to thank my supervisors Prof. Dr. Maria J. Santos and Dr. Christian Rossi for their support, valuable feedback and help throughout the process of writing my thesis. Another thank you goes to Jan Schweizer, for pre-processing and harmonising the APEX products from 2010 and 2013.

I would also like to thank the Swiss National Park for providing all the necessary data. A special thank you goes to Nadja Bernhard and her input and help with ArcGIS Pro, Thomas Rempfler for all the information about red deer data and Benjamin Bar-Gera for inputs about matching red deer GPS positions with red deer activity data.

Finally, I am grateful to all my friends, family and fellow students for their support and interesting discussions throughout this thesis.

Abstract

Herbivores need to deal with a known trade-off between food quality and quantity. While quantity (biomass) usually peaks around mid-summer, forage quality (i.e. nutrients) has its peak in early summer and decrease afterwards. Therefore, herbivores need to balance their forage intake with forage quality and quantity, but also in terms of predators and disturbances. In theory, there are nine possible feeding strategies that herbivores can follow, reaching from favouring both, quantity and quality (++), to prioritising food quantity regardless of quality (+0), to a neutral strategy (00) where neither food quality nor quantity drives habitat selection. The analysed herbivore species in this thesis is red deer in the Swiss National Park (SNP).

The aim of this master thesis is (i) to find out where red deer are found in terms of land cover class in the SNP, (ii) whether red deer reuse their home ranges and feeding locations during the summer, and (iii) which combination of topography, forage quality, and forage quantity best explains red deer feeding habitat selection, in general, for females and for males.

To analyse which forage strategy red deer in grassland areas in the SNP follow during the summer, GPS data (locations and movement data) were used together with in-situ measurements and airborne imaging spectroscopy data. A limitation of airborne imaging spectroscopy data is the long revisit time. Therefore, a multi-temporal approach was used, combining three APEX images via growing degree days to reconstruct one summer and to analyse, whether red deer feeding habitat selection differed throughout the summer. In-situ measurements were used together with imaging spectroscopy data to train a partial least square regression (PLSR) model, which was applied to the whole SNP to get predictions of forage quality (i.e. nitrogen, phosphorus, lignin and fibre) and forage quantity (dry biomass). In a final step, a resource selection function (RSF) was used to analyse the best combination of forage quality and quantity variables explaining red deer feeding habitat selection in the SNP.

Within the SNP, red deer were predominantly found within forest and grassland, with the dominant behaviours lying and feeding. Walking and running were less frequent behaviours. Day-night differences, as well as sex-specific differences were found between the chosen land cover class and the behaviour. Red deer home ranges did not vary spatially across the summer, nor did the feeding locations. Analysing 70 home ranges of red deer showed that they reused their home ranges throughout the summer with a mean overlap of 71.11 ± 16.96 %. The feeding locations were also revisited during the summer, with a mean overlap of 92 % (aggregated for all individuals). However, at GDD 330.95 (late summer), areas around the Ofenpass road (Il Fuorn) and Val Mingèr were more frequently visited compared to GDD 154.7 (early summer) and showed a higher feeding intensity. The overall best model explaining female red deer feeding habitat selection included topography, biomass, nitrogen and the fibre content (ADF), the best model for males included topography, biomass, phosphorus and ADF.

The results come with some limitations, such as less GPS positions of males were available, making this result less robust. Further investigation is needed to determine, whether male red deer feeding habitat selection in the SNP is best explained by a combination of topography, biomass, fibre content and phosphorus, or if this is an artefact. Further, biomass predictions resulted in a lot of zero values, probably underestimating the effect of biomass, influencing the overall result. Nevertheless, this study used for the first time a set of forage quality variables (nitrogen, phosphorus, lignin and fibre) compared to other studies where mostly biomass and nitrogen were used as proxies explaining red deer feeding habitat selection. Further, only actual feeding positions were analysed. However, as only one time span was analysed in more detail, potential short-term shifts in the feeding strategy cannot be fully detected.

Table of Content

List of Figures

List of Tables

List of Abbreviations

ADF	Acid Detergent Fibre
ADL	Acid Detergent Lignin
AIC	Akaike Information Criterion
AICc	corrected Akaike Information Criterion
AOA	Area Of Applicability
APEX	Airborne Prism Experiment
AVIRIS	Airborne Visible/Infrared Imaging Spectrometer
C	Carbon
$CaCO_3$	Calcium carbonate
CI	Confidence Interval
DEM	Digital Elevation Model
DI	Dissimilarity Index
EO-1	Earth Observing-1
ESA	European Space Agency
FMH	Forage Maturation Hypothesis
GDD	Growing Degree Days
GLM	Generalised Linear Model
GLMM	Generalised Linear Mixed Model
GPS	Global Positioning System
GWH	Green Wave Hypothesis
ha	Hectare
HCRF	Hemispherical-Conical Reflectance Factor
ID	Identification number
IID	Independent and Identically Distributed
Int16	Integer 16
iSSA	Integrated Step Selection Analysis
IUCN	International Union for Conservation of Nature
KDE	Kernel Density Estimation
LoCoH	Local Convex Hulls
M	Model
m a.s.l	Metres above sea level
MCP	Minimum Convex Polygon

N	Nitrogen
n	Number
nm	Nanometres
ODMAP	Overview, Data, Model, Assessment and Prediction
P	Phosphorus
PLSR	Partial Least Square Regression
R^2	Coefficient of Determination
RF	Random Forest Method
RMSE	Root Mean Square Error
RSF	Resource Selection Function
SD	Standard Deviation
SDM	Species Distribution Models
SNP	Swiss National Park
SVF	Semi-Variance Function
SWIR	Short-Wave Infrared
TIFF	Tagged Image File Format
UNESCO	United Nations Educational, Scientific and Cultural Organization
VIS	Visible
χ^2	Chi-square

1 Introduction

Herbivores need to deal with a known trade-off between food quality and quantity. Resources that are rich in nutrients (i.e. resources with high food quality) are often less abundant (Fryxell, 1991; Van Soest, 1994). With plant development throughout the summer, biomass increases through accumulation whereas the nutrients peak in the beginning of spring / early summer and decrease with plant maturation (Fryxell, 1991). This relationship is described by the forage maturation hypothesis (FMH). However, as plants mature during the summer, their forage quality declines, while herbivore intake is limited at low biomass. Therefore, to get enough energy, herbivores follow the phenology of the vegetation and select forage with intermediate biomass (Fryxell, 1991; Hebblewhite et al., 2008; Merkle et al., 2016). The food quality-quantity trade-off creates a difficulty for herbivores. They need to get enough energy, which implies that they must find a balance in their diet between abundant resources that are lower in nutrients and high-quality food that peaks at the beginning of the summer and decreases afterwards (Fryxell, 1991; Van Soest, 1994). Furthermore, they need to balance their energy intake with other disturbances such as predators and humans (McArthur et al., 2014).

In theory, there are nine possible feeding strategies (Figure 1) that ungulates can follow during the summer based on the trade-off between food quality and quantity. Herbivores selecting for both high quality and high quantity (++, orange) would select for areas with both high nutrients and high biomass. Herbivores selecting only for biomass (0+, cyan) prioritise food quantity regardless of quality, while a neutral strategy (00, violet) would indicate neither food quality nor quantity drives the habitat selection.

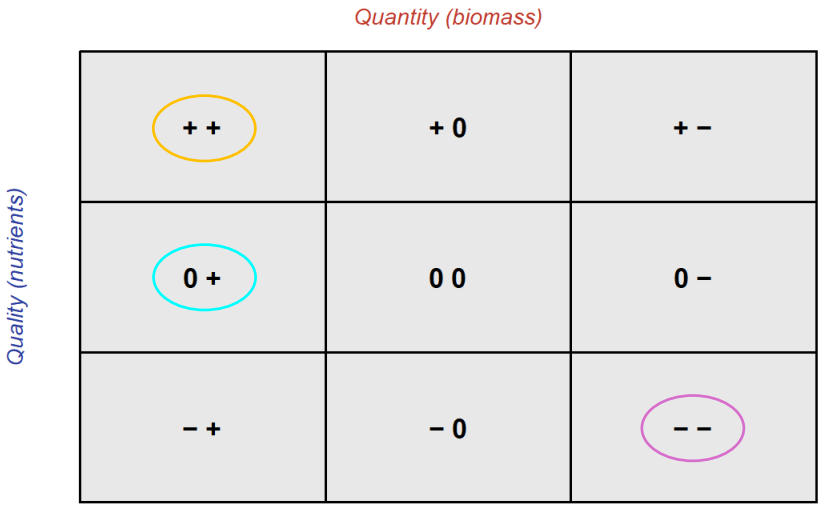

Figure 1: Nine theoretical feeding scenarios that ungulates can follow during the summer. A plus indicates that the species favours this trait, a minus that they avoid it and a zero means this trait is neutral in terms of habitat selection. Quality is on the y-axis, ranging from low to high. Quantity is on the x-axis, ranging from high to low.

How herbivores can deal with the quality-quantity food dilemma depends on their feeding strategy. Hofmann (1989) reviewed morphological studies of ruminants and classified them into three overlapping categories based on their feeding behaviour: concentrate selectors (browsers), grass and roughage eaters (grazers), and intermediate, opportunistic feeders. The analysed herbivore species for this master's thesis is red deer. Red deer fall into the category of intermediate feeders, meaning that they prefer a mixed diet and try to avoid fibres in their diet as long as possible (Hofmann, 1989). Further, they are opportunistic feeders, means, they choose whatever is available for them and they can adapt quite fast to the resources that are currently present. This implies potential shifts in their habitat selection during the summer as a consequence of the food quality-quantity trade-off and their needs.

One possibility for herbivores to maximise their energy intake is to follow the vegetation phenology. In spring, herbivores start to follow vegetation peaks of high quality (Merkle et al., 2016; van der Graaf et al., 2006). They "surf on the green wave" to maximise their energy intake after winter (Merkle et al., 2016). The green wave hypothesis (GWH) represents the spatial extent of the forage maturation hypothesis for large herbivores (Merkle et al., 2016). Especially at the beginning of the summer, studies have shown that red deer benefited from surfing on the green wave compared to individuals that moved slower and were not directly following the green wave (Rivrud et al., 2016). Related to this is the migrating behaviour of red deer from their winter areas to summer areas. Blankenhorn et al. (1978) analysed the migration behaviour of red deer around the Swiss National Park (SNP). They found that most red deer migrate from their winter areas outside the SNP in spring to early summer to their summer areas within the SNP and in autumn back to their winter areas. Not only do preferences change between winter and summer; the preferences can also shift during the summer. At the beginning of the summer, hinds provide maternal care (Clutton-Brock et al., 1982; Merkle et al., 2016) and stags grow their antlers (Clutton-Brock et al., 1982; Mattioli et al., 2022). Further, towards the end of the summer, both need to build up fat reserves for the winter (Clutton-Brock et al., 1982; Mattioli et al., 2022). These changing needs could imply a change in the feeding strategy during the summer.

In this thesis, red deer were analysed in the Swiss National Park (SNP). Founded in 1914, the SNP is a strict nature reserve and the oldest national park in the Alps which is part of the UNESCO Biosphere Reserve Engiadina Val Müstair (Schweizerischer Nationalpark, n.d.). Since the early 1920s, red deer have been present in the SNP with a peak population of over 2000 individuals in the 1980s and nowadays with around 1400 individuals (Schweizerischer Nationalpark, n.d.). Without natural predator, red deer are the dominant species in the SNP and are a strong competitor for other herbivores such as chamois and ibex (Anderwald et al., 2015). Previous studies in the SNP have shown different habitat use by red deer and other herbivores. Schweiger et al. (2015b) analysed the plant biomass and plant nitrogen content of chamois, ibex and red deer in the SNP and found significant differences. Red deer were found in areas where plant biomass was high, and plant nitrogen content was variable. Nitrogen (N) is a proxy for forage quality and often measured and analysed in terms of red deer habitat selection. Nitrogen can have positive effects on the body weight of hinds (Albon and Langvatn, 1992) and therefore influence the survival rate of their offsprings (Borowik et al., 2016). Besides nitrogen, also phosphorus (P) is an important nutrient for herbivores, e.g. for stags that need nutrients to grow their antlers (Landete-Castillejos et al., 2007; Smolko et al., 2022). Phosphorus is often limited in subalpine and alpine grasslands (Thiel-Egenter et al., 2007) and it was shown by Schütz et al. (2006) that red deer preferred phosphorus-rich grassland in the SNP. While nitrogen and phosphorus are favoured by red deer, fibres are avoided as long as possible (Hofmann, 1989). The fibre content was quantified in this thesis with the acid detergent fibre (ADF) which includes cellulose, lignin and ash (Holtzapple, 2003a) and with acid detergent lignin (ADL), the part that is hardest to digest (Holtzapple, 2003b; Katoch, 2023). Fibres are needed to some extent for the rumen (Van Soest, 1994); however, they are very difficult to chew and digest (Van Soest, 1994; Holtzapple, 2003a,b) and are therefore less preferred compared to nitrogen and phosphorus. Forage quantity was quantified in this thesis with dry biomass, the forage quality was quantified with nitrogen, phosphorus, ADL and ADF.

Rapiya et al. (2025) showed that carbon (C), nitrogen, ADF and the ratio C:N:ADF changes over the year and that the season influences these changes. The highest variations were found during late summer. Further, Rempfler et al. (2024) showed that biomass (forage quantity) was more important in habitat selection of red deer in the summer than quality by using Sentinel-2 data. But do red deer always prioritise quantity, or do they shift their strategy during the summer with changing needs? These temporal dynamics during the summer remain unexplored. Furthermore, studies to date used different remote sensing approaches or did not include several nutrient proxies in the same study to assess red deer feeding habitat selection. Until now, nitrogen and biomass were often used as proxies to describe red deer presence, but there might be a better food quality proxy such as phosphorus or ADF. Furthermore, all recorded GPS positions were used in previous analysis, regardless of whether the

animals were feeding or not. However, various behaviours were recorded, and the focus of this thesis will be on actual feeding positions.

To test which of the nine possible feeding strategies red deer follow during the summer in the SNP, this thesis follows a multi-temporal imaging spectroscopy approach using APEX (Airborne Prism Experiment; Schaepman et al., 2015) data. Imaging spectroscopy products can be used to derive vegetation properties such as biomass, nitrogen and phosphorus content at high spatial resolution (Ustin et al., 2004). However, the limitation for continuous measurements so far is the long revisit time. Therefore, a multi-temporal approach is used, where different APEX products from multiple years are combined and matched by the phenological state via the growing degree days (GDD), to construct one summer season with information at the early, mid and late summer. This approach allows to quantify potential temporal shifts in the feeding strategies of red deer during the summer. GPS locations of red deer are used together with image spectroscopy products from APEX and ground measurements of forage quantity (biomass) and forage quality (N, P, ADL, ADF) within the SNP to build a resource selection function (RSF), a special case of a species distribution model (SDM; Figure 2) and to assess red deer feeding habitat selection. SDMs, as well as RSF, are empirical statistical models that characterise a species' niche based on environmental variables and use it to explain the species' distribution (Elith and Leathwick, 2009).

To sum it up, this master thesis focuses on:

1. Using a model to filter the behaviour "feeding" out of all collected GPS information to assess actual red deer feeding habitat selection
2. Using a multi-temporal approach to see how the food diet preferences change during the summer season (early, mid and late summer)
3. Using high resolution imaging spectroscopy data from APEX
4. Including phosphorous, lignin and the fibre content as important nutrients besides nitrogen and biomass in the RSF to assess feeding habitat selection

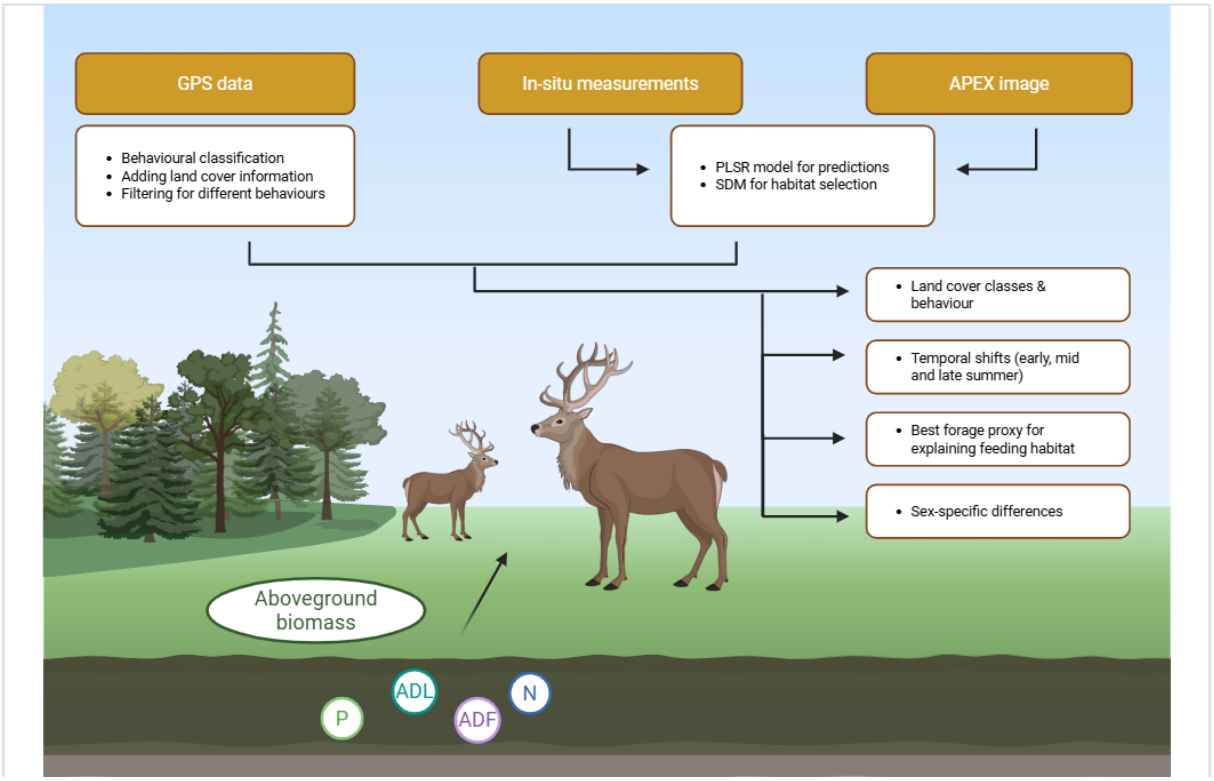

Figure 2: Conceptual diagram showing the steps covered in this thesis (Created by A. Breitling in https://BioRender.com)

1.1 Research questions and hypotheses

This thesis aims to find answers to the following questions:

Q1: Where do we find red deer in the SNP?

Q1.1: What land cover classes do they use?

Q1.2: What is the dominant behaviour within these classes?

Q2: How do red deer home ranges and feeding locations vary spatially across the summer (early, mid and late)?

Q2.1: Do red deer reuse their home ranges across the summer (early, mid and late)?

Q2.2: Do red deer reuse their feeding locations across the summer (early, mid and late)?

Q3: Which combination of topography, forage quality proxies (N, P, ADL and ADF) and forage quantity (biomass) best explains red deer feeding habitat selection?

Q3.1: Topography alone?

Q3.2: Topography and food quantity (biomass)?

Q3.3: Topography together with food quantity (biomass) and quality (N, P, ADL, ADF)?

Q4: Are there sex-specific differences in feeding habitat selection?

By answering these questions, this thesis aims to find out which of the nine theoretical feeding scenarios (see Figure 1) best describes red deer foraging strategy at different time periods during the summer in the SNP. These hypotheses were made:

H1: Red deer are mainly found in the forest and grassland areas with the dominant behaviours lying and feeding.

H2: There are differences in the home ranges and feeding locations across the three phenological stages.

H3: Red deer feeding habitat selection is best explained by topography, biomass and forage quality proxies. They are found at areas with high biomass, variable to high nitrogen content and high phosphorus content. For lignin and fibres, on the other hand, low contents are preferred.

H4: There are no sex-specific differences in feeding habitat selection.

2 Theoretical backgrounds

2.1 Red deer and their diet

Red deer (*Cervus elaphus* Linnaeus, 1758; Figure 3) are a widespread species found in Europe, but also in West and Central Asia (Mattioli et al., 2022). They are very closely related to wapitis and elks; however, they are a nowadays considered as separate species and even the West and Central Asian red deer (*Cervus hanglu*) are seen as separate species (Mattioli et al., 2022). In Europe, there are several subspecies such as the Scottish, the Iberian or the Italian red deer, differentiated through genetic or phenotypic characteristics (Mattioli et al., 2022; Volodin et al., 2013).

Red deer generally prefer woodland areas, but they also need grasslands to feed on, therefore, they are typically found at places with grassland and forests (Mitchell et al., 1977). Due to hunting, deforestation and the trade-off with space for livestock, red deer populations diminished to very few numbers, before in the second half of the 20th century, the populations recovered because of resettlements, better protection of the forest and reducing the interspecific competition with livestock (Mattioli et al., 2022).

Figure 3: Female red deer (hind; own picture)

Depending on the season, there are changes within the physiological cycle of red deer (Arnold, 2020). In spring and over the summer, red deer need to increase their energy intake through forage to compensate for the winter depletion and to prepare for the reproduction cycle and the antler growth (Clutton-Brock et al., 1982; Mattioli et al., 2022). Reproduction needs energy. While hinds are pregnant, they need energy for their foetus to grow, but at the same time energy for themselves (Oftedal, 1985). This extra energy is mainly gained through food or body fat reserves (Oftedal, 1985). Arman et al. (1974) showed that hinds increased their forage intake towards end of the pregnancy by 1.2 to 1.8 times and during lactation even up to 2.4 to 2.6 times compared to a non-reproducing hind. Further, they showed that hinds with calves increased their body weight up to 12 kg in the first 20 to 30 days after the calf was born. However, during lactation, the body fat reserves of the mother decrease again (Clutton-Brock et al., 1982). If this decline is too drastic, the mother and also its calf will most probably not survive the next winter (Clutton-Brock et al., 1982). Therefore, hinds need to gain fat reserves during summer to

prepare for the winter and they reach their highest body weight in November (Mitchell et al., 1976). Stags, on the other hand need to grow their antlers and gain body mass to prepare for the rutting season in autumn (Clutton-Brock et al., 1982). They reach their highest body weight in September, the start of the rut season, however, during the rutting season itself, they barely consume forage and can even lose up to 14 – 17 % of their body weight (Mitchell et al., 1976). Even though red deer consume less forage in winter due to reduced activity, it was shown by Arnold et al. (2015) that nutrients can be better extracted. However, this does not compensate for the general loss in weight in both sexes during winter (Mitchell et al., 1976).

Red deer are opportunistic, intermediate feeders, meaning they prefer a mixed diet and try to avoid fibres as long as possible; however, they can also adapt quite fast to changing resource availability (Hofmann, 1989). Because stags are generally larger than hinds (males: 100 – 220 kg and females: 55 – 130 kg) and grow faster, they need more forage intake (Mattioli et al., 2022). At the same time, they respond more strongly to limited resources than hinds (Clutton-Brock et al., 1982). Even though hinds and stags can generally be found in the same habitats, the habitat use and the forage selection differ between the sexes, known as sexual segregation (Clutton-Brock et al., 1987).

While red deer generally follow the greening up of the vegetation to maximise biomass intake (Hebblewhite et al., 2008; Merkle et al., 2016; Sigrist et al., 2022), they also need nutrients in their diet. The body weight (mass and fat reserves) of hinds is essential for their reproduction and their pregnancy success, as well as for their calves and how hinds manage lactation phase (Mitchell et al., 1976). Reproductive success is therefore related to body condition and high-quality forage (Clutton-Brock et al., 1982). Nitrogen can have positive effects on the body weight of hinds (Albon and Langvatn, 1992) and therefore influence the survival rate of the offspring (Borowik et al., 2016). Stags need nutrients to grow their antlers and make them strong. This is related to the body weight and size (Landete-Castillejos et al., 2007). Besides nitrogen, phosphorus (needed by vertebrates for their bones and the mineralisation of the skeleton (Cotti et al., 2020)) and $CaCO_3$ are also important for producing large antlers (Smolko et al., 2022). The forage intake during lactation phase can already influence the growth of antlers of young stags (Landete-Castillejos et al., 2007). Fibres are not preferred as they are more difficult to digest (Van Soest, 1994; Holtzapple, 2003a,b; Katoch, 2023). With increasing fibre content in plants, the digestibility decreases (Katoch, 2023). However, red deer also need them to some extent for the rumen function (Van Soest, 1994). Whereas fibres are still digestible to some extent, lignin is the part that is hardest to digest and avoided (Holtzapple, 2003b; Katoch, 2023).

2.2 Imaging spectroscopy

In the 1990s, imaging spectroscopy came up as a new research area to analyse and measure processes on Earth (Huete, 2004; Ustin et al., 2004). The underlying concept is based on "interactions between matter and electromagnetic radiation" (Ustin et al., 2004). Solar radiation can interact (i.e. be scattered or absorbed) with the Earth's surface and result in a signal that is received and measured by a sensor (Figure 4; Huete, 2004). This field is rapidly evolving, with new methods and data becoming increasingly available making it now possible to track changes in the environment and analyse different Earth system components such as the cryosphere (e.g. Naegeli et al., 2015), the hydrosphere (e.g. Maire et al., 2025) or the biosphere (e.g. Gamon et al., 2019; Homolová et al., 2013).

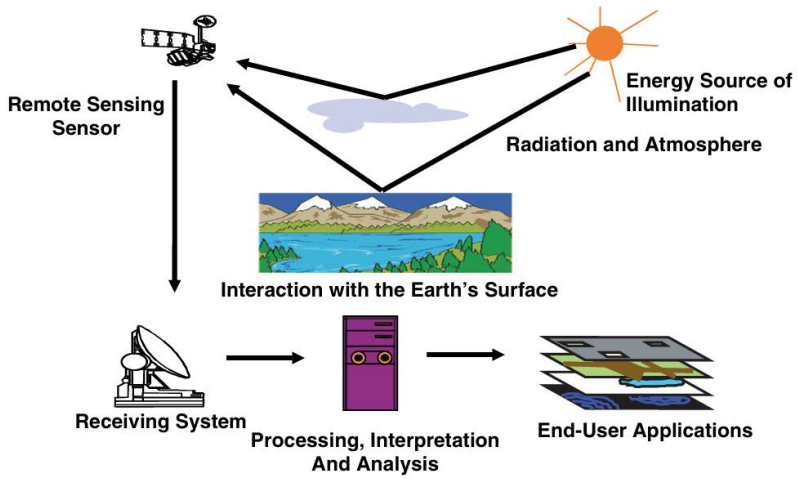

Figure 4: Remote sensing concept (Huete, 2004)

The relevant spectrum goes from the visible range (VIS; 400 nanometres (nm)) to the short-wave infrared (SWIR; 2500 nm; Ustin et al., 2004). Depending on the pigments and constituents in the analysed object, different wavelengths are reflected and absorbed. Water absorbs strongly at the wavelengths 820 nm, 940 nm, 1140 nm, 1400 nm and 1820 nm (Kakuta and Ozawa, 2022; Thompson et al., 2015), whereas vegetation pigments strongly absorb in the VIS and reflect a lot of light in the near infrared (Rouse et al., 1974). However, depending on the purpose, ultraviolet wavelengths can also be useful, e.g. to detect atmospheric pollutants (Huete, 2004).

Whereas sensors of Landsat 8 or Sentinel-2 have their bands at distinct absorption features (see Figure 5 for albedo retrieval from Naegeli et al. (2017)), imaging spectrometers, also called "hyperspectral" imagers, have hundreds of narrow bands to capture the full spectrum (Ustin et al., 2004). Sensors can either be on satellites or on aircraft. Whereas Hyperion (operated 2000 – 2017), was on board the Earth Observing-1 (EO-1) satellite (NASA, n.d.), AVIRIS (Airborne Visible/Infrared Imaging Spectrometer) and APEX (Airborne Prism Experiment) are used on board of an aircraft.

Sensors can also be characterised by their resolution. Those are nicely described by Huete (2004) for satellite sensors. The spatial resolution describes how large a pixel on Earth is, measured by the sensor. The higher the spatial resolution, the more objects are resolved. The spectral resolution is defined be the number of bands and the bandwidths and the temporal resolution is defined as how long it takes to take an image of the same area again. However, there is a trade-off between the spectral, the spatial and the temporal resolution (Key et al., 2001). For example, the higher the spatial resolution (i.e. more features are resolved), the lower the temporal resolution, and the spectral resolution is lower as well (Key et al., 2001). The hyperspectral sensors build on these trade-offs and try to circumvent them by having a high spectral resolution and at the same time a high spatial resolution. Therefore, defining the goal and purpose of the analysis and selecting accordingly the right spatial, spectral, and temporal resolution together with the right sensor is very important (Key et al., 2001; Warner et al., 2009).

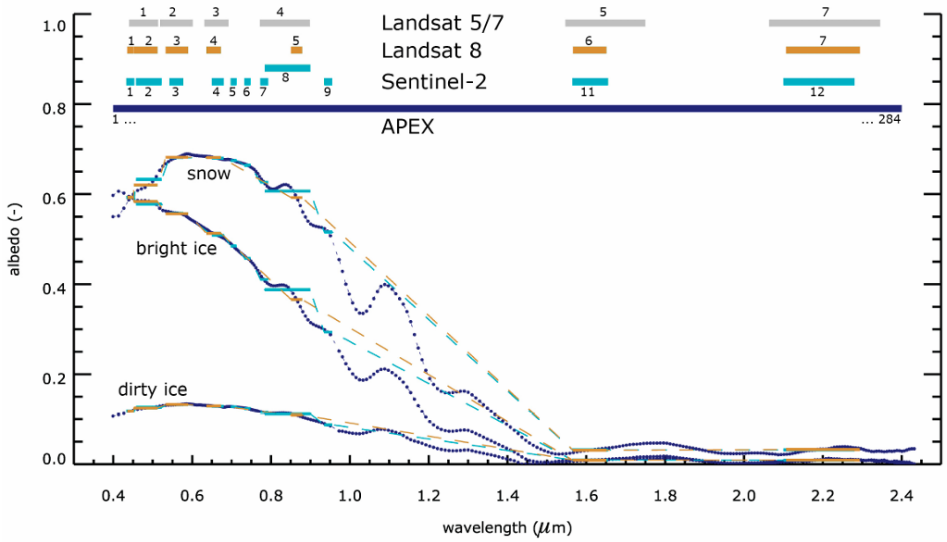

Figure 5: Comparison of the position of bands for the sensors of Landsat 5/7, Landsat 8, Sentinel-2 and APEX for albedo retrieval (Naegeli et al., 2017)

The sensors (e.g. APEX) on board of an aircraft measure a signal. To be able to use this information, several pre-processing steps are necessary. One is the radiometric calibration. There are many user guides on how to plan and perform the radiometric calibration (e.g. Tansock et al., 2015). The radiometric calibration is necessary to characterise the sensors' performance, to calibrate the data and to account for electronic and optical effects (Tansock et al., 2015). Besides that, the measured signal in digital numbers needs to be converted into a radiance signal in W m^{-2} sr^{-1} (Ustin et al., 2004). After the radiometric calibration, the spectral calibration is also of importance, to ensure that each spectral band is assigned to its correct wavelength (e.g. described by Kuhlmann et al., 2016). Due to aircraft movement and the relief of the terrain, geometric distortions can occur. To account for those, algorithms need to be applied to get an orthorectified image, in which every pixel is assigned to a geographic position (Schläpfer and Richter, 2002). However, there are also many processes within the atmosphere and on the Earth's surface, that influence the measured signal, such as scattering of radiation on molecules or aerosols, the absorption of energy at gases and scattering processes depending on the surface topography (Huete, 2004). These signals are included in the measured radiance; however, the "true" radiance from the surface is only one part of it. Radiative transfer models (e.g. ATCOR) are used to "compensate" for processes in the atmosphere and the topography such as the path radiance, the slope, the viewing and scan angle and adjacency scattering processes (Richter and Schläpfer, 2002). The product of these radiative transfer models is the surface reflectance, which can then be further used to derive information (Ustin et al., 2004).

At higher spatial scale, vegetation is much better resolved, thus, also introducing shadow and reflectance anisotropy effects due to the heterogeneity of the vegetation (Damm et al., 2015). These effects influence the retrieved surface reflectance. While they cannot yet be entirely avoided, there are promising ideas, like optimising the observation angle (Neneman et al., 2020) or via empirical correction approaches (Weyermann et al., 2014). However, at very small scale (i.e. of individual trees), correcting for these effects is still an active area of research (Damm et al., 2015).

2.3 Species distribution model

Species distribution model (SDMs) and are used to assess whether a species is present in an environment or not (Elith and Leathwick, 2009; Godsoe and Harmon, 2012). Resource selection functions (RSF) represent a special case of SDMs. The workflow of a RSF is similar and to the one of a SDM (here generally described for SDMs), but in RSFs one accounts for variations between individuals (Gillies et al., 2006; McCabe et al., 2021). The workflow for a SDM starts with collecting appropriate data on species occurrence and environmental predictors and combining them in a model with presence-absence data to get information about the environmental space of a species that can be applied to the geographic space (see Figure 6 from Soley-Guardia et al., 2024). Most SDMs are based on a regression between the species occurrence and a combination of predictor variables (Elith and Leathwick, 2009). Depending on the type of the response variable, different models (e.g. a generalised linear model (GLM) when the response variable is binomial) can be used to build an SDM. These different approaches are well summarised in Table 1 of Guisan and Zimmermann (2000).

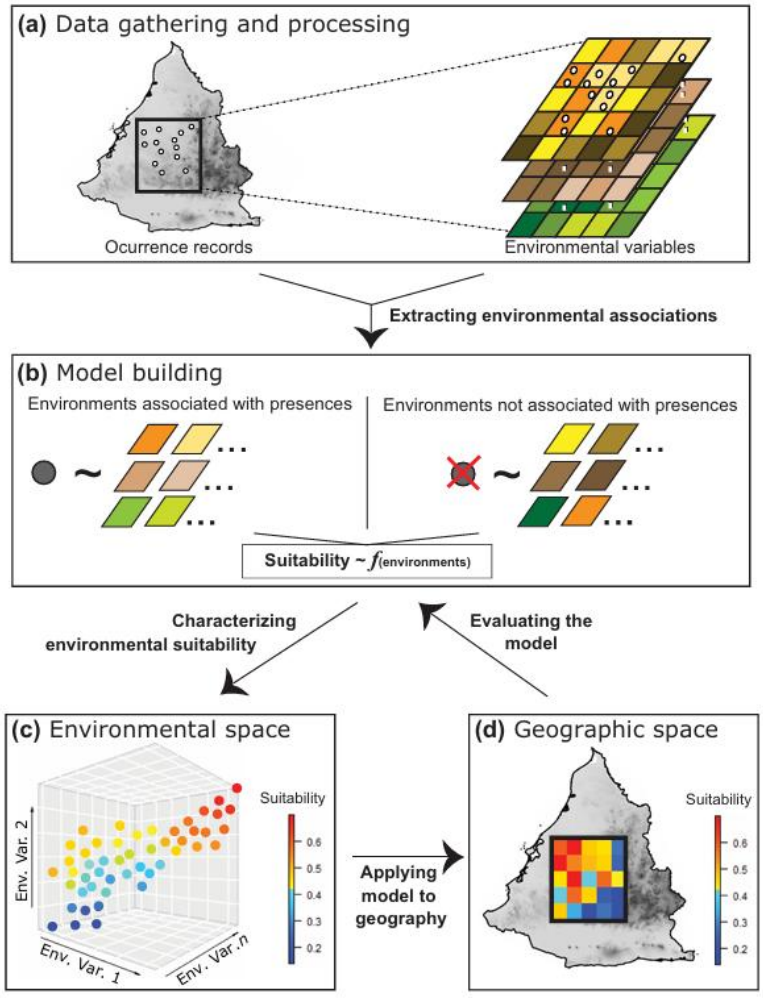

Figure 6: Workflow for a SDM from gathering the data to building the model and applying the model to the environmental and geographic space (Soley-Guardia et al., 2024)

Methodological difficulties in setting up an SDM include for example, how to include species interactions and how to handle presence only data, as most SDMs require presence-absence data. Godsoe and Harmon (2012) described how biotic interactions influence the results of SDMs and Poggiato et al. (2025) showed that trophic interactions can be included in SDM by incorporating Bayesian statistics. If only presence data are available, some "background" or "pseudo-absence" points need to be generated. Background points are generated over the whole study area and describe the environment (Phillips et al., 2009). On the other hand, pseudo-absence points (i.e. potential positions where the species was

absent) can be generated in many ways, e.g. randomly or weighted (Engler et al., 2004; Ferrier et al., 2002; Zaniewski et al., 2002). Pseudo-absence points can also be generated as a buffer around a location (e.g. VanDerWal et al., 2009) or by incorporating the step length and the turning angle of the animal with an integrated step selection analysis (iSSA; Avgar et al., 2016).

Several studies have shown that including absence points increases the model accuracy (Elith et al., 2006; Phillips et al., 2009). However, the choice of the best method how to generate the absence points is not trivial. Barbet-Massin et al. (2012) provided guidelines on how to choose the correct parameters to build robust SDMs. Further, Phillips et al. (2009) describe how to deal with problems like sampling bias of presence data. Besides that, spatial autocorrelation needs to be considered as the assumption of independence does not hold for clustered points (Guisan and Zimmermann, 2000).

Besides methodological challenges, there are also conceptual challenges. SDMs are based on the concept of the niche, i.e. the position of a species within its environment. There are different definitions, of which the following three are the most important ones for the niche concept (Wang, 1995). The first who used the term niche was Grinnell (1917) who defined the niche as a species' distribution, also referred to as "habitat". Elton (1927) extended the concept and included in the niche the position a species has within its community. Hutchinson (1957) defined the niche as "n-dimensional hypervolume", where all environmental parameters are captured. He also defined the terms realised and fundamental niche. Whereas the fundamental niche spans the whole environment where a species could exist based on abiotic factors, the realised niche is the area where the species actually occurs based on biotic interactions (Putman and Wratten, 1984). It's a large debate, whether the fundamental or the realised niche is modelled in SDMs and Araújo and Guisan (2006) addressed this issue in their paper. Depending on the used concept, the SDM output needs to be interpreted differently.

Besides that, SDMs can serve for different purposes and questions that one wants to answer. SDMs can be used to explain, predict or project species distributions (Araújo et al., 2019). Explanatory models investigate the dependency between the environment and the occurrence of the species to identify potential drivers of species distribution and provide or test hypotheses about these drivers. Predictive models use the learned relationship between environment and species and predict the distribution of the species within the same space and time. Projections extend this model to predict suitable habitats in the past or the future and do predictions also in other geographic regions.

Depending on the purpose, different evaluation purposes are appropriate. For explanatory SDMs, Elith and Leathwick (2009) suggest using statistical tests and incorporate that with what is known. For predictive SDM they suggest using data resampling (e.g. by splitting the samples, via cross-validation or bootstrapping) to test the model or use independent data.

SDMs come with a set of assumptions. One is that the "species are at equilibrium with their environments, and that relevant environmental gradients have been adequately sampled" (Elith and Leathwick, 2009). However, Guisan and Zimmermann (2000) describe that for species, which are rather bounded to their environment and react more slowly to changes in the environment, such as alpine species, this assumption can be relaxed. Furthermore, SDMs work best, if the species does not move over large distances and stays within a defined area (Elith and Leathwick, 2009).

Despite all the methodological and conceptual challenges, SDMs have become a widely used tool in ecology. SDMs can be used to model species niches and analyse how they will change under climate change but are also useful for conservation purposes and management (Willis et al., 2015). However, the implementation is not yet consistent leading to low quality models and non-comparable results. Soley-Guardia et al. (2024) described in their paper some of the problems, i.e. that there is a lot of software and literature available and that SDMs are easy to implement, but the real understanding is often lacking. Araújo et al. (2019) analysed 400 modelling studies and made clear, that standards for setting up a SDM are still lacking. They provide guidelines and standards to improve the model quality, make them transparent and transferable. Related to this is the idea of Zurell et al. (2020). They developed

the “ODMAP (Overview, Data, Model, Assessment and Prediction) protocol, as its components reflect the main steps involved in building SDMs and other empirically-based biodiversity models” (Zurell et al., 2020). The goal of this protocol is to guide authors through the workflow of SDMs and how to report and communicate the results to make them comparable.

3 Material

3.1 Study area

The study area was the Swiss National Park (SNP), covering 170 km^2 in the canton of Grisons in Switzerland (Figure 7; Schweizerischer Nationalpark, n.d.). The SNP is a strict nature reserve where animals and plants are protected from human disturbances. The International Union for Conservation of Nature (IUCN) categorised the SNP in the highest class of protection, category 1a, where only hiking on trails and scientific work is allowed (Schweizerischer Nationalpark, n.d.). The elevation range is between 1400 and 3174 metres above sea level (m a.s.l.; Schweizerischer Nationalpark, n.d.). Around half of the area (51 %) is mountainous terrain consisting of scree and rocks, 21 % are alpine grasslands and 28 % of the area is covered with forest, of which are almost all coniferous trees (Schweizerischer Nationalpark, n.d.). The climate is dry and cool. The climate at Buffalora weather station (1971 m a.s.l.) just outside the SNP (see Figure 7) was characterised by a mean annual temperature of 1.17 ± 0.53 °C (mean ± SD) and mean annual precipitation of 812.33 ± 236.21 mm (1991-2020; MeteoSwiss, n.d.). Summer months (June – August) had a mean temperature of 10.28 ± 0.84 °C and a mean precipitation of 314.12 ± 69.83 mm (1991-2020; MeteoSwiss, n.d.). The plant growing season in alpine vegetation is usually from mid-May to mid-September (Anderwald et al., 2015) for three to four months (Vorkauf et al., 2021). Red deer are mainly present in the SNP during summer, with approximately 1400 individuals, and leave the SNP in autumn for their winter areas outside the SNP (Schweizerischer Nationalpark, n.d.).

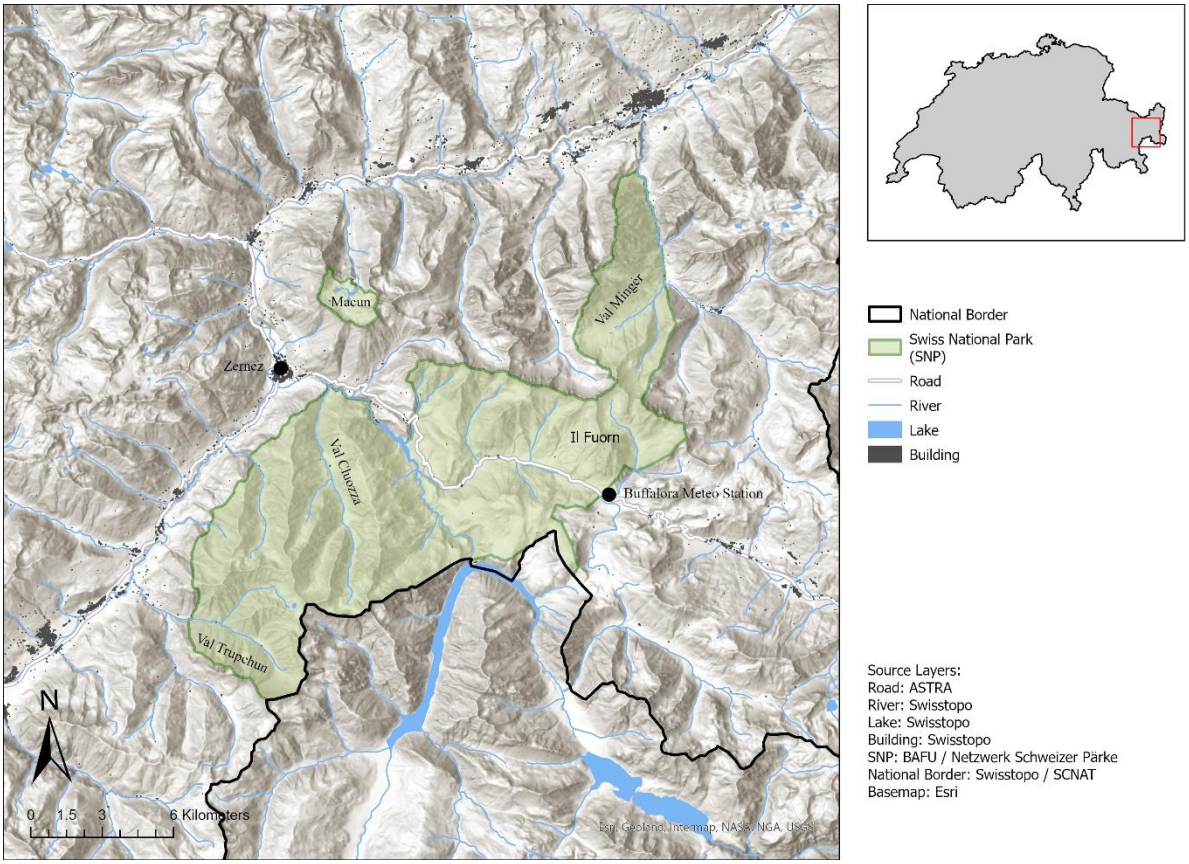

Figure 7: Extent of the SNP shown in green. Some valley names are added for a better orientation. The map was produced in ArcGIS Pro (version 3.6.0).

3.2 Data

3.2.1 Red deer summer locations

GPS positions of red deer were collected by the SNP for the Project Ingio Via for the years 2010-2019 (Rempfler, n.d. for the SNP). Over this time, 82 different individuals were captured and equipped with a GPS collar. The sensor was set to record the individual's GPS position approximately every hour, sometimes up to four hours and lasted around two years, before the sensor was dropped off, ran out of battery or the animal died. The GPS coordinates spatial accuracy was 11.3 ± 4.7 m (Schweiger et al., 2015b). Besides that, 73 of those individuals (55 females and 18 males) were also equipped with an accelerometer (Figure 8) to measure their movement, starting in the autumn 2010 with one individual. This special GPS collar (VERTEX Plus Collar) was from VECTRONIC Aerospace GmbH (VECTRONIC Aerospace GmbH, 2016) and collected the acceleration in x- and y-direction every five minutes. Again, the accelerometer recorded data for around two years, before the collars were dropped off or ran out of battery. Out of these data, for this study the GPS summer positions (June – August) were used as red deer presence data and together with the movement data to identify feeding locations.

Figure 8: Red deer equipped with a GPS collar including an accelerometer (Schweizerischer Nationalpark, n.d.).

3.2.2 Temperature data for summer phenology

The temperature data was downloaded for Buffalora weather station from Meteo Swiss (MeteoSwiss, n.d.). The station (1971 m a.s.l.) is located just outside the SNP (see Figure 7 under section 3.1). From 01.01.1917 until present, the station records weather parameters like the air temperature. Used here were the daily minimum and maximum air temperature, measured 2 m above the ground every day for calculating the growing degree days (GDD). With the GDDs, different growing stages throughout the summer could be assigned to the phenology.

3.2.3 Plant trait data: Airborne imaging spectroscopy data and ground measurements of forage quantity and forage quality

I used imaging spectroscopy data collected with APEX (Schaepman et al., 2015) over the SNP (SNP et al., n.d.). APEX operates as an airborne pushbroom system with 1000 pixels in across track direction and depending on the flight height, the swath-width ranges from 2.5 – 5 km (Schaepman et al., 2015). The data were collected as 284 spectral bands between 450 to 2500 nm (Schaepman et al., 2015) with spectral resolution in the visible and near infrared of 2.6 – 13.5 nm and in the short-wave infrared (SWIR) 5.6 – 9.9 nm.

The APEX data were available for five years (2010, 2013, 2015, 2016 and 2019) where the whole SNP was covered by a flight. The images were provided in 545 individual tiles, each consisting of 550 x 550 pixels and 284 bands. With a spatial resolution of 2 x 2 m, each tile covers an area of 1100 m x 1100 m (= 1.21 km^2). The product was a surface reflectance product containing hemispherical-conical reflectance factor (HCRF) values, stored as Int16.

Ground measurements of forage quantity (biomass) and forage quality proxies (among others N, P, ADF and ADL) were collected by Schweiger et al. (2015a) for the SNP at different locations within the SNP or its nearby surroundings (Figure 9) for different years. They established 51 plots in 2010 and 82 in 2013 with a size of 6 x 6 m. On 24 June 2010 and on 12 July 2013 (the days of the APEX flights, see Table 2 under Section 4.2.1) biomass was clipped 1 cm above the ground within a 1 x 1 m grid in the centre of each plot and the fresh weight was measured (Schweiger et al., 2015a). The samples were then dried and ground, and forage quality variables were determined in the lab (Schweiger et al., 2015a). Whereas for the year 2010, 11 different vegetation characteristics were measured, only seven were also measured in 2013 and the following years. The vegetation characterises of interest are shown in Table 1 and were used to describe forage quantity (dry biomass) and forage quality (N, P, ADF and ADL) within the SNP. These proxies were used to determine which combination of forage quantity and forage quality best explained red deer feeding habitat selection. The measurements in 2013 were mainly collected in Val Trupchun, while the measurements from 2010 were also conducted in other areas within the SNP (Il Fuorn and Val Mingèr) covering the different elevation and vegetation characteristics within the SNP.

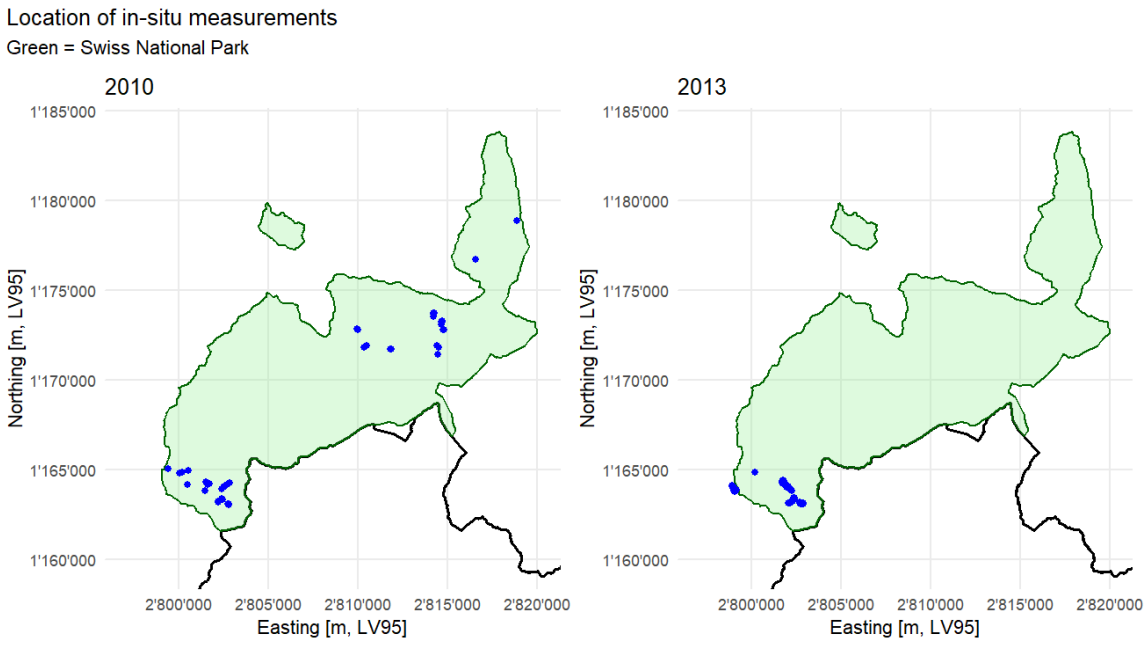

Figure 9: Location of in-situ measurements collected within the Swiss National Park (green) and its nearby surroundings for 2010 (left) and 2013 (right).

Table 1: Variables describing forage quantity (biomass) and forage quality (N, P, ADF and ADL), together with the available data, the number of plots and the parameter range.

Variable	Available data	Number of plots	Range
Biomass dry [g/m^2]	2010 + 2013	133	7.19 - 443.30
Nitrogen [%]	2010 + 2013	133	1.16 - 4.00
ADL [%]	2010 + 2013	133	1.85 - 20.98
ADF [%]	2010 + 2013	133	21.55 - 44.19
Phosphorus [%]	2010	51	0.08 - 0.18

3.2.4 Topographic variables

The topographic variables (elevation, slope and aspect) were extracted from the digital elevation model (DEM; Swisstopo, n.d.) with a 2 x 2 m spatial resolution covering Switzerland. In the DEM, the elevation levels were directly stored, slope and aspect were retrieved.

4 Method

4.1 Red deer locations

4.1.1 Identifying feeding locations from accelerometer data

As the objective was to analyse how red deer selected their summer (June – August) feeding habitat with respect to forage quantity and quality, only actual feeding positions were of interest. To identify different behaviours from accelerometer data, the predictive model developed by Bar-Gera et al. (2025) was used. The model used acceleration measurements in x- (back and forth) and y-direction (left and right) and converted them into discrete behavioural categories using linear discriminant analysis. The classification was conducted following their provided R-script.

To match the activity data including the predicted behaviour (recorded every five minutes) with the GPS locations (recorded roughly every hour, sometimes up to four hours), a temporal matching approach was used. For every GPS location, all activity data within a ± 20-minute window were identified. This window was found with a sensitivity analysis, where different time windows (± 5; ± 10; ± 15; ± 20; ± 25 and ± 30 minutes) were tested. The sensitivity analysis tested how sensitive the number of GPS positions is in respect to the time window. The ± 20-minute window was the best in terms of having enough positions (seven to nine) within the window to identify a majority behaviour and assigning this majority behaviour to the respective GPS position. By aggregating the activity data to GPS data within a ± 20-minute window, temporal autocorrelation between the GPS locations was reduced. Further, a diversity index was calculated by using the Simpson diversity index which is directly bounded between 0 and 1 and used to assess the homogeneity of the behaviour at each GPS location. In ecology, the Simpson diversity index describes “the probability of two randomly sampled individuals belonging to different species” (He and Hu, 2005). This was adapted and applied to different behaviours (0: low heterogeneity and the same behaviour within the window; 1: high heterogeneity and with diverse behaviours). 2286 GPS positions had no matching activity data within the time window and were excluded, representing 1 % of all GPS positions. These missing activity data came from three different individuals, where two of them had three and seven missing activity data respectively, that were not recorded. The individual with the animal ID 20168 had 2276 missing activity data (no activity data was recorded).

For later analysis, when only feeding positions were of interest, only GPS positions with the dominant behaviour “feeding” and a Simpson index ≤ 0.3 were kept. This value worked well with the data and ensured a homogeneous behaviour within the time window of ± 20 minutes, as a maximum of three out of seven to nine positions differed from the majority behaviour.

4.1.2 Identifying GPS positions from land cover and by time of the day

To identify the corresponding land cover to each GPS position, the land cover class layer from ESA with a 10-meter resolution (ESA WorldCover project [2021] / Contains modified Copernicus Sentinel data ([2021]) processed by ESA WorldCover consortium; Zanaga et al., 2022) was used (input by Hijmans (2024)). To analyse day-night differences, the time between sunrise (06:00) and sunset (21:00) was defined as day, the rest as night (for June – August; for all the years).

As for later data analysis, only red deer positions in open habitat were of interest, the land cover layer (Zanaga et al., 2022) was used to produce a “grassland” mask. For doing so, the layer was projected into the Swiss Coordinate System and resampled to 2 m resolution to fit the spatial resolution of the APEX image. Land cover class grassland, cropland, bare/sparse vegetation and moss and lichen were counted for the grassland mask and the rest (e.g. forest) was excluded. Even though forest made up a large proportion of observations, the imaging spectroscopy data would only provide information on the vegetation of the tree canopies, which were not informative of red deer feeding, and were therefore excluded.

4.2 Summer dynamics

4.2.1 Assigning phenological stages via growing degree days

The study used imaging spectroscopy data collected from several years in the SNP (Table 2) to represent different phenological stages of the summer season. The goal was to construct one summer (June – August) season to test, whether red deer feeding habitat preferences change throughout the summer. There was only one flight per year, so a temporal matching of the different years via the growing degree days (GDD; McMaster and Wilhelm, 1997) was done to construct one summer. The GDDs were calculated based on the formula below (McMaster and Wilhelm, 1997). Days with an average temperature below the base temperature did not contribute to the GDD.

$$GDD = \frac{(\max. temperature + \min. temperature)}{2} - base\ temperature$$

For calculating the GDD, a base temperature of 4 °C was taken, as suggested by Rauschkolb et al. (2025) for herbaceous species in Central Europe. This also aligns with the long-term (1971 – 2004) phenological monitoring project in the Swiss Alps, where 4 °C was chosen as an intermediate value for species blooming from early spring to summer (Project MeteoSwiss Cost 725; Studer et al., 2005). GDD are a good proxy for the phenological stage of plants and are better suited than calendar days, as GDD account for thermal conditions (Quaglia et al., 2020). Usually, alpine plants need around three to four months for their growing cycle (Vorkauf et al., 2021). Based on this, the GDD values were assigned approximately to phenological stages, representing approximately the main growing phase of alpine plants.

Table 2: Available APEX data for the SNP with the calculated GDD of the APEX flight, the calendar day and assigned phenological stage. Highlighted in green are the three chosen GDD for further analysis.

Year	GDD of APEX flight	Calendar day	Phenological stage
2010	154.7	24.06.2010	Early season
2013	239.95	12.07.2013	Mid season
2015	268.6	03.07.2015	Mid season
2016	284.75	16.07.2016	Mid season
2019	330.95	18.07.2019	Late season

For further analysis, the GDD 154.7, 239.95 and 330.95 were chosen representing early, mid and late season in terms of vegetation growth. Further, the number of GDDs between early and mid and mid to late summer were similar when using GDD 154.7, 239.95 and 330.95. These three GDD periods were used to construct the summer season and to analyse whether red deer feeding habitats changed throughout the summer. The summer temperature (June – August) in these years (2010, 2013 and 2019) was 10.66 °C, 10.35 °C and 11.59 °C with total summer precipitation of 272.2 mm, 238.3 mm and 282.4 mm (MeteoSwiss, n.d.).

4.2.2 Assessing red deer home range fidelity across phenological stages

Home ranges were calculated to check whether red deer reused the same locations throughout the three phenological stages. All available summer GPS positions (including all behaviours and all land cover classes) for the years 2010 to 2019 were used and only filtered for the respective GDD with a window of + 5 days. The window of + 5 days was used to find out whether red deer were attracted to the location or not and to avoid duplicates of GPS positions when using a broader window. The GPS data were checked for temporal autocorrelation (R package ctmm, version: 1.3.0; Fleming and Calabrese, 2025) by calculating the semi-variance function (SVF) and fitting continuous-time movement models (Silva et al., 2022). Model selection via the corrected Akaike Information Criterion (AICc; corrected for small sample sizes) identified the independent and identically distributed (IID) anisotropic model as best model for 207 out of 210 individual-GDD period combinations with IID isotropic for the remaining

three individuals. Further, the mean ratio between the effective sample size and the absolute sample size across all individuals and GDD periods was 0.994, indicating minimal temporal autocorrelation (Silva et al., 2022) and the median time interval between two GPS positions across all individuals and GDD periods was 1.6 hours. As the GPS positions had minimal temporal autocorrelation, the assumptions of independent and identically distributed data for a standard kernel density estimation (KDE) were met (Van Winkle, 1975; Worton, 1989). Therefore, there was no need of using autocorrelated KDE to correct for spatial or temporal autocorrelation. To calculate the home range overlap, the tutorial by Paterson (2023) was followed using the R package amt (version 0.3.0.0, Signer et al., 2019) with the function *hr_overlap* to calculate home ranges based on the KDE method. Home ranges can be calculated in different ways. There are geometric and probabilistic methods, summarised in Figure 1 by Signer and Fieberg (2021) and compared in Table 5.1 by Kernohan et al. (2001). Into the category of geometric home range estimations fall all methods where the (outermost) points were used to construct a polygon around, e.g. like for the minimum convex polygon (MCP; Mohr, 1947) or the local convex hulls (LoCoH, Getz and Wilmers, 2004). Probabilistic methods, like the kernel density estimation (KDE; Van Winkle, 1975; Worton, 1989), use the underlying density and utilisation distribution to estimate the home range. The different home range estimation methods come with advantages and disadvantages. Whereas the KDE method includes the underlying density function to characterizes potential core areas and their utilisation, the sample size and the selection of the smoothing parameter (h) determine the performance of KDE and are not trivial (Kernohan et al., 2001). Further, area bias and therefore underestimations are a problem in normal KDE, motivating a new family, called autocorrelated KDEs (Fleming et al., 2015). The geometric methods on the other hand are very easy to compute and understand and good to compare to other studies (Kernohan et al., 2001). However, these methods are influenced by the sample size, and outliers, and often result in overestimation (Kernohan et al., 2001). As the goal here was to determine the home range overlap, rather than the actual home range size, the choice of the home range calculation method likely to have little impact on the overall result.

To make the home ranges comparable between the GDD periods, only individuals that were present in all three periods were kept (n = 70). Further, a minimum of 30 GPS points per individual was set to calculate robust KDE home ranges, as was done by Jarnemo et al. (2023). For calculating the KDE, the bandwidth was calculated with the *hr_kde_ref* function (h = 175; similar bandwidth value as found by Richard et al., 2011) and the raster resolution was set to 100 m to balance computational efficiency and the spatial detail.

4.2.3 Assessing red deer feeding location fidelity across phenological stages

To analyse not only summer home ranges, but also whether red deer reused their actual feeding locations during the summer, feeding locations were used (as filtered in section 4.1.1) together with the land cover filter (section 4.1.2). To quantify feeding intensity and spatially concentrated feeding areas, the number of feeding events within a radius of 500 m around each feeding location was calculated. This radius was chosen following Rempfler et al. (2024), who used this radius to analyse temporal revisits. Positions with fewer than three events were excluded. To assess whether red deer reused feeding locations across the GDD periods, spatial point-based overlap (i.e., the percentage of feeding locations from one GDD period that fell within 500 m buffer of the feeding location from another GDD period) was calculated.

4.3 Red deer habitat predictors

4.3.1 Pre-processing imaging spectroscopy data for trait modelling

Before using the imaging spectroscopy data for training the model for plant trait predictions, pre-processing steps were needed. The spectral data were scaled by dividing by 10’000 to get the reflectance values between 0 and 1 (fraction of solar radiation that was reflected from a surface) and normalised for their brightness before fitting the PLSR model. The brightness normalisation accounts for anisotropy

effects, differences in viewing geometry and shade and was applied following Feilhauer et al. (2010). To do so, each spectrum was divided by its Euclidean vector length, resulting in a unit vector of uniform brightness.

To account for the spatial autocorrelation in the data, spatial cross-validation was conducted with the k-means method. The k-means method clusters data into k groups with the goal of grouping datapoints that are spatially close to each other (MacQueen, 1967). The training data was split into five spatial similar groups. With a splitting of 80:20, each group then served once as validation group while the other four groups were the training data.

4.3.2 Linking field measurements to spectral data via PLSR

The goal was to build a model that predicted biomass and forage quality parameters for the whole SNP by linking field measurements with imaging spectroscopy data. As red deer reused the same feeding locations during the phenological periods, only one GDD period was analysed in more detail with an APEX image and ground measurements, here GDD 239.95 (year 2013). However, for phosphorus, only data from 2010 were available, whereas for biomass, nitrogen, ADL and ADF ground measurements and spectral information from 2010 and 2013 were available. Therefore, the two APEX images from 2010 and 2013 were radiometrically homogenised between the years by applying a regression correction using invariant features (image of 2013 was taken as reference). This allowed to get more trainings data and to get better models for the plant traits, when data from 2010 and 2013 were used.

I used partial least square regression (PLSR; Feilhauer et al., 2010; Wold et al., 2001) to model the relationship between spectral data and the content of nutrients and biomass. Originally designed for applying statistical methods to chemical datasets (chemometrics; Wold et al., 2001), PLSR became an important tool for analysing remote sensing datasets (Feilhauer et al., 2010). PLSR can be used to analyse hyperspectral datasets with hundreds of bands that are also highly correlated, as a principal component analysis is performed within the model process (Wold et al., 2001). Another often used method is the random forest (RF) method (Breiman, 2001). As shown by several studies (e.g. Habibi et al., 2021; Wang et al., 2020), the RF model performed better compared to the PLSR, however, the PLSR points with being quite simple and easy to understand and interpret (Wold et al., 2001). However, finding the optimal number of components in a PLSR model is important to avoid overfitting (Wold et al., 2001). As suggested by Wold et al. (2001), the optimal components were found through spatial cross validation (k = 5 folds).

For the PLSR analysis, all spectral bands that were not interpolated by the radiative transfer model ATCOR were filtered and used for the analysis. The ATCOR model converts measured radiance into reflectance values and corrects hyperspectral imagery for topography and atmospheric effects (Richter and Schläpfer, 2002). As atmospheric effects are wavelength-dependent, the ATCOR model can also be used to interpolate bands, that were reduced e.g. due to noise. As the uncertainty is higher for the interpolated band, these bands were excluded, and only non-interpolated bands were used. These bands (n = 186) were used as predictor variables in the PLSR analysis. The steps in the practice guide of Burnett et al. (2021) were followed for the PLSR with the pls package (version 2.8-5, Liland et al., 2024; script: spectra-trait_reseco_lma_plsr_example.R by Serbin (2024)). All variables were checked for normality as this can lead to better PLSR results (Burnett et al., 2021). The distribution of biomass was slightly skewed to the left, and nitrogen and ADL both had a slightly long tail (see Supplementary Figures 1 - 5). A square root transformation was tested for biomass and log-transformations for ADL and nitrogen. Three different models were developed (i) 2010 data only (n = 51), (ii) 2013 data only (n = 82) and (iii) the combined data (n = 133)). For phosphorus, only one model with the data from 2010 (n = 51) was developed.

The optimal number of components in each PLSR for each vegetation variable was tested by using the procedure recommended by Burnett et al. (2021). A total of 1 to 20 components were plotted and assessed for their model performance with the coefficient of determination (R^2). The PLSR models were

then trained on all data with the optimal components. The model performance was evaluated with the coefficient of determination (R^2) and the root mean square error (RMSE).

4.3.3 Plant trait predictions for the whole SNP

The PLSR model for each vegetation variable was used to infer the predictions to the entire SNP, by predicting variable values for the entity of the APEX image. Only non-interpolated bands (n = 186) were used, like for model training. To mask out pixels with values, that the model had not seen in the training, the area of applicability (AOA) was calculated (Meyer and Pebesma, 2021). The AOA is defined as n-dimensional space covered by the training data. Points outside the AOA are extrapolated predictions, that differ from the training data and may be quite uncertain. For each pixel, the dissimilarity index (DI) in the n-dimensional space was calculated as Euclidean distance to the nearest training sample (Meyer and Pebesma, 2021). If the distance was larger than the threshold ("maximum DI of the training data derived via cross-validation" (Meyer and Pebesma, 2021)), the value 0 was assigned, for points within the threshold 1. To calculate the AOA, the online tutorial by Meyer (2025) was followed. All predictor variables (same bands as used for the PLSR) got the same weight and were equally treated. Because the data were spatially clustered, the k-means clustering was again used to produce different groups (same as for training). The threshold (0.415; for Phosphorus 0.432, because of only data from 2010) was then calculated within the CAST function (version 1.0.4, Meyer et al., 2026) "based on distances to a nearest data point not located in the same spatial cluster" (Meyer, 2025). Finally, all negative predicted values were set to zero.

The predictions for the whole SNP were done for each tile (n = 545) and variable individually. The AOA mask was applied to only get meaningful predictions. The individual tiles were then combined to one prediction layer. The grassland mask was applied with the *mask* function from the terra package (version 1.8-86, Hijmans, 2025) to the AOA predictions to get a final map and only predictions within the grassland mask. To compare the maps, quantiles with five classes were used on each variable to categorise the values into very low, low, medium, high and very high.

4.4 Data analysis

4.4.1 Using species distribution models to understand red deer feeding behaviour

The last step was to determine, if (i) topography alone, (ii) topography and food quantity or (iii) topography together with food quantity and quality best explained red deer feeding behaviour. These hypotheses were tested with a species distribution model (SDM). However, accounting for variations between individuals has been shown to improve the models (Gillies et al., 2006; McCabe et al., 2021) as done in resource selection functions (RSFs), representing a special case of SDMs. The goal was to describe the relationship between red deer occurrence and the environment, so an "explanatory" SDM (Araújo et al., 2019). RSF was implemented with a generalised linear mixed model (GLMM) framework (Bolker et al., 2009) because the independence assumption was violated due to multiple datapoints per individual. The GLMMs are a combination of a mixed model framework and a generalised linear model (GLM) and are well suited if data are e.g. in binary structure and random effects need to be accounted for (Bolker et al., 2009). The presence data were the feeding locations that were previously filtered (see Section 4.1.1). Additionally, the data were filtered for only the GDD period 239.95 ± 10 days, independent of the year and only positions within the grassland mask and the mosaic were kept. This resulted in 3061 GPS positions and 41 individuals. As the GPS data, which were not temporarily autocorrelated (see Section 4.2.2), were further reduced and filtered, temporal autocorrelation was also minimised. Pseudo-absence data were then generated within a buffer around the GPS location (VanDerWal et al., 2009) following the steps on the webpage of Hijmans and Elith (2024). To define a buffer size, from where random points were sampled, the home range areas of each individual were used. The buffer was set to 1 km, based on the median radius of 940 m, which was appropriate given

the spatial extent of the SNP with 170 km^2 (Schweizerischer Nationalpark, n.d.). The buffer thus defined the area that red deer could potentially use for feeding. A constraint was included so that random points were only produced within the grassland mask. Following Muff et al. (2020), pseudo-absence points were generated in a relation of approximately 1:10, consistent with their framework for unmatched RSF. Because points could lie outside the AOA mask, 30 pseudo-absence points were generated first. For each GPS location, the individual information from the generated GPS position was reused for the generated absence points. After, all produced locations without a value (i.e. outside the AOA mask) were excluded and then randomly resampled to 10 pseudo-absence points per GPS location. 544 presence points were lost because they were located outside the AOA mask. The final dataset still contained enough positions for the RSF analysis containing 2517 presence and 24924 absence points (1:9.9).

In ArcGIS Pro, the digital elevation model (DEM; SwissALTI3D 2m DEM - DHM – MNT from Swisstopo (n.d.)) was cut to the extent of the SNP and downloaded from ArcGIS Pro (version 3.6.0). The elevation was extracted directly with the *extract* function from the terra package (version 1.8-86), the slope and aspect were calculated with *terrain* and after extracted (Hijmans, 2025). As the GPS has an accuracy of 11.3 ± 4.7 m (Schweiger et al., 2015b), a buffer of 10 m around each GPS location was created and the mean value was extracted. The variable values (biomass, nitrogen, ADL, ADF and phosphorus) were then extracted in the same way, also with a buffer of 10 m, from the TIFF-files (input from Hijmans (2024)) and combined with the feeding locations of the red deer.

Correlations between the predictor variables (Figure 10) were checked using Pearson correlation (collinearity if $r > 0.7$; Dormann et al., 2013). The only correlation with a value of 0.8 was found between nitrogen and phosphorus (black square). Therefore, nitrogen and phosphorus were not included in the same model.

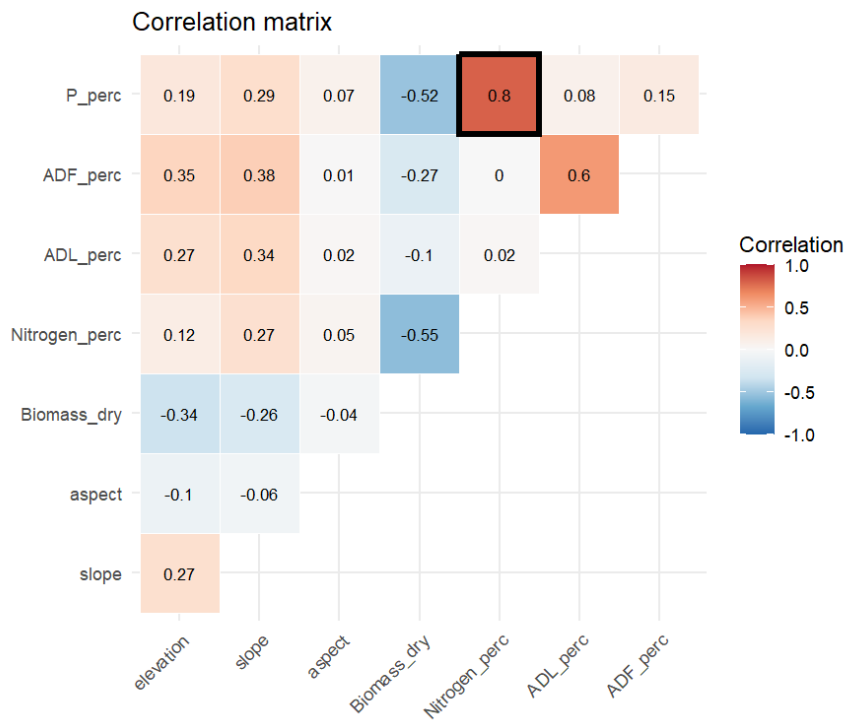

Figure 10: Correlation matrix showing the Pearson correlation of all predictor variables.

Including topographic variables can improve the model performance of SDMs, as shown e.g. by Pottier et al. (2014). Elevation, slope and aspect were used as topographic variables. Further, Donini et al. (2025) showed that red deer occurrence was correlated to the elevation squared. Therefore, elevation was used as squared elevation in the SDM. Due to the hierarchical principle, the elevation was also used without the squared term in the equation (The Pennsylvania State University, n.d.). While slope describes the "change in elevation" in degrees, aspect describes whether a slope is directed to the sun or not (Olaya, 2009). Expressed in degrees, 0° (and 360°) was defined as North, where cos(α) can be used to describe the northing and sin(α) the easting (King et al., 1999; Olaya, 2009).

Because the different parameters are in different units, the data were centred and scaled prior to model fitting to a mean = 0 and SD = 0.5 (Gelman, 2008; Rempfler et al., 2024) to make the outputs directly comparable. Muff et al. (2020) reviewed studies using GLMMs for habitat selection and highly recommended including random intercepts and random slopes in the model to avoid biased and overconfident results when modelling RSFs. Further they suggest fixing the intercept variance at a large value (10^6) to avoid shrinkage and bias and giving weights to the datapoints (presence = 1, available = 1000). Before the GLMMs were fitted, the number of positions recorded for each individual were checked. Out of 41 individuals, 11 had less than 10 presence points and were therefore excluded, resulting in 28 individuals (26796 points) for the analysis. All GLMMs were fitted with the glmmTMB package (version 1.1.14, Brooks et al., 2017) in R (version 4.5.1). To have a comparable RSF / SDM, the ODMAP protocol by Zurell et al. (2020) was followed (Supplementary Table 4), summarising the relevant elements for a good SDM.

To test the three hypotheses (explaining red deer feeding behaviour by (i) topography alone, (ii) topography and food quantity or (iii) topography together with food quantity and quantity), three model categories were created (see Table 3 with three different colours). M0 was used as null model with only the random effect. M1 (orange category) tested whether topography alone was a good explanation of red deer feeding behaviour and M2 (blue category) whether topography together with food quantity (biomass) was better. To determine which quality proxy described the red deer presence the best, all the different quality variables were tested, as well as some 2-way-interactions of forage quality together with biomass (M3 – M8, green category). The models were compared with the Akaike information criterion (AIC).

For M2 – M8, the models were once fitted with a random intercept only and once with random slopes (tested with biomass and the respective quality variable). The best model was then identified, and the parameter uncertainty was checked via the confidence interval. To check for spatial autocorrelation, the model residuals (5000 random points chosen due to computational constraints) were analysed with the Moran's I following the steps on the webpage by Gimond (2019). The Moran's I is a measure for spatial autocorrelation and describes how similar points are due to their geographic proximity, ranging from -1 to 1 with values close to 0 indicating no spatial autocorrelation. The Moran's I ($I = 0.003$, p-value = 0.005), indicated only minimal spatial autocorrelation.

Table 3: All models were fitted with fixed weights (presence = 1, available = 1000) and a fixed intercept variance of 10^6. The table shows only the model with the random intercept, but for models M2 – M8, also random slopes were fitted (not shown for clarity). M0 serves as reference model, the three colours (orange, blue and green) represent the three categories of the tested hypothesis (i, ii and iii).

Model	Fitted parameters	Formula
M0	Random effect only (individual)	Presence ~ (1|Individual)
M1	Topography	Presence ~ elevation + elevation^2 + slope + aspect_cos + aspect_sin + (1| Individual)
M2	Topography + Biomass	Presence ~ elevation + elevation^2 + slope + aspect_cos + aspect_sin + Biomass + (1| Individual)
M3	Topography + Biomass × Nitrogen	Presence ~ elevation + elevation^2 + slope + aspect_cos + aspect_sin + Biomass * Nitrogen + (1| Individual)
M4	Topography + Biomass × Phosphorus	Presence ~ elevation + elevation^2 + slope + aspect_cos + aspect_sin + Biomass * Phosphorus + (1| Individual)
M5	Topography + Biomass × ADL	Presence ~ elevation + elevation^2 + slope + aspect_cos + aspect_sin + Biomass * ADL + (1| Individual)
M6	Topography + Biomass × ADF	Presence ~ elevation + elevation^2 + slope + aspect_cos + aspect_sin + Biomass * ADF + (1| Individual)
M7	Topography + Biomass × ADF × N	Presence ~ elevation + elevation^2 + slope + aspect_cos + aspect_sin + Biomass * ADF * Nitrogen + (1| Individual)
M8	Topography + Biomass × ADF × P	Presence ~ elevation + elevation^2 + slope + aspect_cos + aspect_sin + Biomass * ADF * Phosphorus + (1| Individual)

4.4.2 Sex-specific analysis

Hinds and stags can have different food preferences. To test whether feeding behaviour differed between females and male, a sex-specific analysis was conducted. The dataset was split into females and males, however, it was not possible to further distinguish the females into hinds with calves and those without. Originally, there were 55 females and 18 males with GPS and activity information. After filtering for the respective GDD period, 34 females and 18 males were left. There were 34 different female individuals, however, 11 of those had fewer than 10 presence points. Therefore, those 11 individuals were excluded, and 23 individuals (15024 GPS positions = sample size) were left for the analysis. 18 males were left and 11 of those males were outside the SNP (see Supplementary Figure 7) and also outside the APEX image coverage. Therefore, data from seven males were available; however, two individuals had one and three presence points respectively and were excluded. Five males (11772 GPS positions = sample size) were left for the analysis. The number of individuals and the sample size for males was smaller, therefore the results needed to be interpreted with care.

All the possible combinations of models (see Table 3 under Section 4.4.1) with random intercept and also random slopes were tested. For each sex, the best model was identified via the AIC, and the model parameter uncertainty was checked with the confidence intervals.

To test whether habitat selection differed between sexes, the two best models (M7d and M8b) were used and fitted on the full dataset three times. Once without sex, once with sex as main effect and once with sex as interaction term. These models were compared using AIC and a likelihood ratio test (anova()).

To check for spatial autocorrelation, the model residuals (5000 random points chosen due to computational constraints for hinds, and 2000 random points for stags due to the lower number of GPS points) were analysed with the Moran's I following the steps on the webpage by Gimond (2019). The Moran's I indicated only minimal spatial autocorrelation (for hinds: $I = 0.006$, p-value = $1.87 * 10^{-6}$; and for stags: $I = -0.002$, p-value = 0.76).

5 Results

5.1 Animal summer locations

In total, 73 individuals were monitored over 9 years (2011 – 2019) and a total of 219447 GPS positions of red deer were recorded (Figure 11). These were all recorded positions before any filters were applied. Although GPS positions were recorded from 2010 onwards, the first individual equipped with an accelerometer recorded from autumn 2010 onwards, resulting in no summer locations for 2010. Red deer in the SNP were predominantly found in four land cover classes: forest, grassland, moss and lichen and bare/sparse vegetation (Figure 11). More than half of all positions (63.6 %) were recorded in forest, followed by grassland with 28.1 %. The other land cover classes (moss and lichen: 6.0 %; bare/sparse vegetation: 1.7 %) were less visited by red deer, and land cover classes such as shrubland, snow and ice, or cropland were very rarely visited.

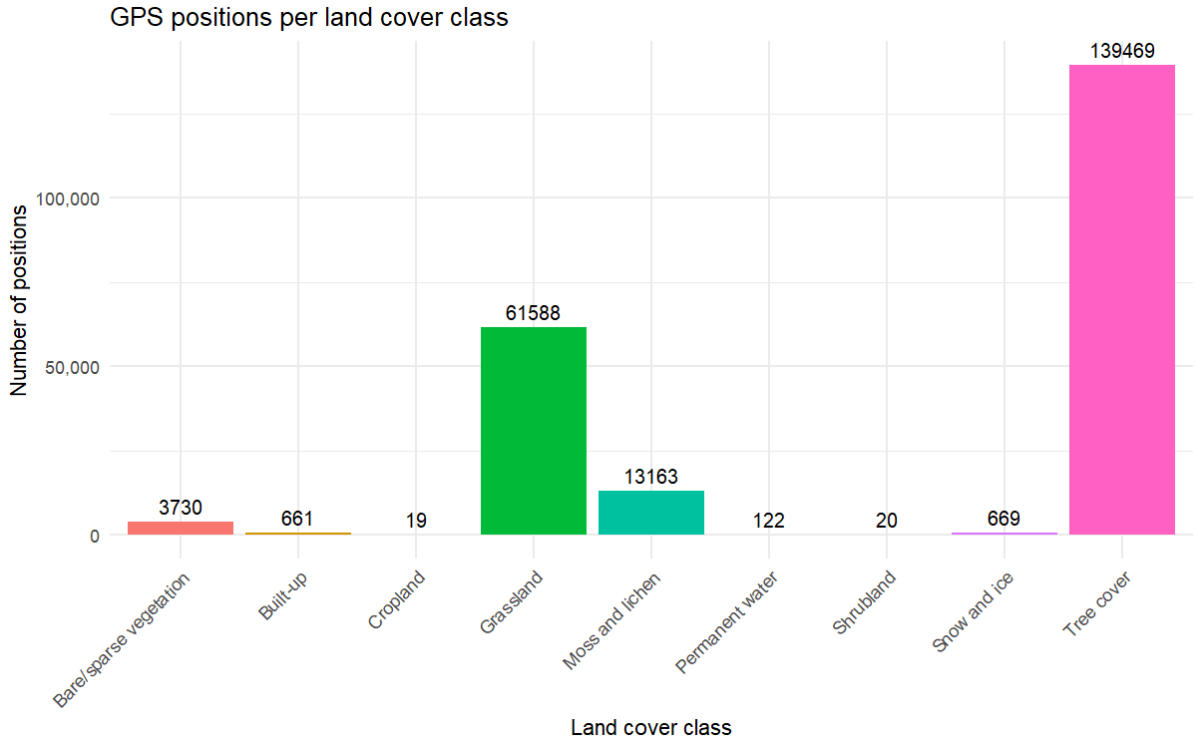

Figure 11: Recorded GPS positions of 73 red deer for the summer months 2011 – 2019 for different land cover classes showing the absolute values. Total number of positions per land cover class is added on top of each bar.

The behaviour varied between land cover classes (Figure 12). In relative terms, feeding was the dominant behaviour in moss and lichen (52.7 %) and shrubland (75 %), indicating that these two land cover classes were mainly used for feeding. In forest and grassland, the proportion of feeding positions was 26.9 % and 37.7 % respectively. Within forest, the dominant behaviour was lying (63.4 %), followed by feeding (26.9 %), walking (6.6 %) and running (3.1 %). In contrast, grassland showed a more balanced distribution between feeding and lying (37.7 % and 42.3 %, respectively), while walking and running were again less dominant (12.3 % and 7.7 %).

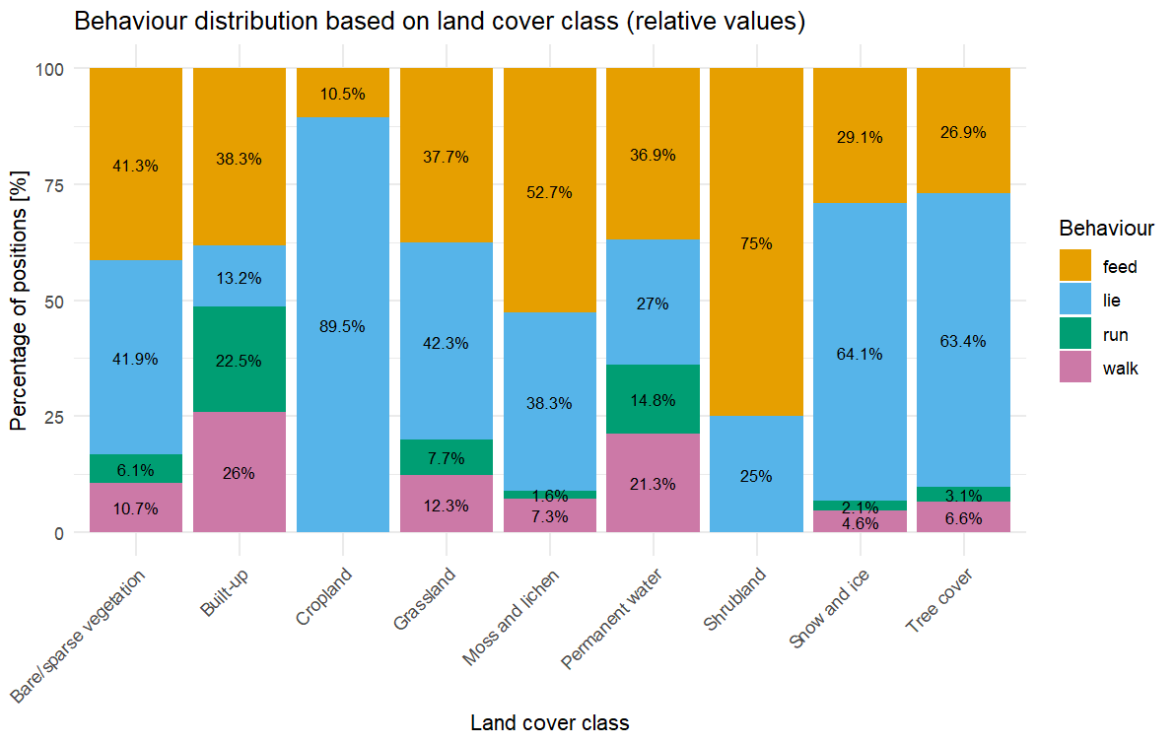

Figure 12: Behavioural distribution of red deer for different land cover classes showing the relative values.

During the day, red deer preferred forested areas, followed by grassland and moss and lichen (Figure 13). Forest was mainly chosen for lying, followed by feeding. Grassland was chosen equally during the day for feeding and lying. During the night, red deer selected either grassland or forest locations, with both land cover classes showing almost equal numbers of positions (37'685 and 38'916, representing 17.2 % and 17.7 % of all positions). These two land cover classes were used for feeding and lying during the night.

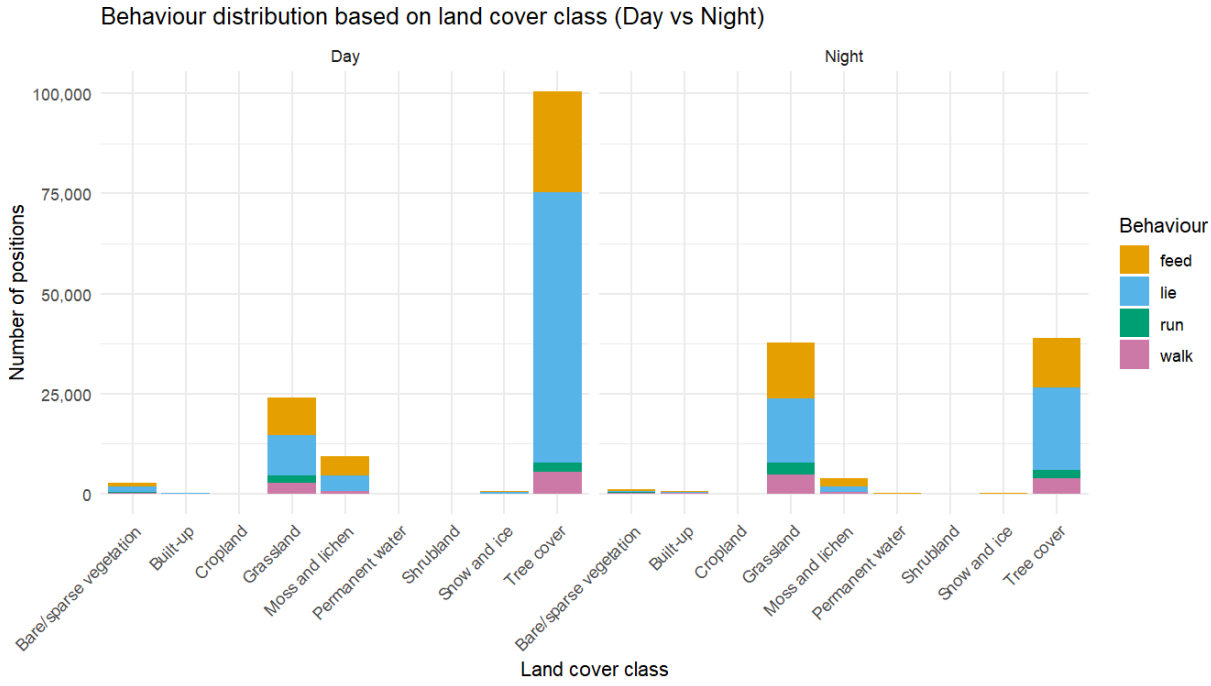

Figure 13: Behavioural distribution for red deer based on land cover class and day-night differences.

5.1.1 Animal summer locations by sex

Females and males showed different distributions per land cover class. In total, 55 females and 18 males were monitored, resulting in 158105 and 61336 GPS positions, respectively. Both sexes were mainly found in forest, grassland and moss and lichen (Figure 14). However, females used forest much more compared to males. While females used grassland, forest and moss and lichen mainly for feeding and lying, forest was less important for males in terms of feeding but more for lying (Figure 15). For both females and males, the behavioural distribution per land cover class between day and night was similar to that of the overall population.

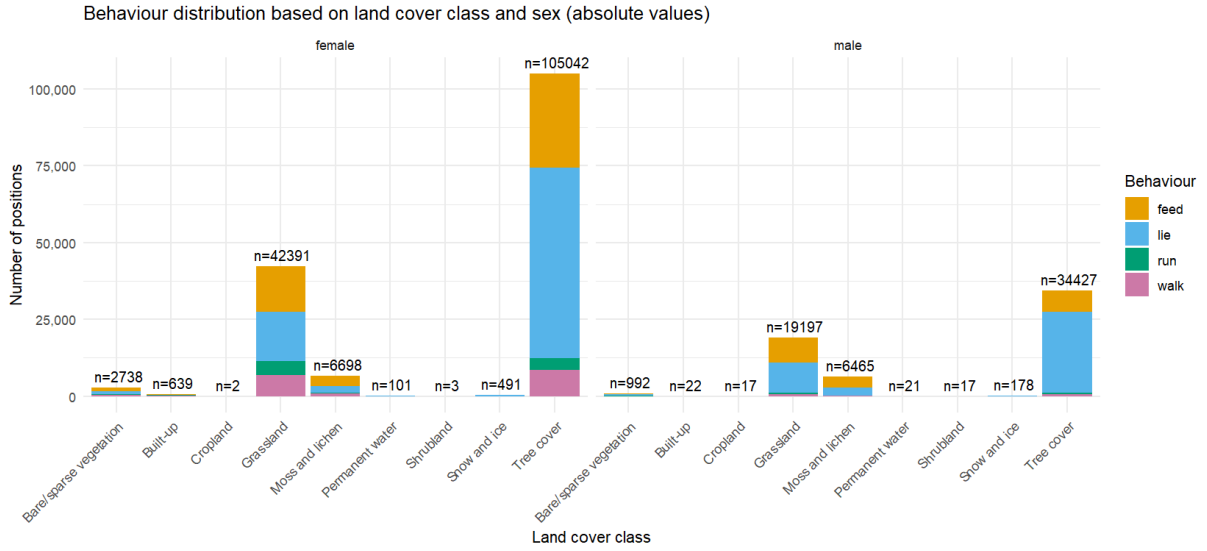

Figure 14: Behavioural distribution of females and males for different land cover classes showing the relative values.

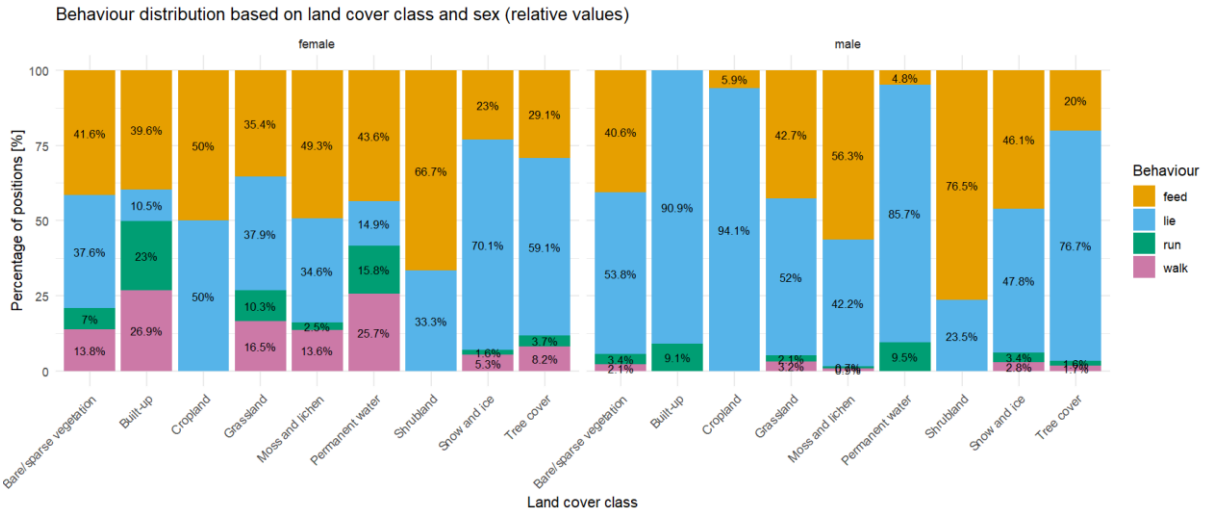

Figure 15: Behavioural distribution of red deer for different land cover classes and sex showing the relative values.

5.2 Home ranges across the summer

During the nine analysed years (2011 to 2019), there were 70 individuals with recorded GPS positions for all the three GDD periods (154.7, 239.95 and 330.95), each individual tracked for approximately two years. Figure 16 shows the home ranges of red deer for the three GDD periods, indicating that some areas were heavily used. Val Trupchun, the region around the Ofenpass round (Il Fuorn) and Val Mingèr were predominantly used. Different colours indicate different individuals. Visually, there was a substantial overlap between the home ranges at the three phenological stages. The largest overlap was between GDD 239.95 and 330.95 with 72.9 %. The smallest overlap was between GDD 154.7 and 330.95 with 68.1 %. The overall mean overlap between the three GDD periods was 71.11 ± 16.96 % (mean ± SD, Supplementary Figure 6). This suggested that red deer reused the same home ranges throughout the summer justifying the analysis of only one GDD period in more detail for the RSF. However, the large standard deviation indicated that there are differences between individuals. Table 4 shows the size of the home ranges at the three phenological stages. The areas were all similar in their size with the home ranges at GDD 330.95 slightly smaller (279.9 ± 120.9 ha) compared to the other two time periods (315.7 ± 167.7 ha and 318.8 ± 149.5 ha for GDD 154.7 and 239.95, respectively).

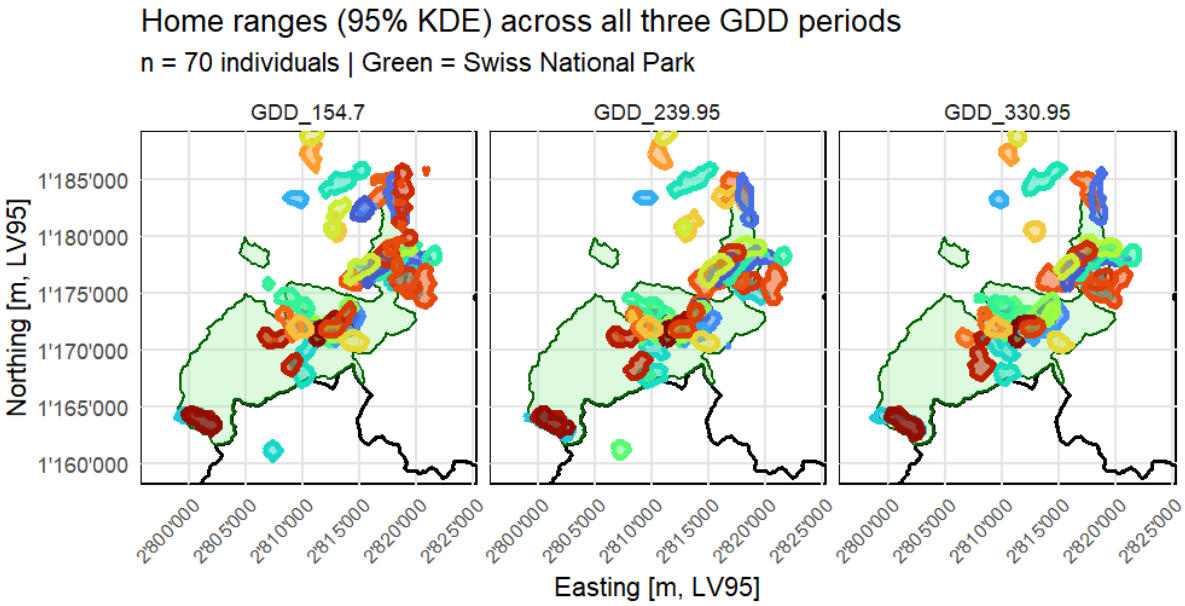

Figure 16: Home ranges for all 70 individuals across the three GDD periods. Each period was filtered for the GDD +5 days. Only individuals with more than 30 recorded GPS locations and those that were present in all three GDD periods are shown. Different colours indicate different individuals.

Table 4: Red deer home range area statistics

Red deer home range statistics 95 % kernel density estimates across phenological stages					
Phenological stage	N	Mean Area [ha]	SD Area [ha]	Mean Radius [m]	SD Radius [m]
GDD 154.7 (early)	70	315.7	167.7	971	251
GDD 239.95 (mid)	70	318.8	149.5	983	222
GDD 330.95 (late)	70	279.9	120.9	923	201

5.3 Feeding locations across the summer

Overall, the feeding locations of red deer in the SNP did not vary spatially across the three phenological stages (Figure 17). However, at a smaller spatial scale, there were some differences with a shift in the intensity of the used feeding locations around Val Mingèr and in Val Cluozza between GDD 154.7 and GDD 330.95. Later in the season (GDD 330.95) there were more feeding events (larger circles and brighter colours). Also, around the Ofenpass road and Il Fuorn, there were more revisited feeding locations for GDD 330.95 than for GDD 239.95 or for GDD 154.7. The largest overlap was between the feeding areas of GDD 154.7 and GDD 239.95 with 94.4 %, followed by 93.2 % for GDD 239.95 and GDD 330.95. The smallest overlap was between the first and the last phenological stage (GDD 154.7 and GDD 330.95) with 88.5 %. The mean overlap, aggregated for all individuals, was 92 %. This aligned with the findings that red deer not only reused their home ranges, but also their actual feeding locations across the summer.

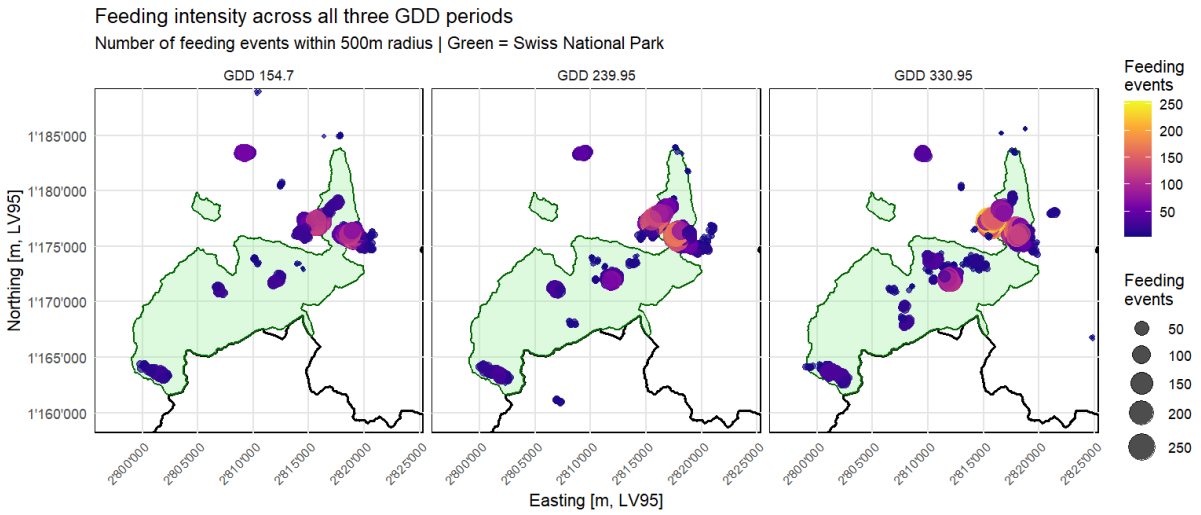

Figure 17: Red deer feeding locations across the three GDD periods. Larger circles and brighter colours indicate more revisits.

5.4 Model performance

The model performance of the training data with the PLSR ranged between an R^2 value of 0.331 for phosphorus to 0.475 for biomass (Table 5). However, neither the square root nor the log transformations improved the R^2 value for biomass (R^2 0.469 vs. 0.475), nitrogen (R^2 0.445 vs. 0.462) nor ADL (R^2 0.333 vs. 0.416). Therefore, no transformations were applied. For biomass, nitrogen, ADF and ADL, the model with data from 2010 and 2013 performed better compared to the single models, therefore, the combined model was used for those variables.

Table 5: Model performance of the training data with the PLSR model evaluated by the coefficient of determination (R^2) and the root mean square error for each variable, together with the number of datapoints and the found optimal component.

Variable	Dataset	Number of data	Optimal component	Mean R^2	SD	Mean RMSE
Biomass	2010 + 2013	133	9	0.475	0.163	68.174
Nitrogen	2010 + 2013	133	11	0.462	0.417	0.616
ADF	2010 + 2013	133	18	0.402	0.368	5.454
ADL	2010 + 2013	133	14	0.416	0.368	2.239
Phosphorus	2010	51	12	0.331	0.324	0.030

5.5 Prediction maps of food quality and quantity

The prediction maps are shown for each variable individually (Figure 18 to 22). Biomass predicted values ranged from 0 to 683.77 g/m^2 (Figure 18). However, the AOA mask was more aggressive for biomass than for the other variable predictions leading to a lot of zero values (negative predictions were set to zero; left-skewed distribution), making up the first 20 % of the data (first quantile). Therefore, the yellow category only contains zero values. The predicted values for the other four variables (N, P, ADL and ADF) showed a normal distribution, with medium levels more prominent compared to very low or very high values. Nitrogen predictions (Figure 19) ranged from 0 to 7.12 %, while phosphorus (Figure 20) predicted values ranged from 0 to 0.29 %. The predicted value range for ADL (Figure 21) was 0 to 46 % and for ADF (Figure 22) 0 to 79.54 %.

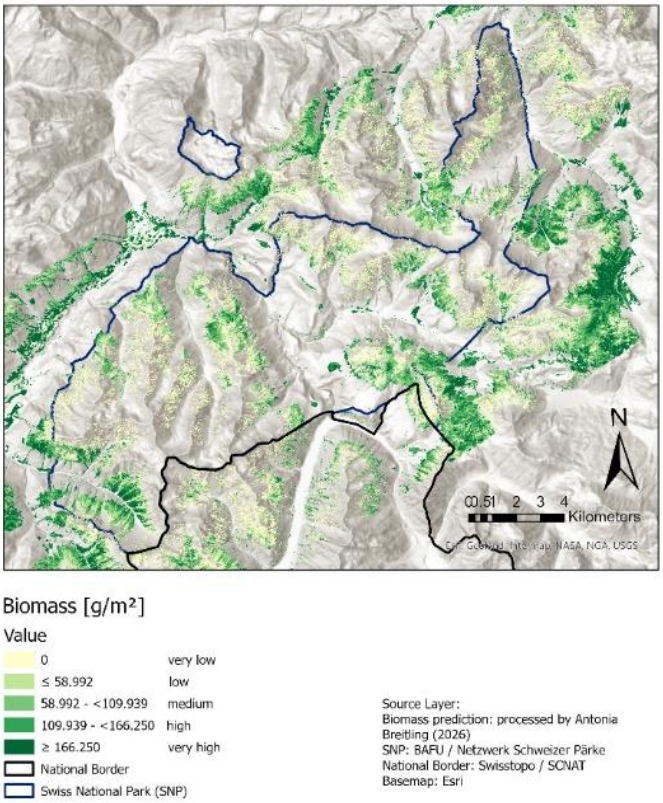

Figure 18: Biomass predictions in g/m² for the SNP masked for grassland. The values are split into quantiles with five categories (very low, low, medium, high and very high). Due to a lot of predictions with the value zero, the first quantile only contains zeros. Map produced in ArcGIS Pro.

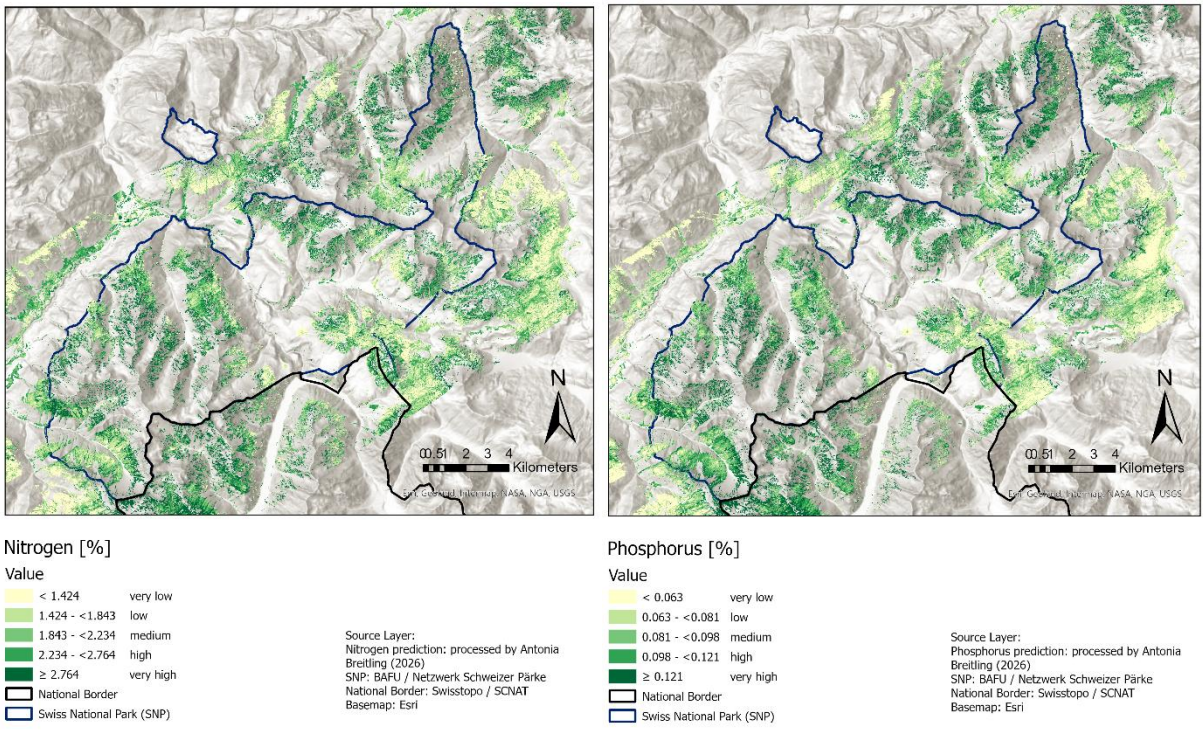

Figure 19: Nitrogen predictions in percentage for the SNP masked for grassland. The values are split into quantiles with five categories (very low, low, medium, high and very high). Map produced in ArcGIS Pro.

Figure 20: Phosphorus predictions in percentage for the SNP masked for grassland. The values are split into quantiles with five categories (very low, low, medium, high and very high). Map produced in ArcGIS Pro

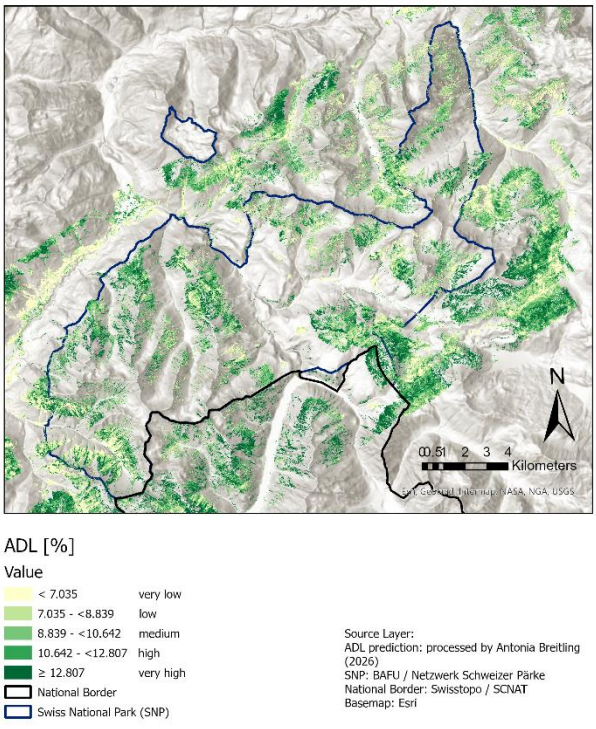

Figure 21: ADL predictions in percentage for the SNP masked for grassland. The values are split into quantiles with five categories (very low, low, medium, high and very high). Map produced in ArcGIS Pro.

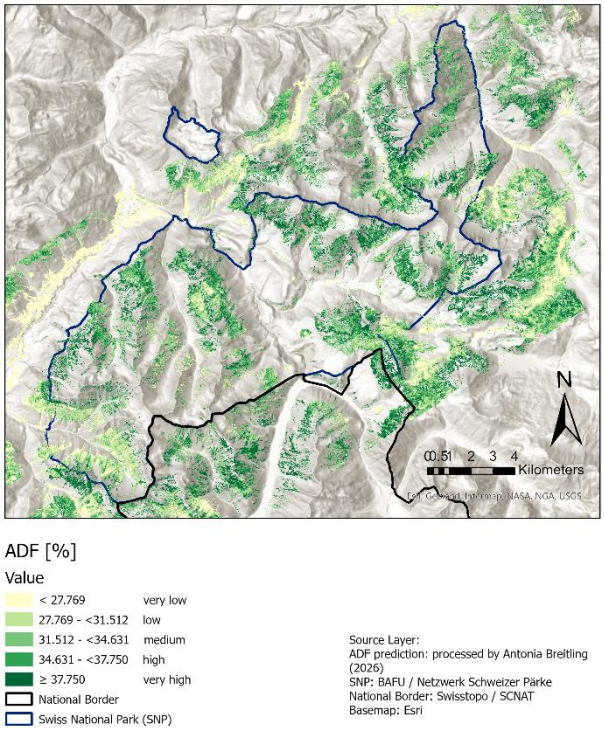

Figure 22: ADF predictions in percentage for the SNP masked for grassland. The values are split into quantiles with five categories (very low, low, medium, high and very high). Map produced in ArcGIS Pro.

5.6 Characterisation of red deer feeding locations

Red deer feeding locations were found at slightly lower elevation levels (2280.77 ± 175.89 m) and flatter slopes (26.54 ± 11.47 °) compared to absence points (2303.33 ± 175.00 and 30.49 ± 11.88 ° respectively); Table 6 and Figure 23. Further, red deer were more often located at slopes directed to the south (Northing: -0.105) and to the east (Easting: 0.138). Compared to the absence points, red deer presence was in higher biomass areas (presence: 115.25 ± 74.04 g/m^2; absence: 79.41 ± 71.53 g/m^2) and lower ADF areas (presence: 31.71 ± 6.07 %; absence: 34.13 ± 5.98 %). Nitrogen, ADL and phosphorus values were similar between presence and absence.

Table 6: Descriptive statistics of red deer feeding locations.

Descriptive statistics of feeding locations and pseudo-absences																
	Elevation [m]		Slope [°]		Aspect [°]		Biomass [g/m^2]		Nitrogen [%]		ADF [%]		ADL [%]		Phosphorus [%]	
Group	Mean	SD	Mean	SD	Mean	SD	Mean	SD	Mean	SD	Mean	SD	Mean	SD	Mean	SD
Absence	2303.33	175.00	30.49	11.88	165.65	100.71	79.41	71.53	2.02	0.63	34.13	5.98	9.58	3.33	0.09	0.03
Presence	2280.77	175.89	26.54	11.47	146.27	84.23	115.25	74.04	1.95	0.52	31.71	6.07	9.08	3.80	0.09	0.02

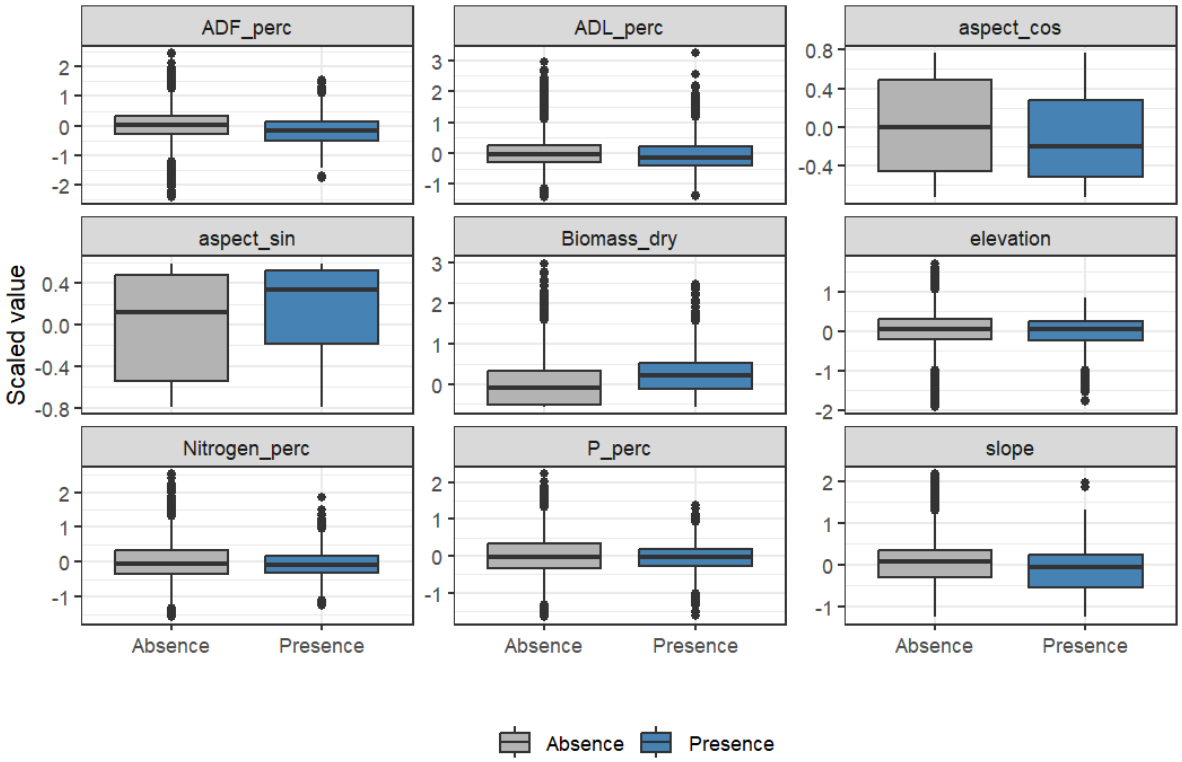

Figure 23: Descriptive statistics of red deer feeding locations, after the variables had been scaled for the presence and absence data.

5.7 Explaining red deer presence

In total, there were 26796 GPS points (28 individuals) for the analysis. The different models represented different tested hypotheses to assess which combination of biomass and food quality proxy best explained red deer presence (Table 7). Including topography (M1) increased model performance compared to only the random effect (ΔAIC: 910, χ^2 = 919.58, p-value < 0.001). Similar, including biomass together with topography also improved model performance compared to the model with only topography. Accounting for individual differences in respect to biomass (M2b; random slopes for biomass) decreased the ΔAIC by 398 (χ^2 = 401.78, p-value < 0.001), showing that different individuals reacted differently to biomass values.

M3 to M8 tested the hypothesis whether topography, biomass and forage quality best explained red deer presence. Model M7d (for summary output see Supplementary Figure 8), was the model with the lowest AIC and identified as the best model, supporting the hypothesis that red deer presence was best explained by topography, biomass and forage quality. This model included topography, biomass, nitrogen and fibre content, allowing the 3-way interaction and accounting for random slopes of ADF. Individuals showed different responses to the fibre content with four individuals showing a negative slope, while the others showed a neutral to slightly positive response, with confidence intervals including the value zero (Figure 24).

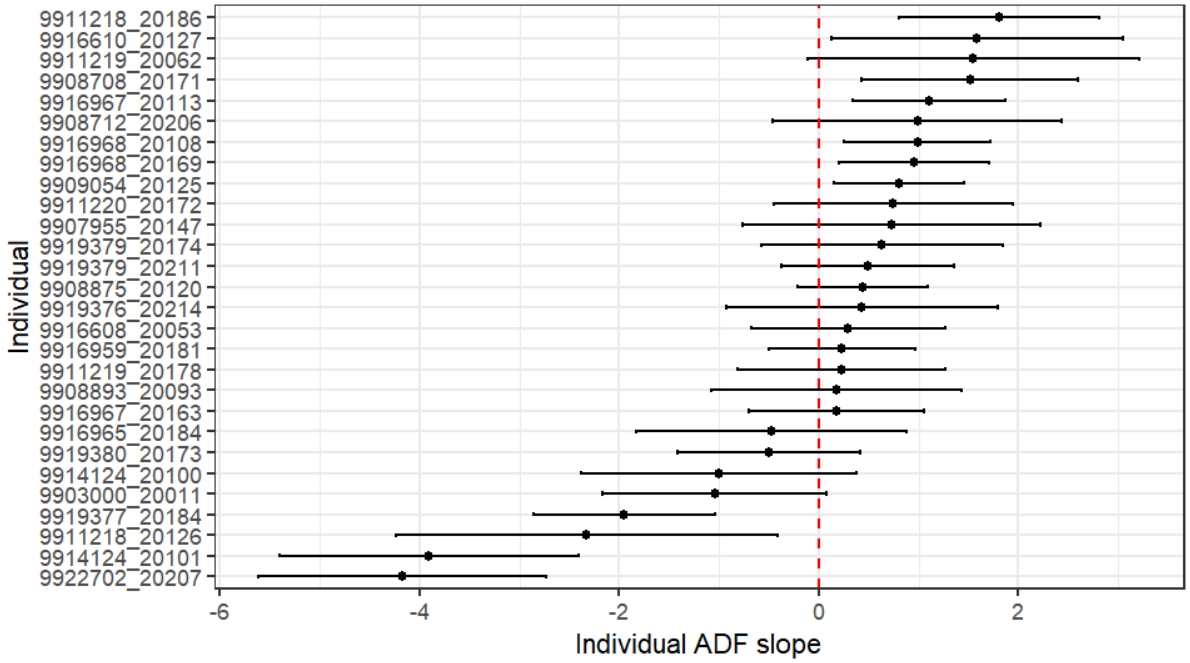

Figure 24: Estimate on fibre content for M7d for each individual (n = 28) showing the different preferences for each individual. The large CI interval for some of the individuals are due to the slightly less recorded GPS positions, but still more than 10 positions (e.g. Individual 20126 and 20062).

All parameters except the intercept and the 3-way interaction were significant (model estimates in the log odds scale; Figure 25). This aligns with the findings summarised in Table 6 (Section 5.6). Red deer preferred higher elevations (positive estimate); however, the negative estimate for the squared elevation showed that this effect is reduced at very high elevations. Thus, medium levels were most suitable for red deer. Furthermore, red deer were found in flatter terrain, slopes facing south and east. They clearly selected higher biomass values and higher nitrogen values but lower ADF values. All 2-way interactions were significant. At high biomass values, the negative effect of ADF was reduced. Further, at higher biomass values, higher nitrogen values were preferred and again, at higher nitrogen values, the negative effect of ADF was reduced. Figure 26 summarises the effect size (95 % CI) of each fixed model parameter in log odds scale.

Spatial autocorrelation was tested on the residuals of the best model (M7d) using the Moran's I (I = 0.003, p-value = 0.005), indicating only minimal spatial autocorrelation.

For all the models, accounting for random slopes increased the model performance (see Table 7 and compare e.g. M3a, M3b and M3c). This showed that red deer reacted differently to food quality parameters and biomass. When biomass was modelled either with nitrogen or phosphorus, the model with random slopes for biomass was better. Therefore, red deer reacted more individually to different biomass values compared to nitrogen or phosphorus. However, if lignin or fibres were included together with biomass, these two proxies as random slopes increased the model. Therefore, red deer showed a greater variation in response to lignin and fibres content than to biomass.

Table 7: Overview of the model performance characterised by the AIC and the ΔAIC value. The best model is highlighted in green.

Model	Degree of Freedom	AIC	ΔAIC
M0: random effects only	1	50637.52	1845.33
M1: Topography	6	49727.94	935.75
M2a: Topography + Biomass (random intercept only)	7	49451.17	658.98
M2b: Topography + Biomass (random slopes)	8	49330.16	537.97
M3a: Topography + Biomass * N (random intercept only)	9	49245.74	453.55
M3b: Topography + Biomass * N (random slope for Biomass)	10	49112.84	320.65
M3c: Topography + Biomass * N (random slope for N)	10	49172.67	380.48
M4a: Topography + Biomass * P (random intercept only)	9	49294.28	502.09
M4b: Topography + Biomass * P (random slopes for Biomass)	10	49124.14	331.95
M4c: Topography + Biomass * P (random slopes for P)	10	49235.82	443.63
M5a: Topography + Biomass * ADL (random intercept only)	9	49443.30	651.11
M5b: Topography + Biomass * ADL (random slopes for Biomass)	10	49313.63	521.44
M5c: Topography + Biomass * ADL (random slopes for ADL)	10	49206.63	414.44
M6a: Topography + Biomass * ADF (random intercept only)	9	49189.33	397.14
M6b: Topography + Biomass * ADF (random slopes for Biomass)	10	49049.01	256.82
M6c: Topography + Biomass * ADF (random slopes for ADF)	10	48979.71	187.52
M7a: Topography + Biomass * ADF * N (random intercept only)	13	49007.73	215.54
M7b: Topography + Biomass * ADF * N (random slopes for Biomass)	14	48856.30	64.11
M7c: Topography + Biomass * ADF * N (random slopes for N)	14	48931.19	139
M7d: Topography + Biomass * ADF * N (random slopes for ADF)	14	48792.19	0
M8a: Topography + Biomass * ADF * P (random intercept only)	13	49043.90	251.71
M8b: Topography + Biomass * ADF * P (random slopes for Biomass)	14	48865.90	73.71
M8c: Topography + Biomass * ADF * P (random slopes for P)	14	48982.46	190.27
M8d: Topography + Biomass * ADF * P (random slopes for ADF)	14	48850.21	58.02

Predictor	Estimate	2.5%	97.5%
(Intercept)	-0.001	-370.311	370.309
elevation	0.189	0.055	0.323
I(elevation^2)	-0.746	-0.929	-0.563
slope	-0.527	-0.642	-0.412
aspect_cos	-0.662	-0.764	-0.560
aspect_sin	0.676	0.584	0.768
Biomass_dry	1.118	1.010	1.225
ADF_perc	-1.451	-2.087	-0.814
Nitrogen_perc	0.531	0.400	0.661
Biomass_dry:ADF_perc	0.970	0.796	1.144
Biomass_dry:Nitrogen_perc	0.960	0.763	1.157
ADF_perc:Nitrogen_perc	0.858	0.614	1.101
Biomass_dry:ADF_perc:Nitrogen_perc	0.216	-0.143	0.575

Figure 25: Coefficient table including estimate and 95 % CI of the overall best model (M7d). All estimates are in log odds scale.

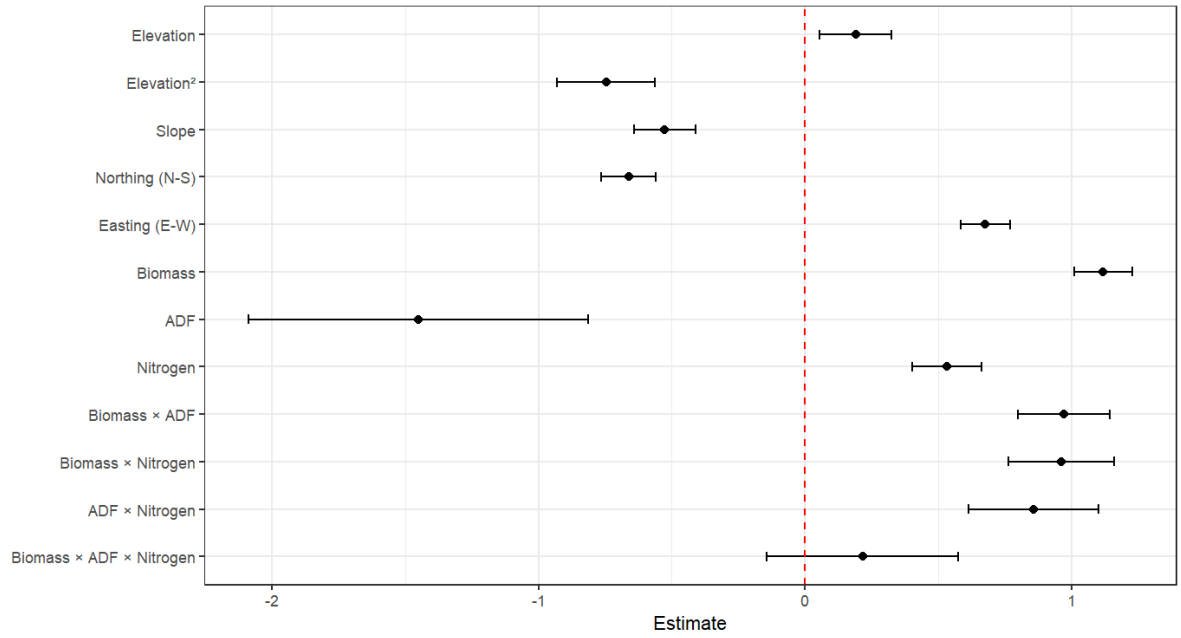

Figure 26: Effect size plot of the overall best model (M7d), showing the fixed effects estimates with a 95 % CI on the log odds scale. The dashed red line indicates no effect (estimate = 0).

5.7.1 Sex-specific feeding habitat differences

Stags were more often found outside the SNP (see Supplementary Figure 7) compared to hinds which were found more within the SNP, resulting in 23 hinds (15024 GPS positions) and 5 stags (11772 GPS positions) available for the analysis.

The best model explaining female red deer distribution was also M7d (see Table 7 under Section 5.7), including topographic variables, biomass, nitrogen and ADF and accounting for random slopes for ADF (Figure 27; values in log odds scale). Again, most variables were significant (for summary output see Supplementary Figure 9), except the intercept, nitrogen and the 3-way interaction. Females were found in lower elevations and flatter terrain. Nitrogen as main effect did not describe where female red deer were found (estimate = 0.08, p-value = 0.42, Supplementary Figure 9). However, in the 2-way

interactions, nitrogen played an important role through its interactions with biomass and ADF. For higher biomass values, higher nitrogen values were preferred and at high nitrogen values, the effect of ADF was reduced.

Predictor	Estimate	2.5%	97.5%
(Intercept)	-0.001	-408.675	408.673
elevation	-1.159	-1.382	-0.936
I(elevation^2)	-1.386	-1.645	-1.127
slope	-0.402	-0.558	-0.247
aspect_cos	-0.687	-0.817	-0.557
aspect_sin	0.836	0.715	0.957
Biomass_dry	0.534	0.360	0.708
ADF_perc	-1.620	-2.496	-0.744
Nitrogen_perc	0.082	-0.118	0.281
Biomass_dry:ADF_perc	0.386	0.121	0.652
Biomass_dry:Nitrogen_perc	0.671	0.352	0.990
ADF_perc:Nitrogen_perc	1.103	0.743	1.463
Biomass_dry:ADF_perc:Nitrogen_perc	-0.114	-0.663	0.435

Figure 27: Coefficient table including estimate and 95 % CI of the best model explaining female red deer presence. All estimates are in log odds scale.

Generally, all models for males performed better when modelling random slopes for biomass (see Supplementary Table 1) than for a food quality proxy. This indicated that males reacted differently to different biomass values. However, because fewer GPS positions (11772) were available for stags, the output needed to be interpreted with care. The best model explaining male red deer presence was M8b, including topographic variables, biomass, phosphorus and ADF and accounting for random slopes for biomass (Figure 28; values in log odds scale). Analysing the best model for male red deer (M8b) showed that most parameters were significant (for summary output see Supplementary Figure 10; all in log odds scale), except for the intercept and the 2-way interaction of ADF with phosphorus. Compared to females that preferred lower elevations, elevation had a strong positive effect on males, indicating that male red deer strongly preferred higher elevations. However, the squared elevation term showed that too high elevations were not preferred. Males preferred higher biomass and phosphorus values but avoided high ADF values. Males showed a weaker response to ADF (-0.906) compared to females (-1.620), but at the same time a stronger response to biomass (males: 1.407; females: 0.534). At high biomass values, the negative ADF effect was reduced, and high phosphorus values were preferred. The 3-way interaction was slightly significant (Supplementary Figure 10). Figure 29 summarises the effect size (95 % CI) of each fixed model parameter in log odds scale for males and females. Elevation had the overall strongest effect on male red deer presence, ADF had the strongest effect on females.

Predictor	Estimate	2.5%	97.5%
(Intercept)	0.000	-876.660	876.659
elevation	2.082	1.792	2.372
I(elevation^2)	-2.315	-2.780	-1.850
slope	-0.776	-0.945	-0.607
aspect_cos	-0.578	-0.743	-0.413
aspect_sin	0.431	0.287	0.574
Biomass_dry	1.407	0.919	1.895
ADF_perc	-0.906	-1.076	-0.735
P_perc	0.864	0.690	1.038
Biomass_dry:ADF_perc	0.376	0.116	0.635
Biomass_dry:P_perc	1.223	0.941	1.505
ADF_perc:P_perc	-0.279	-0.613	0.054
Biomass_dry:ADF_perc:P_perc	-0.560	-1.097	-0.022

Figure 28: Coefficient table including estimate and 95 % CI of the best model explaining male red deer presence. All estimates are in log odds scale.

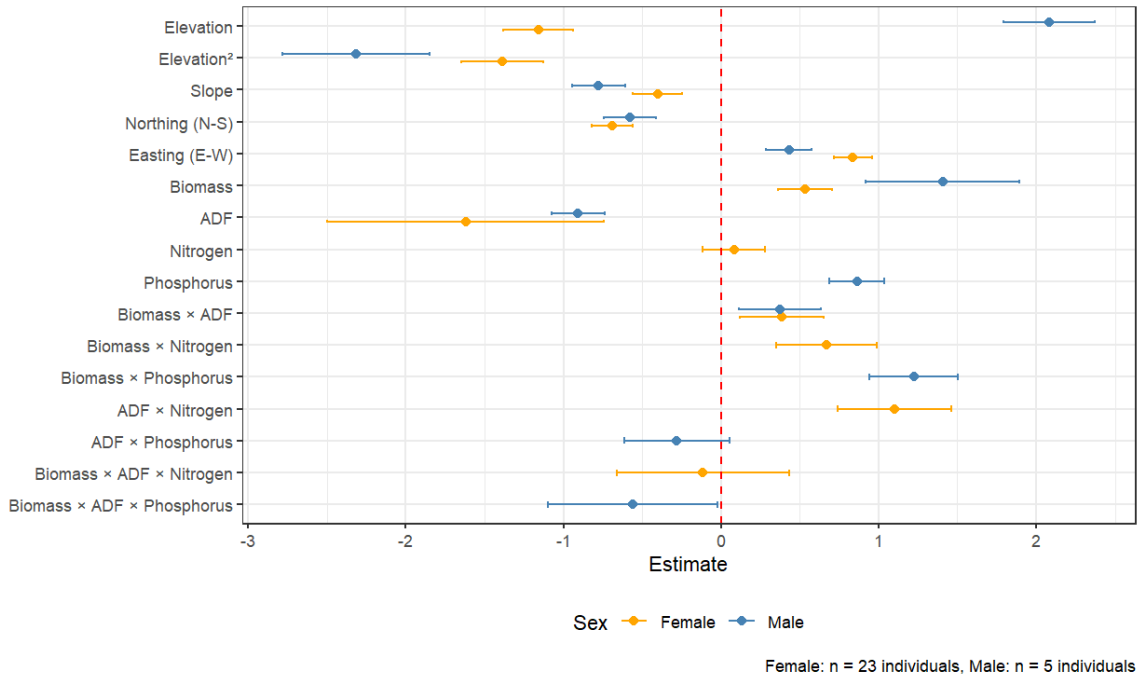

Figure 29: Effect size plot of the parameters for the best model for females (M7d) and the best model for male (M8b), showing the fixed effects estimates with a 95 % CI on the log odds scale. The dashed red line indicates no effect (estimate = 0). Females are shown in orange, males in blue.

The two best models (M7d and M8b) were used to test whether sex significantly influenced habitat selection. Adding sex as main effect to M7d did not improve the model (ΔAIC: 2, $\chi^2 = 0$, $p = 0.9998$), however, adding sex with interactions did improve the model (ΔAIC: 80.66, $\chi^2 = 96.658$, $p < 0.001$). The same was true for M8b. Adding sex as main effect to M8 did not improve the model (ΔAIC: 2, $\chi^2 = 0$, $p = 0.9999$), however, adding sex with interactions did improve the model (ΔAIC: 101.69, $\chi^2 = 117.69$, $p < 0.001$). This indicated that females and males showed sex-specific differences in their habitat selection, especially for elevation and food quality proxies. While females selected for nitrogen in combination with ADF, males selected for phosphorus and ADF. This suggested different nutritional priorities between the sexes, however, with only five males, this difference needed to be interpreted with care.

Spatial autocorrelation was tested on the residuals of the best model for hinds and stags using the Moran's I (M7d for hinds: I = 0.006, p-value = $1.87 * 10^{-6}$; M8b for stags: I = -0.002, p-value = 0.76), indicating only minimal spatial autocorrelation.

6 Discussion

Red deer were predominantly found in four land cover classes, with forest (63.6 %) having the largest number of positions, followed by grassland (28.1 %), moss and lichen (6 %) and bare/sparse vegetation (1.7 %). The dominant behaviour within forest was lying (63.4 %), followed by feeding (26.9 %), walking (6.6 %) and running (3.1 %). In grassland, the behaviour was more balanced between lying and feeding (42.3 % and 37.7 %, respectively), followed by walking (12.3 %) and running (7.7 %). During the day, red deer were mainly found in the forest, with the dominant behaviour lying. During the night, they either selected grassland or forest with more balanced behaviours between feeding and lying. Sex-specific differences in terms of land cover and behaviour were found.

Red deer home ranges did not vary spatially across the summer. The summer home range sizes were 315.7 ± 167.7 ha, 318.8 ± 149.5 ha and 279.9 ± 120.9 ha for GDD 154.7, 239.95 and 330.95, respectively. Analysing 70 home ranges of red deer showed that they reused their home ranges throughout the summer with a mean overlap of 71.11 ± 16.96 %. The home ranges were spread over the whole SNP, with some individuals in Val Trupchun, but most of them around the Ofenpass road (Il Fuorn) and Val Mingèr. Besides the home ranges, the feeding locations were also revisited during the summer, with a mean overlap of 92 % (aggregated for all individuals). However, at GDD 330.95, areas around the Ofenpass road (Il Fuorn) and Val Mingèr were more frequently visited compared to GDD 154.7 and showed higher feeding intensity.

The overall best model explaining red deer feeding habitat selection included topography, biomass together with nitrogen and fibre content. Sex-specific differences in feeding habitat selection were found between females and males. While female red deer feeding habitat selection could be best explained by topography, biomass, nitrogen and fibre content, the best model for males included topography, biomass, phosphorus and fibre content.

6.1 Behavioural distribution per land cover and time of the day

The land cover classes where red deer have been predominantly found are proportional to the most frequent land cover classes in the SNP (51 % mountainous terrain out of scree and rocks, 21 % alpine grasslands and 28 % forest (Schweizerischer Nationalpark, n.d.)). These findings partially align with the results by Rempfler et al. (2024), who only analysed open areas (i.e. forest was excluded). These authors found 74 % of the summer locations in grassland, followed by moss and lichen with 24 %, bare/sparse vegetation with 2 % and cropland with 0.07 %.

The observed behavioural differences between day and night align with the results of Willisch et al. (2024), who found red deer to select forest during the day and open areas during the night. Previous studies suggested that forests provide protection from human disturbance and are therefore preferred during the day when human activities are high (Sibbald et al., 2011). However, in the Swiss National Park, human impact is minimal (Schweizerischer Nationalpark, n.d.), and the choice of forests might be due to other factors. Still, day-night differences were observed, although they are not as strong as in unprotected areas (Rempfler et al., 2025). Red deer habitat selection in the SNP can therefore result from ecological effects, especially in terms of forests choice. Forests are identified to be important for red deer and previous explanations include a diversity of alternative food types found within the forest (Eggers et al., 2026; Suter et al., 2004), protection from temperature exposure (Widén et al., 2025) and a safe location to rest and protect the calves (Eggers et al., 2026). Further, red deer are important in seed dispersal and provide therefore useful ecosystem services (Garcia et al., 2025). Given that forests are selected during the day, all of these factors – beyond avoidance of human influence – may be playing a role in red deer habitat use. Further, red deer need to balance disturbances and forage intake. Predators can also be a contributing factor, influencing the feeding behaviour and the selection of feeding places (McArthur et al., 2014). During the analysed time (2010 until 2019), only one wolf was present within

the SNP (Schweizerischer Nationalpark, n.d.). Therefore, the predation risk was very low in the analysed time and did most probably not influence red deer habitat selection.

While red deer mainly lay in the forest during the day, they used grassland and forests during night for feeding. Godvik et al. (2009) showed that forest areas provide some food resources for red deer. This was also supported by Suter et al. (2004), who analysed red deer pellets in the SNP and showed that red deer feed mainly on grassland but also on plant species found within the forest. This explains why feeding behaviour was also found within the forest. Red deer also need time to ruminate their food, preferably in undisturbed areas while resting or lying (Clutton-Brock et al., 1982). Lying also has the positive effect of providing protection from flies (Espmark and Langvatn, 1979). This explains why red deer were found lying in the forest. Grassland areas were preferably used during the night, where forage was sufficient available (Godvik et al., 2009). Further, during the night, temperatures are lower thus enabling red deer to remain in open habitats and complement their feeding therein. These day-night movements between different habitat types are known as complementary habitat hypothesis, previously identified for similar species (i.e. roe deer; De Groeve et al., 2023). Often times, this complementary is interpreted as a strategy in human modified landscapes (De Groeve et al., 2023), and for the SNP this might represent a legacy of that behaviour. Within the SNP, red deer are protected (Schweizerischer Nationalpark, n.d.), therefore, day-night differences are expected to be less strong affected by human activities (Rempfler et al., 2025), even though there are still recreational activities.

These results are limited to the summer months and to GPS data that is used for the behavioural assignments. Uncertainty and transferability need to be addressed before direct transferability to other regions in the world. The observed behaviour patterns were analysed within a protected area for red deer. Yet the use of GPs data is crucial to allow behaviours to be assigned without the need to observe and follow red deer for a long time in their habitat thus providing measurements without observer biases.

6.2 Explaining summer home ranges and feeding locations in the SNP

Several studies have shown (e.g. Jarnemo et al., 2023; Jerina, 2012) that stags have generally larger home ranges than hinds. Female summer home ranges (n = 53) were 275.1 ± 121.6 ha, 279.0 ± 107.8 ha and 271.4 ± 112.9 ha for GDD 154.7, 239.95 and 330.95, respectively and male summer home ranges (n = 17) were larger with 423.6 ± 247.3 ha, 421.1 ± 206.5 ha and 284.1 ± 141.5 ha for GDD 154.7, 239.95 and 330.95, respectively (hinds: Supplementary Table 2; stags: Supplementary Table 3).

The summer home range sizes lay within the range of home range sizes found in other studies using a KDE approach. Female red deer in the Vosges mountains in the northeast of France had smaller summer home ranges of 156.66 ± 12.69 ha (n = 23; Richard et al., 2011). Furthermore, female red deer in Germany had also smaller summer home ranges of 966 ± 550 ha (n = 6; Gillich et al., 2021). Kropil et al. (2015), on the other hand, analysed stags (n = 10) in the Kremnica Mountains in Slovakia and found home ranges of 1947 ± 1610 ha for migrating red deer by using a kernel home range of 90 %. Jarnemo et al. (2023) analysed home ranges in Norway in two different landscapes, one more forest-dominated and one more agriculturally based. Summer home ranges for hinds were 307 ha for the forest area (n = 13) and 512 ha (n = 12) for the more agriculture-based landscape. The ratio of stags to hinds' home range size is reported to be 2.6 for red deer across 18 studies (Jarnemo et al., 2023). Whereas hinds prioritise protection of their young (Bonenfant et al., 2004), stags prioritise food quality to get strong for the rutting season (Main et al., 1996). Home range size of hinds increased slightly at mid summer and decreased towards the end of the summer most likely reflecting the high nutritional demands during lactation and when the calves were growing (Clutton-Brock et al., 1982). Home range sizes of stags were already largest at early summer and decreased towards end summer. This may be related to reproduction strategies, as they prepare for the upcoming rutting season. Home range area at GDD

330.95 was smaller than for the other GDD periods suggesting a better food availability to that time and shorter distances to travel (Rivrud et al., 2010). Further, most individuals had their summer home ranges around the Ofenpass road (Il Fuorn) and Val Mingèr implying better habitat conditions. These areas coincidence with the land cover classes preferred by red deer, as well as with the elevation ranges.

The feeding intensity was higher for GDD 330.95 compared to the earlier GDD periods. The energy intake of red deer from vegetation was shown by Arnold et al. (2015) to be lowest in winter and to increase continuously from spring to October. Additionally, Sigrist et al. (2022) analysed red deer habitat selection in alpine regions related to the green wave and found strong selection for high biomass in the later summer, when the green wave was coming to an end. GDD 330.95 represents the latest of the three GDD stages coinciding with good food quality and high energy intake, which may reflect the build-up of fat reserves as preparation for the rutting season and winter.

A more local study within the SNP (Rempfler et al., 2024), however, showed that the summer home ranges (June to August of 2017 to 2021) of 70 individuals were considerably smaller than the ones found in this study. The median for females was approximately 10 km^2 and for males approximately 25 km^2, (visually determined from Figure 2b in Rempfler et al. (2024)). The difference may be explained by the different method used to estimate home range size (minimum convex polygon (MCP 100 %) in their study and kernel density in this study) and that only open habitat locations were included in their study (i.e. excluding forest positions).

The home range size is influenced by several factors, namely body size, energetic needs, trophic structure, etc. Body size and related metabolic rate have been posited to influence the home range size of mammals, explaining why males have generally larger home ranges than females (e.g. Lindstedt et al., 1986), yet this is still to be settled (Kelt and Van Vuren, 2001) with new findings suggesting that home range size is more related to available resources (Clutton-Brock et al., 1982), landscape fragmentation (Haskell et al., 2002), physiological needs and disturbances (Nickel et al., 2021). Landscape composition influences the home range size of red deer by defining how far red deer need to walk to reach the next suitable area for feeding or resting (Bevanda et al., 2015). Migration can result in generally larger home ranges compared to stationary red deer, as shown by Luccarini et al. (2006), who analysed home ranges in the Italian Alps and Kropil et al. (2015), who analysed home ranges of stags in the Kremnica Mountains in Slovakia. However, the analysed time in this thesis was the summer, therefore, red deer should already be at their summer home ranges as migration into the SNP usually starts in spring / early summer and back to their winter areas in October (Anderwald et al., 2015; Blankenhorn et al., 1978). But they are generally migrating (20 to 30 km between summer and winter areas; Anderwald et al., 2015), therefore, the home ranges can still be larger compared to only resident individuals.

Also, climate influences home range size, as shown by Rivrud et al. (2010) for female red deer in Norway. The direction of influence of temperature and precipitation depends on the temporal scale analysed and can either be direct (on short term) or indirect (on longer terms via plant growth). Food availability can also influence the home range size. If the home range area contains good food quality, the home ranges were found to be smaller (Rivrud et al., 2010); alternatively, if roads or high red deer density occur in an area, also the home ranges are affected (Jerina, 2012)

Red deer reused their home ranges throughout the summer with a mean overlap of 71.11 ± 16.96 %, indicating a strong fidelity to their summer home ranges, as well as their feeding locations. These findings do not support the starting hypothesis, H2. Yet, Kamler et al. (2008) showed that both, hinds and stags, reused their summer home ranges in different years. Contrary to my results, where hinds showed a stronger mean overlap of 72.2 ± 17.4 % compared to stags with 64.5 ± 14 %, Kamler et al. (2008) found stronger overlaps for stags in summer than for hinds (92.3 ± 2.1% and 83.1 ± 7 %, respectively). These differences may be interpreted as forage quality was most probably not as good within the home range of hinds in the study area of Kamler et al. (2008), and therefore hinds had to change their feeding locations more, showing a lower fidelity. Further, the large standard deviation in

the mean summer home range overlap, suggests differences between individuals (e.g. hinds with calves and without), which can further explain these differences (hinds with calves have a higher energy demand compared to hinds without calves (Clutton-Brock et al., 1982)).

6.3 Modelling vegetation characteristics that relate to habitat quality

Generally, trait prediction model performance was slightly higher for the training model compared to the test model (see Table 5 under Section 5.4). This is not surprising as the training model is directly fitted to the training data, and then extrapolated to the test model. Model performance, R^2 value, for biomass (0.43) and nitrogen (0.34) lie within the range of performances of other models in the SNP, even though performance for biomass lies at the lower end. Reported model performance for aboveground biomass predictions in grassland and alpine environments include $R^2 = 0.52$ in different grassland systems in Northern Italy (Pinna et al., 2025) and $R^2 = 0.60$ (Rempfler et al., 2024) and $R^2 = 0.57$ (Schweiger et al., 2015b) in the SNP. For nitrogen, Rempfler et al. (2024) modelled an $R^2 = 0.34$, Schweiger et al. (2015b) had an adjusted $R^2 = 0.43$ (mean across 4 years).

The difference may be explained by the different methods used, the number of sampled plots and the time frame. Rempfler et al. (2024) used a RF model trained with a high number of plots (322 between 2011 and 2013 and additional 52 plots between 2016 and 2018). Further, several years were used for the training data, to capture year-to-year variability in the vegetation. The model performance for biomass is better, however, that for nitrogen is similar. This suggests that nitrogen predictions may be easier to achieve and are more stable across the years. Biomass prediction, on the other hand, might benefit from training data over several years to capture year-to-year variability. Schweiger et al. (2015b) used simple spectral ratio indices. Model performance for both, biomass and nitrogen, are higher than herein, however, the study area was only in the Val Trupchun and not the entire SNP. The number of plots were similar (51 plots in 2010 and 2011 but 100 plots in 2012 and 2013), however, over data was used over 4 consecutive years for model training.

The model performance of the other variables (ADL, ADF and P) was also within the expected range, even though no comparison to studies conducted in the SNP could have been done due to no available studies addressing this topic. Zhang et al. (2025) estimated phosphorus in alpine grassland using a field spectroradiometer in the Qinghai-Tibet Plateau and reported an $R^2 = 0.39$ using PLSR. This value is in the same range as the value obtained in this study with $R^2 = 0.33$. The slightly lower model performance may be explained by differences in the data acquisition approach. While Zhang et al. (2025) used a handheld spectroradiometer, this study used airborne imaging spectroscopy data (APEX) together with in-situ measurements, resulting in larger pixels (2 x 2 m) with potentially mixed pixels effects. Wijesingha et al. (2020) estimated the fibre content (ADF) in different grassland types in Germany and reported an $R^2 = 0.39$ (median) by using PLSR. Even though they used a multi-point spectrometer on a drone to measure the spectra, their model performance value is in the same range as the one in this study ($R^2 = 0.40$). The obtained model performance value for lignin (ADL; $R^2 = 0.42$) is comparable to the range reported in other studies analysing lignin on grasslands, although lignin estimation with remote sensing techniques is still challenging. Thulin et al. (2012) showed that the model performance for lignin in grassland derived from a field spectrometer varied depending on spectral preprocessing and transformations used, with reported adjusted R^2 values from practically zero to around 0.41.

Model performance is also affected by choices made during the modelling procedure. In RSFs, the choice of absence or “pseudo-absence” data is known to affect model performance. When the numbers are unbalanced, there are biases in where the data are selected from and whether they represent “true” absence. To build the RSF and to account for variations between the individuals, the information about the individual had to be available. Therefore, neither the background points nor completely random

points were sampled, however for each individual, a buffer radius was constructed within the optimal area (grassland mask) and randomly sampled from there. If the buffer size is either too broad or too narrow, the model performance is reduced, highlighting the choice of an intermediate buffer size (VanDerWal et al., 2009).

6.4 Red deer feeding habitat selection in the SNP

The best model explaining red deer feeding habitat selection in the SNP included two forage quality proxies, namely nitrogen and fibres. Compared to other studies, these insights are new, as often biomass and nitrogen were used to characterise red deer feeding habitats (Rempfler et al., 2024; Schweiger et al., 2015b). Consistent with these two studies, biomass had a stronger predictive effect on red deer feeding compared to nitrogen. However, acid detergent fibre (ADF) had an even greater effect and was strongly avoided (negative sign). ADF relates to plant cell wall thickness and composition, which strongly influence the digestibility of nutrients (Spalinger et al., 1986). Therefore, fibre fractions serve as an indicator for low forage quality and digestibility (Van Soest, 1994) suggesting that areas with high ADF content will likely be less preferred by red deer. This is supported by Zweifel-Schielly et al. (2012) who analysed the diet of migrating red deer throughout the different seasons of the alpine landscape and showed that red deer selected plant groups with low ADF content, especially during the growing season.

Lignin (ADL), the part that is hardest to digest (Holtzapple, 2003b; Katoch, 2023), was not good in explaining red deer presence. The reason might be, that lignin is already part of ADF (correlation of 0.6; see Figure 10), already capturing the effect of digestibility.

The best performing model (M7d) had random slopes for ADF, indicating that red deer individuals responded differently to ADF content. This finding is supported by Čupić et al. (2021) who analysed faecal samples of deer in a controlled environmental setup. According to these authors, reproduction, age, body weight and season influenced the amount of nitrogen and ADF in the diet. While reproduction only slightly influenced the diet composition with approximately 4 % variability, season showed a strong influence (17 % on average), as well as age and body weight (18 %).

All 2-way interactions were significant. At high biomass values, the negative effect of ADF was reduced, suggesting that higher biomass values are more important than fibre content and compensating the negative effect of it. At higher biomass values, higher nitrogen values were preferred and again, at higher nitrogen values, the negative effect of ADF was reduced, suggesting that nitrogen-rich vegetation slightly compensates for higher ADF values. The interaction between biomass and food quality is shown by Langvatn and Hanley (1993). It was shown that the intake of digestible protein (estimated via the nitrogen balance) and digestible dry matter increased with increasing biomass for young grasses of good quality. However, for older plants, the biomass value was high, while the digestible protein and digestible dry matter were low. As biomass more strongly influenced digestible dry matter compared to digestible protein (Langvatn and Hanley, 1993), this suggests that high biomass values can partially compensate for high ADF values, but not for nitrogen values. Further, Zweifel-Schielly et al. (2012) were able to relate high protein values in plant groups with low fibre contents in summer. This supports the hypothesis that nitrogen-rich vegetation can slightly compensate for higher ADF values.

Topography explained some variance in red deer presence. Red deer preferred elevation levels of 2280.77 ± 175.89 m during summer months. Compared to their winter areas in the Engadin and Val Müstair (Blankenhorn et al., 1978), these elevation values are higher. This can be explained by a higher abundance of forage quality at higher elevations as shown by Mysterud et al. (2017), where migrating red deer had access to higher forage quality during summer as they moved to higher elevations compared to the resident red deer. Besides the better forage quality at higher elevations, also the temperature decreases with increasing elevation (6.5 Celsius per 1 km; Daidzic, 2019). Therefore, higher elevations

provide cooler temperatures, likely because it enables better body thermal regulation (Widén et al., 2025).

Further, red deer were found in flatter terrain and slopes facing south and east. This aligns with the findings of other studies conducted in the SNP, where red deer were mainly found in flatter areas (Schweiger et al., 2015b) especially hinds, likely, because these areas confer safe grounds for the young (Rempfler et al., 2024). Additionally, Sigrist et al. (2022) found red deer in less steep areas and migrating red deer preferred slopes with more solar radiation. These areas provide better forage availability as south facing slopes get more radiation, are therefore snow free faster and have an earlier start of vegetation growth compared to slopes facing north, as shown by Hebblewhite et al. (2008).

6.4.1 Explaining sex-specific feeding habitat differences

Sex-specific differences in feeding habitat selection were found between hinds and stags refuting H4. While female red deer feeding habitat selection could be best explained by topographic variables, biomass, nitrogen and ADF, the best explaining model for stags included topographic variables, biomass, phosphorus and ADF.

Whereas Rempfler et al. (2024) only found slight differences in the habitat selection of male and female red deer in the SNP, Garcia et al. (2023) found differences in the diet of Iberian male and female red deer in Portugal. Especially during spring and autumn, differences in spring were associated with reproduction, i.e. birth and lactation for hinds vs. start of growth of antlers for stags. Rempfler et al. (2024) conducted their study during summer (June – August), where calves had already been born and the differences within the diet might be smaller, explaining why only weak differences were found.

The found differences in this thesis might arise because within one study, a more comprehensive set of quality proxies were included, compared to Rempfler et al. (2024) and Schweiger et al. (2015b) where only biomass and nitrogen were included in the models, or Schütz et al. (2006), which included only phosphorus in models for the SNP. Nitrogen, measured as crude protein, was shown to be positively correlated with the body weight of female red deer (Albon and Langvatn, 1992). Besides the age of hinds (highest probability of pregnancy found at four years) the body condition is essential for the survival of their offsprings (Borowik et al., 2016; Clutton-Brock et al., 1982). Hinds with access to high quality forage are likely to have a better body condition, which in turn also influences the growth and survival of their young (Borowik et al., 2016). This may explain why nutrient-rich forage, especially nitrogen, was an important factor explaining female red deer habitat selection. However, the main effect of nitrogen was not significant, but in the 2-way interaction it was, suggesting that nitrogen is still important in female red deer habitat selection.

Stags need nutrients to build up their antlers. Antlers are the fastest growing bone among vertebrates starting to grow in spring and then the speed increases towards the end of the summer (Goss, 1983). This was only partially supported by Gomez et al. (2013), who showed that antler growth of Iberian red deer lay between day 28 and 156 with the highest need of minerals around day 100 due to maximal mineralisation. However, the antler growth depends on the nutrients in the forage and is thus related to the body weight and size (Clutton-Brock et al., 1982; Landete-Castillejos et al., 2007). Smolko et al. (2022) were able to show that $CaCO_3$, phosphorus and nitrogen in the soil resulted in larger antlers, highlighting the need of nutrients during antler growth. However, already at very young stages, the forage intake can influence the growth of the antlers. Landete-Castillejos et al. (2007) showed that weight gains during lactation were important for mineral composition of antlers. For phosphorus, 69 % of the variability could be explained by lactation. As phosphorus is essential for all vertebrates for their bones and the mineralisation of the skeleton (Cotti et al., 2020), this might explain why phosphorus was important to include in the model describing male habitat selection. However, as stag data was only from five males, this result might not be very robust and needs further investigation, i.e. whether phosphorus really explains red deer presence better than nitrogen. Grasman and Hellgren (1993) analysed the effect of phosphorus on white-tailed deer and found that antler growth was not limited by

phosphorus. Furthermore, nitrogen and phosphorus tend to be highly correlated in vegetation (correlation of 0.8; see Figure 10), making a separation of their individual effects difficult in habitat selection models.

Hinds tend to occur more often within the SNP compared to stags, who were found more north of the SNP and close to the border to Austria. This aligns with the findings of Rempfler et al. (2024) who found hinds in flatter areas and closer to the forest and more within the SNP compared to stags, as they are more sensitive to human disturbances. Therefore, only five stags were available for the analysis, compared to 23 females. Although individual was included in the model as random effect to account for the different sampling sizes, the overall result is likely dominated by females. This explains, why the overall model is very similar to the model only containing hinds. Even though the GPS positions were relatively similar (for males and females 11772 and 15024 GPS positions, respectively), the difference between the individuals (5 vs. 23) does influence the model.

6.5 Limitations

The thesis comes with a set of limitations, especially regarding model training, model predictions, and the predictors in the RSF. Two types of models were used: PLSR for modelling plant traits and RSF (using as input the predictions from PLSR models). The PLSR linked in situ-measurements of plant traits with airborne imaging spectroscopy reflectance information to train the model, and to do predictions of biomass and other forage quality proxies for the whole SNP. However, the predicted solution is unlikely to be unique, as multiple combinations between in-situ measurements and airborne measurements may occur. The reason is that different chemical compounds (e.g. water and lignin) absorb in the same wavelength region, making it difficult to assign a wavelength to a specific chemical compound (Curran, 1989). This means, several combinations of reflectance data can result in the same biomass prediction, even though the biomass value should be different due to differences in the vegetation composition or structure. Further, shade and the viewing angle of the airborne sensor can result in different reflectance measurements for the same material, influencing the predictions (Feilhauer et al., 2010). Therefore, a brightness correction for the PLSR model was applied following Feilhauer et al. (2010), however, noise introduced by the sensor could not be accounted for with the brightness normalisation. This could have led to uncertainties in the predictive values that were used in the analysis of habitat selection.

The data that were used to train the PLSR model consisted of in-situ measurements and spectral information collected from 2010 and 2013 for the variables biomass, nitrogen, ADL and ADF. A variable number of plots were sampled in the different years: 51 plots were collected in 2010, 82 plots in 2013, summing up to 133 plots. Whereas the 51 plots from 2010 were spread over the whole SNP, capturing different elevation levels, vegetation types and properties and areas (Val Trupchun and Il Fuorn; Schweiger et al., 2015a), the 82 plots from 2013 were all sampled within Val Trupchun. This might put greater weight on vegetation conditions found within Val Trupchun, explaining why the model for the whole SNP might had a lower model performance compared to the model by Schweiger et al. (2015b) within Val Trupchun. Further, phosphorus was only measured in 2010, but not in 2013. Therefore, only 51 plots provided data for training the model. Even though the sample size is smaller compared to the training data used for the other predictions, the plots captured different environmental conditions within the SNP.

Further, the bedrock in the SNP differs between a limestone and calcareous bedrock in Val Trupchun and a dolomite bedrock around Il Fuorn (Schweiger et al., 2015a). Even though it was shown by Schweiger et al. (2015a) that the model performance for predicting aboveground biomass differed between the two sites ($R^2 = 0.60$ for Val Trupchun and $R^2 = 0.30$ Il Fuorn), only one model for the SNP was used. The model performance for biomass for the whole SNP was 0.43, similar to the performance achieved by Schweiger et al. (2015a) for their regional model ($R^2 = 0.44$).

Additionally, even though vegetation can have year-to-year variation due to external factors like temperature, precipitation and how long the snow-free period was (Choler, 2015), this variation was not explicitly accounted for in the RSF model for red deer habitat selection. Instead, the GDD, which accounts for the thermal conditions (Quaglia et al., 2020), was instead used as phenological standardisation to ensure comparability across the years. However, as temperatures slightly increased between 2010 and 2019, GDD 330.95 was reached earlier in 2019 compared to the other years. Therefore, its possible that the three defined GDD periods may not have captured the full summer. Further, Trepel et al. (2024) analysed 297 studies in their meta-analysis to see the effect of large herbivores on the ecosystem and its function. These effects covered nutrient concentrations in the soil (e.g. phosphorus), the soil compaction, responses on the vegetation (i.e. on plant nitrogen), heterogeneity of the vegetation, and responses with other animals. All these effects were not accounted for in this analysis.

The residuals of the best identified habitat models (overall, for hinds and for stags) were tested for spatial autocorrelation using Moran's I. The GPS data were also previously tested for temporal autocorrelation for the home range analysis and the feeding locations. Further, as only one "fix" timespan (GDD 239.95 ± 10 days) was analysed in the RSF, the temporal component was not considered in the RSF. As the GPS had a spatial accuracy of 11.3 ± 4.7 m (Schweiger et al., 2015b), variable values used for the RSF were extracted within a buffer of 10 m (mean value was assigned).

The pseudo-absence points were generated within a buffer around the presence location (measured by the GPS). Within the buffer, 30 random points were generated with the constraint, that these points lie within the grassland mask. This ensured that absence points were only generated within open areas that are used by red deer for feeding. Nevertheless, it could have been possible, that mountain ridges are within the buffer, but on the mountain slopes, it could have grassland and these areas could have been used for the absence points. However, red deer can't "jump" over mountains ridges and might not be able to feed at these places. This can make some of the pseudo-absence points unrealistic.

Even though the home ranges and the feeding locations were quite similar between the three GDD stages with high overlaps (mean home range overlap between the three GDD periods was 71.11 ± 16.96 % and for the feeding locations 92 % (aggregated for all individuals)), the vegetation properties can still change. Rapiya et al. (2025) analysed carbon, nitrogen, ADF and the ratio C:N:ADF in natural rangelands in South Africa with Sentinel data and found seasonal changes in the concentration and the ratio of these constituents. In late summer, the C:N:ADF ratio was highest, with high concentrations of C and N and low ADF concentrations. These underlying changes within the vegetation were not considered and only one GDD period was analysed further to define red deer feeding habitat selection. Therefore, the question whether red deer shift their feeding strategy through the summer cannot be fully answered in this thesis.

Despite the performance of the prediction model laying within the range of that for other models within the SNP, the biomass predictions resulted in a high number of zero value predictions. Further, the AOA mask seemed to be very conservative for biomass (i.e. reduced the predictions space), compared to the other predictions. Whereas all predictions of forage quality (N, P, ADL and ADF) showed a normal distribution of predicted values, the distribution of the predicted biomass values was left skewed with a lot of values at zero. As all negative predictions were set to zero, it could either mean, a lot of negative values had been predicted, that were then set to zero, or a lot of zero values were directly predicted. Zero is still a value, however, it could have influenced the result of red deer habitat selection. It is, however, unlikely that there is no biomass for these regions, likely leading to an underestimate of the effect of biomass.

The position of the red deer relied on the GPS positions recorded. Each GPS collar recorded for approximately two years, sometimes even shorter, before the sensor ran out of battery, was dropped off or the animal died. Therefore, over the nine analysed years, different individuals were tracked and included in the analysis. The question is, how representative is one individual for the whole red deer

population? As shown with the different slopes in M7d, red deer do respond quite differently to nutrients. Although individual differences were accounted for in the model with the random effect, nevertheless, inter-individual differences in habitat selection could still introduces bias.

Besides that, the behavioural assignments relied on a discriminant analysis (Bar-Gera et al., 2025), a method that enables to classify the movements into groups of behaviours. Originally five different behaviours (feeding, lying, standing, walking, running) could be identified with their model (Bar-Gera et al., 2025). However, walking, standing and running occurred on average for shorter times (lying: 34.77 min, compared to standing: 1.49 min, walking: 1.16 min and running: 2.39 min) compared to the 5-minute interval. Therefore, mixed intervals were used, where one behaviour was made up at least half of the time of the interval. Further, standing was not further distinguished from the other categories and was not treated as separate behaviour. However, mixed intervals lead to misclassification as one behaviour does not fill the full interval. The input data for training their models were observations together with GPS data, however, the accuracy of GPS data within a forest is lower compared to the grassland (Piedallu and Gégout, 2005). This might also result in some misclassifications.

7 Conclusion

The aim of this thesis was to determine which of the nine theoretical feeding strategies red deer follow during the summer. The best scenario describing their feeding strategy included both high forage quantity (biomass) and high forage quality (i.e. high nitrogen or phosphorus content and low fibre content), corresponding to the (++) strategy. As stated in hypothesis H1, red deer were predominantly found in the forest and grassland areas with the dominant behaviours lying and feeding. Hypothesis H2, was not supported, as no spatial differences in the home ranges or feeding locations across the three phenological stages were found. Similarly, hypothesis H4, was not supported, as sex-specific differences in red deer feeding habitat selection were identified. Red deer habitat selection was best explained by topography, biomass and forage quality proxies, supporting hypothesis H3. Specially, red deer were found in areas with high biomass and high nitrogen or phosphorus content, but low lignin and fibre content. Comparing forage quality and quantity, biomass (quantity) had a stronger predictive effect on red deer feeding compared to nitrogen or phosphorus (quality). However, acid detergent fibre (ADF) had an even greater effect compared to biomass for hinds and the general model. Males showed a weaker response to the fibre content compared to females, but at the same time a stronger response to biomass. Elevation had the overall strongest effect on male red deer presence, the fibre content had the strongest effect on females.

This study used a set of combination of forage quality proxies (N, P, ADL and ADF) together with forage quantity and topography to explain red deer feeding habitat selection in the SNP. Only actual feeding locations were analysed, by applying successfully the behavioural classification model developed by Bar-Gera et al. (2025). Further investigation is needed to assess a potential underestimation of the biomass effect due to a high number of zero predictions, and to determine whether phosphorus is truly a better explanatory variable for male red deer feeding habitat selection or whether this finding is an artefact of the low number of GPS positions and individuals available for this analysis (n = 5). As red deer reused their summer home ranges and feeding locations throughout the summer, analysing only one time period was justified. However, potential short-term shifts during the summer in the feeding strategy cannot be fully detected. Nevertheless, this thesis provides new insights into red deer feeding habitat selection in the SNP by filtering GPS locations for feeding behaviour, using a multi-temporal imaging spectroscopy approach and using a set of forage quality proxies. In a next step, the model identified to explain red deer feeding habitat the best could be used and applied to generate a probability map, showing where red deer are most likely found within the SNP and if these places match with the actual recorded GPS locations.

8 References

Albon, S.D., Langvatn, R., 1992. Plant Phenology and the Benefits of Migration in a Temperate Ungulate. Oikos 65, 502–513. https://doi.org/10.2307/3545568

Anderwald, P., Herfindal, I., Haller, R.M., Risch, A.C., Schütz, M., Schweiger, A.K., Filli, F., 2015. Influence of migratory ungulate management on competitive interactions with resident species in a protected area. Ecosphere 6, 1–18. https://doi.org/10.1890/ES15-00365.1

Araújo, M.B., Anderson, R.P., Márcia Barbosa, A., Beale, C.M., Dormann, C.F., Early, R., Garcia, R.A., Guisan, A., Maiorano, L., Naimi, B., O'Hara, R.B., Zimmermann, N.E., Rahbek, C., 2019. Standards for distribution models in biodiversity assessments. Science Advances 5, eaat4858. https://doi.org/10.1126/sciadv.aat4858

Araújo, M.B., Guisan, A., 2006. Five (or so) challenges for species distribution modelling. Journal of Biogeography 33, 1677–1688. https://doi.org/10.1111/j.1365-2699.2006.01584.x

Arman, P., Kay, R.N.B., Goodall, E.D., Sharman, G. a. M., 1974. THE COMPOSITION AND YIELD OF MILK FROM CAPTIVE RED DEER (CERVUS ELAPHUS L.). Reproduction 37, 67–84. https://doi.org/10.1530/jrf.0.0370067

Arnold, W., 2020. Review: Seasonal differences in the physiology of wild northern ruminants. animal 14, 124–132. https://doi.org/10.1017/S1751731119003240

Arnold, W., Beiglböck, C., Burmester, M., Guschlbauer, M., Lengauer, A., Schröder, B., Wilkens, M., Breves, G., 2015. Contrary seasonal changes of rates of nutrient uptake, organ mass, and voluntary food intake in red deer (Cervus elaphus). Am J Physiol Regul Integr Comp Physiol 309, R277–R285. https://doi.org/10.1152/ajpregu.00084.2015

Avgar, T., Potts, J.R., Lewis, M.A., Boyce, M.S., 2016. Integrated step selection analysis: bridging the gap between resource selection and animal movement. Methods in Ecology and Evolution 7, 619–630. https://doi.org/10.1111/2041-210X.12528

Barbet-Massin, M., Jiguet, F., Albert, C.H., Thuiller, W., 2012. Selecting pseudo-absences for species distribution models: how, where and how many? Methods in Ecology and Evolution 3, 327–338. https://doi.org/10.1111/j.2041-210X.2011.00172.x

Bar-Gera, B., Anderwald, P., Evans, A.L., Rempfler, T., Signer, C., 2025. Comparing the accuracy of machine learning methods for classifying wild red deer behavior based on accelerometer data. Anim Biotelemetry 13, 9. https://doi.org/10.1186/s40317-025-00401-9

Bevanda, M., Fronhofer, E.A., Heurich, M., Müller, J., Reineking, B., 2015. Landscape configuration is a major determinant of home range size variation. Ecosphere 6, 1–12. https://doi.org/10.1890/ES15-00154.1

Blankenhorn, H.-J., Buchli, C., Voser, P., 1978. Wanderungen und jahreszeitliches Verteilungsmuster der Rothirschpopulationen (Cervus elaphus L.) im Engadin, Münstertal und Schweizerischen Nationalpark. Revue suisse de zoologie 85, 779–789. https://doi.org/10.5962/bhl.part.82268

Bolker, B.M., Brooks, M.E., Clark, C.J., Geange, S.W., Poulsen, J.R., Stevens, M.H.H., White, J.-S.S., 2009. Generalized linear mixed models: a practical guide for ecology and evolution. Trends in Ecology & Evolution 24, 127–135. https://doi.org/10.1016/j.tree.2008.10.008

Bonenfant, C., Loe, L.E., Mysterud, A., Langvatn, R., Stenseth, N.Chr., Gaillard, J.-M., Klein, F., 2004. Multiple causes of sexual segregation in European red deer: enlightenments from varying breeding phenology at high and low latitude. Proc. R. Soc. Lond. B 271, 883–892. https://doi.org/10.1098/rspb.2003.2661

Borowik, T., Wawrzyniak, P., Jędrzejewska, B., 2016. Red deer (Cervus elaphus) fertility and survival of young in a low-density population subject to predation and hunting. J Mammal 97, 1671–1681. https://doi.org/10.1093/jmammal/gyw133

Breiman, L., 2001. Random Forests. Machine Learning 45, 5–32. https://doi.org/10.1023/A:1010933404324

Brooks, M., E., Kristensen, K., Benthem, K., J. ,van, Magnusson, A., Berg, C., W., Nielsen, A., Skaug, H., J., Mächler, M., Bolker, B., M., 2017. glmmTMB Balances Speed and Flexibility Among Packages for Zero-inflated Generalized Linear Mixed Modeling. The R Journal 9, 378–400. https://doi.org/10.32614/RJ-2017-066

Burnett, A.C., Anderson, J., Davidson, K.J., Ely, K.S., Lamour, J., Li, Q., Morrison, B.D., Yang, D., Rogers, A., Serbin, S.P., 2021. A best-practice guide to predicting plant traits from leaf-level

hyperspectral data using partial least squares regression. Journal of Experimental Botany 72, 6175–6189. https://doi.org/10.1093/jxb/erab295
Choler, P., 2015. Growth response of temperate mountain grasslands to inter-annual variations in snow cover duration. Biogeosciences 12, 3885–3897. https://doi.org/10.5194/bg-12-3885-2015
Clutton-Brock, T.H., Guinness, F.E., Albon, S.D., 1982. Red Deer: Behavior and Ecology of Two Sexes, Wildlife Behavior and Ecology series. University of Chicago Press, Chicago.
Clutton-Brock, T.H., Iason, G.R., Guinness, F.E., 1987. Sexual segregation and density-related changes in habitat use in male and female Red deer (Cerrus elaphus). Journal of Zoology 211, 275–289. https://doi.org/10.1111/j.1469-7998.1987.tb01534.x
Cotti, S., Huysseune, A., Koppe, W., Rücklin, M., Marone, F., Wölfel, E.M., Fiedler, I.A.K., Busse, B., Forlino, A., Witten, P.E., 2020. More Bone with Less Minerals? The Effects of Dietary Phosphorus on the Post-Cranial Skeleton in Zebrafish. Int J Mol Sci 21, 5429. https://doi.org/10.3390/ijms21155429
Čupić, S., García, A.J., Holá, M., Ceacero, F., 2021. Evaluation of factors inducing variability of faecal nutrients in captive red deer under variable demands. Sci Rep 11, 2394. https://doi.org/10.1038/s41598-021-81908-y
Curran, P.J., 1989. Remote sensing of foliar chemistry. Remote Sensing of Environment 30, 271–278. https://doi.org/10.1016/0034-4257(89)90069-2
Daidzic, N.E., 2019. On Atmospheric Lapse Rates. IJAAA 6. https://doi.org/10.15394/ijaaa.2019.1374
Damm, A., Guanter, L., Verhoef, W., Schläpfer, D., Garbari, S., Schaepman, M.E., 2015. Impact of varying irradiance on vegetation indices and chlorophyll fluorescence derived from spectroscopy data. Remote Sensing of Environment 156, 202–215. https://doi.org/10.1016/j.rse.2014.09.031
De Groeve, J., Van de Weghe, N., Ranc, N., Morellet, N., Bonnot, N.C., Gehr, B., Heurich, M., Hewison, A.J.M., Kröschel, M., Linnell, J.D.C., Mysterud, A., Sandfort, R., Cagnacci, F., 2023. Back and forth: day–night alternation between cover types reveals complementary use of habitats in a large herbivore. Landsc Ecol 38, 1033–1049. https://doi.org/10.1007/s10980-023-01594-1
Donini, V., Pedrotti, L., Ferretti, F., Iacona, E., Lorenzetti, L., Nelli, L., Cozzi, F., Corlatti, L., 2025. Can camera traps predict habitat-species associations? A comparison with GPS-based habitat selection in red deer. Landsc Ecol 40, 38. https://doi.org/10.1007/s10980-025-02051-x
Dormann, C.F., Elith, J., Bacher, S., Buchmann, C., Carl, G., Carré, G., Marquéz, J.R.G., Gruber, B., Lafourcade, B., Leitão, P.J., Münkemüller, T., McClean, C., Osborne, P.E., Reineking, B., Schröder, B., Skidmore, A.K., Zurell, D., Lautenbach, S., 2013. Collinearity: a review of methods to deal with it and a simulation study evaluating their performance. Ecography 36, 27–46. https://doi.org/10.1111/j.1600-0587.2012.07348.x
Eggers, J., Seidl, R., Maroschek, M., Reiner, R., 2026. Where forage meets safety: The role of forest disturbances in red deer adaptation to human pressure. Forest Ecology and Management 602, 123383. https://doi.org/10.1016/j.foreco.2025.123383
Elith, J., Graham, C.H., Anderson, R.P., Dudík, M., Ferrier, S., Guisan, A., Hijmans, R.J., Huettmann, F., Leathwick, J.R., Lehmann, A., Li, J., Lohmann, L.G., Loiselle, B.A., Manion, G., Moritz, C., Nakamura, M., Nakazawa, Y., Overton, J.McC., Peterson, A.T., Phillips, S.J., Richardson, K., Scachetti-Pereira, R., Schapire, R.E., Soberón, J., Williams, S., Wisz, M.S., Zimmermann, N.E., Araujo, M., 2006. Novel Methods Improve Prediction of Species' Distributions from Occurrence Data. Ecography 29, 129–151. https://doi.org/10.1111/j.2006.0906-7590.04596.x
Elith, J., Leathwick, J.R., 2009. Species Distribution Models: Ecological Explanation and Prediction Across Space and Time. Annual Review of Ecology, Evolution, and Systematics 40, 677–697. https://doi.org/10.1146/annurev.ecolsys.110308.120159
Elton, C.S., 1927. Animal Ecology. Sidgwick and Jackson., London.
Engler, R., Guisan, A., Rechsteiner, L., 2004. An improved approach for predicting the distribution of rare and endangered species from occurrence and pseudo-absence data. Journal of Applied Ecology 41, 263–274. https://doi.org/10.1111/j.0021-8901.2004.00881.x
Espmark, Y., Langvatn, R., 1979. Lying down as a means of reducing fly harassment in red deer (Cervus elaphus). Behav Ecol Sociobiol 5, 51–54. https://doi.org/10.1007/BF00302694
Feilhauer, H., Asner, G.P., Martin, R.E., Schmidtlein, S., 2010. Brightness-normalized Partial Least Squares Regression for hyperspectral data. Journal of Quantitative Spectroscopy and Radiative Transfer 111, 1947–1957. https://doi.org/10.1016/j.jqsrt.2010.03.007

Ferrier, S., Watson, G., Pearce, J., Drielsma, M., 2002. Extended statistical approaches to modelling spatial pattern in biodiversity in northeast New South Wales. I. Species-level modelling. Biodiversity and Conservation 11, 2275–2307. https://doi.org/10.1023/A:1021302930424
Fleming, C.H., Calabrese, J.M., 2025. ctmm: Continuous-Time Movement Modeling. https://doi.org/10.32614/CRAN.package.ctmm
Fleming, C.H., Fagan, W.F., Mueller, T., Olson, K.A., Leimgruber, P., Calabrese, J.M., 2015. Rigorous home range estimation with movement data: a new autocorrelated kernel density estimator. Ecology 96, 1182–1188. https://doi.org/10.1890/14-2010.1
Fryxell, J.M., 1991. Forage Quality and Aggregation by Large Herbivores. The American Naturalist 138, 478–498. https://doi.org/10.1086/285227
Gamon, J.A., Somers, B., Malenovský, Z., Middleton, E.M., Rascher, U., Schaepman, M.E., 2019. Assessing Vegetation Function with Imaging Spectroscopy. Surv Geophys 40, 489–513. https://doi.org/10.1007/s10712-019-09511-5
Garcia, F., Alves da Silva, A., Freitas, H., Sousa, J.P., Alves, J., 2025. The essential, but complex, role of red deer as an ecosystem service provider: a comprehensive review across Europe. Eur J Wildl Res 71, 46. https://doi.org/10.1007/s10344-025-01922-7
Garcia, F., Alves da Silva, A., Ruckstuhl, K., Neuhaus, P., Coelho, C., Wang, M., Sousa, J.P., Alves, J., 2023. Differences in the Diets of Female and Male Red Deer: The Meaning for Sexual Segregation. Biology (Basel) 12, 540. https://doi.org/10.3390/biology12040540
Gelman, A., 2008. Scaling regression inputs by dividing by two standard deviations. Statistics in Medicine 27, 2865–2873. https://doi.org/10.1002/sim.3107
Getz, W.M., Wilmers, C.C., 2004. A local nearest-neighbor convex-hull construction of home ranges and utilization distributions. Ecography 27, 489–505. https://doi.org/10.1111/j.0906-7590.2004.03835.x
Gillich, B., Michler, F.-U., Stolter, C., Rieger, S., 2021. Differences in social-space–time behaviour of two red deer herds (Cervus elaphus). acta ethol 24, 185–195. https://doi.org/10.1007/s10211-021-00375-w
Gillies, C.S., Hebblewhite, M., Nielsen, S.E., Krawchuk, M.A., Aldridge, C.L., Frair, J.L., Saher, D.J., Stevens, C.E., Jerde, C.L., 2006. Application of random effects to the study of resource selection by animals. Journal of Animal Ecology 75, 887–898. https://doi.org/10.1111/j.1365-2656.2006.01106.x
Gimond, M., 2019. A basic introduction to Moran's I analysis in R [WWW Document]. URL https://mgimond.github.io/simple_moransI_example/ (accessed 4.3.26).
Godsoe, W., Harmon, L.J., 2012. How do species interactions affect species distribution models? Ecography 35, 811–820. https://doi.org/10.1111/j.1600-0587.2011.07103.x
Godvik, I.M.R., Loe, L.E., Vik, J.O., Veiberg, V., Langvatn, R., Mysterud, A., 2009. Temporal scales, trade-offs, and functional responses in red deer habitat selection. Ecology 90, 699–710. https://doi.org/10.1890/08-0576.1
Gomez, S., Garcia, A.J., Luna, S., Kierdorf, U., Kierdorf, H., Gallego, L., Landete-Castillejos, T., 2013. Labeling studies on cortical bone formation in the antlers of red deer (*Cervus elaphus*). Bone 52, 506–515. https://doi.org/10.1016/j.bone.2012.09.015
Goss, R.J., 1983. 7 - Developmental Anatomy of Antlers, in: Goss, R.J. (Ed.), Deer Antlers. Academic Press, pp. 133–171. https://doi.org/10.1016/B978-0-12-293080-5.50011-7
Grasman, B.T., Hellgren, E.C., 1993. Phosophorus Nutrition in White-Tailed Deer: Nutrient Balance, Physiological Responses, and Antler Growth. Ecology 74, 2279–2296. https://doi.org/10.2307/1939581
Grinnell, J., 1917. The Niche-Relationships of the California Thrasher. The Auk 34, 427–433. https://doi.org/10.2307/4072271
Guisan, A., Zimmermann, N.E., 2000. Predictive habitat distribution models in ecology. Ecological Modelling 135, 147–186. https://doi.org/10.1016/S0304-3800(00)00354-9
Habibi, L.N., Watanabe, T., Matsui, T., Tanaka, T.S.T., 2021. Machine Learning Techniques to Predict Soybean Plant Density Using UAV and Satellite-Based Remote Sensing. Remote Sensing 13, 2548. https://doi.org/10.3390/rs13132548
Haskell, J.P., Ritchie, M.E., Olff, H., 2002. Fractal geometry predicts varying body size scaling relationships for mammal and bird home ranges. Nature 418, 527–530. https://doi.org/10.1038/nature00840

He, F., Hu, X.-S., 2005. Hubbell's fundamental biodiversity parameter and the Simpson diversity index. Ecology Letters 8, 386–390. https://doi.org/10.1111/j.1461-0248.2005.00729.x
Hebblewhite, M., Merrill, E., McDermid, G., 2008. A Multi-Scale Test of the Forage Maturation Hypothesis in a Partially Migratory Ungulate Population. Ecological Monographs 78, 141–166. https://doi.org/10.1890/06-1708.1
Hijmans, R.J., 2025. terra: Spatial Data Analysis. https://doi.org/10.32614/CRAN.package.terra
Hijmans, R.J., 2024. Spatial Data Science with R and "terra" [WWW Document]. rspatial. URL https://rspatial.org/index.html (accessed 2.11.26).
Hijmans, R.J., Elith, J., 2024. Species distribution modeling [WWW Document]. rspatial. URL https://rspatial.org/sdm/index.html (accessed 2.11.26).
Hofmann, R.R., 1989. Evolutionary steps of ecophysiological adaptation and diversification of ruminants: a comparative view of their digestive system. Oecologia 78, 443–457. https://doi.org/10.1007/BF00378733
Holtzapple, M.T., 2003a. HEMICELLULOSES, in: Encyclopedia of Food Sciences and Nutrition. Elsevier, pp. 3060–3071. https://doi.org/10.1016/B0-12-227055-X/00589-7
Holtzapple, M.T., 2003b. LIGNIN, in: Encyclopedia of Food Sciences and Nutrition. Elsevier, pp. 3535–3542. https://doi.org/10.1016/B0-12-227055-X/00699-4
Homolová, L., Malenovský, Z., Clevers, J.G.P.W., García-Santos, G., Schaepman, M.E., 2013. Review of optical-based remote sensing for plant trait mapping. Ecological Complexity 15, 1–16. https://doi.org/10.1016/j.ecocom.2013.06.003
Huete, A.R., 2004. Remote Sensing for environmental monitoring, in: Artiola, J.F., Pepper, I.L., Brusseau, M.L. (Eds.), Environmental Monitoring and Characterization. Elsevier Academic Press, UK, USA, pp. 183–206. https://doi.org/10.1016/B978-012064477-3/50013-8
Hutchinson, G.E., 1957. Concluding remarks, in: Old Spring Harbor Symposia on Quantitative Biology. pp. 415–427.
Jarnemo, A., Nilsson, L., Wikenros, C., 2023. Home range sizes of red deer in relation to habitat composition: a review and implications for management in Sweden. Eur J Wildl Res 69, 92. https://doi.org/10.1007/s10344-023-01719-6
Jerina, K., 2012. Roads and supplemental feeding affect home-range size of Slovenian red deer more than natural factors. J Mammal 93, 1139–1148. https://doi.org/10.1644/11-MAMM-A-136.1
Kakuta, N., Ozawa, S., 2022. Near-infrared imaging of water vapour in air. Meas. Sci. Technol. 33, 075403. https://doi.org/10.1088/1361-6501/ac6082
Kamler, J.F., Jędrzejewski, W., Jędrzejewska, B., 2008. Home Ranges of Red Deer in a European Old-Growth Forest. The American Midland Naturalist 159, 75–82. https://doi.org/10.1674/0003-0031(2008)159%255B75:HRORDI%255D2.0.CO;2
Katoch, R., 2023. Forage Quality Components, in: Katoch, R. (Ed.), Techniques in Forage Quality Analysis. Springer, Singapore, pp. 17–32. https://doi.org/10.1007/978-981-19-6020-8_4
Kelt, D.A., Van Vuren, D.H., 2001. The Ecology and Macroecology of Mammalian Home Range Area. The American Naturalist 157, 637–645. https://doi.org/10.1086/320621
Kernohan, B.J., Gitzen, R.A., Millspaugh, J.J., 2001. Analysis of Animal Space Use and Movements, in: Radio Tracking and Animal Populations. Academic Press, pp. 125–166. https://doi.org/10.1016/B978-012497781-5/50006-2
Key, T., Warner, T.A., McGraw, J.B., Fajvan, M.A., 2001. A Comparison of Multispectral and Multitemporal Information in High Spatial Resolution Imagery for Classification of Individual Tree Species in a Temperate Hardwood Forest. Remote Sensing of Environment 75, 100–112. https://doi.org/10.1016/S0034-4257(00)00159-0
King, D., Bourennane, H., Isambert, M., Macaire, J.J., 1999. Relationship of the presence of a non-calcareous clay–loam horizon to DEM attributes in a gently sloping area. Geoderma 89, 95–111. https://doi.org/10.1016/S0016-7061(98)00124-4
Kropil, R., Smolko, P., Garaj, P., 2015. Home range and migration patterns of male red deer Cervus elaphus in Western Carpathians. Eur J Wildl Res 61, 63–72. https://doi.org/10.1007/s10344-014-0874-4
Kuhlmann, G., Hueni, A., Damm, A., Brunner, D., 2016. An Algorithm for In-Flight Spectral Calibration of Imaging Spectrometers. Remote Sensing 8, 1017. https://doi.org/10.3390/rs8121017

Landete-Castillejos, T., Garcia, A., Gallego, L., 2007. Body weight, early growth and antler size influence antler bone mineral composition of Iberian Red Deer (*Cervus elaphus hispanicus*). Bone 40, 230–235. https://doi.org/10.1016/j.bone.2006.07.009
Langvatn, R., Hanley, T.A., 1993. Feeding-patch choice by red deer in relation to foraging efficiency. Oecologia 95, 164–170. https://doi.org/10.1007/BF00323486
Liland, K.H., Mevik, B.-H., Wehrens, R., 2024. pls: Partial Least Squares and Principal Component Regression. https://doi.org/10.32614/CRAN.package.pls
Lindstedt, S.L., Miller, B.J., Buskirk, S.W., 1986. Home Range, Time, and Body Size in Mammals. Ecology 67, 413–418. https://doi.org/10.2307/1938584
Luccarini, S., Mauri, L., Ciuti, S., Lamberti, P., Apollonio, M., 2006. Red deer (*Cervus elaphus*) spatial use in the Italian Alps: home range patterns, seasonal migrations, and effects of snow and winter feeding. Ethology Ecology & Evolution 18, 127–145. https://doi.org/10.1080/08927014.2006.9522718
MacQueen, J.B., 1967. Some methods for classification and analysis of multivariate observations, in: Cam, L.M.L., Neyman, J. (Eds.), Proceedings of the Fifth Berkeley Symposium on Mathematical Statistics and Probability. University of California Press, Berkeley and Los Angeles, pp. 281–297.
Main, M.B., Weckerly, F.W., Bleich, V.C., 1996. Sexual Segregation in Ungulates: New Directions for Research. J Mammal 77, 449–461. https://doi.org/10.2307/1382821
Maire, L., Gege, P., Damm, A., Odermatt, D., 2025. Differentiating phytoplankton taxa in lakes using hyperspectral *in situ* reflectance and imaging microscopy. Science of The Total Environment 1003, 180718. https://doi.org/10.1016/j.scitotenv.2025.180718
Mattioli, S., Zachos, F.E., Rossi, L., Lister, A.M., Corlatti, L., 2022. Red Deer Cervus elaphus Linnaeus, 1758, in: Hackländer, K., Zachos, F.E. (Eds.), Handbook of the Mammals of Europe. Handbook of the Mammals of Europe. Springer, Cham, pp. 1–37. https://doi.org/10.1007/978-3-319-65038-8_19-1
McArthur, C., Banks, P.B., Boonstra, R., Forbey, J.S., 2014. The dilemma of foraging herbivores: dealing with food and fear. Oecologia 176, 677–689. https://doi.org/10.1007/s00442-014-3076-6
McCabe, J.D., Clare, J.D., Miller, T.A., Katzner, T.E., Cooper, J., Somershoe, S., Hanni, D., Kelly, C.A., Sargent, R., Soehren, E.C., Threadgill, C., Maddox, M., Stober, J., Martell, M., Salo, T., Berry, A., Lanzone, M.J., Braham, M.A., McClure, C.J.W., 2021. Resource selection functions based on hierarchical generalized additive models provide new insights into individual animal variation and species distributions. Ecography 44, 1756–1768. https://doi.org/10.1111/ecog.06058
McMaster, G.S., Wilhelm, W.W., 1997. Growing degree-days: one equation, two interpretations. Agricultural and Forest Meteorology 87, 291–300. https://doi.org/10.1016/S0168-1923(97)00027-0
Merkle, J.A., Monteith, K.L., Aikens, E.O., Hayes, M.M., Hersey, K.R., Middleton, A.D., Oates, B.A., Sawyer, H., Scurlock, B.M., Kauffman, M.J., 2016. Large herbivores surf waves of green-up during spring. Proc. R. Soc. B. 283, 20160456. https://doi.org/10.1098/rspb.2016.0456
MeteoSwiss, n.d. Climate stations - Homogeneous data series [WWW Document]. URL https://www.meteoswiss.admin.ch/ (accessed 12.6.25).
Meyer, H., 2025. Area of applicability of spatial prediction models [WWW Document]. R-universe. URL https://hannameyer.r-universe.dev/articles/CAST/cast04-AOA-tutorial.html (accessed 2.6.26).
Meyer, H., Milà, C., Ludwig, M., Linnenbrink, J., Schumacher, F., 2026. CAST: “caret” Applications for Spatial-Temporal Models. https://doi.org/10.32614/CRAN.package.CAST
Meyer, H., Pebesma, E., 2021. Predicting into unknown space? Estimating the area of applicability of spatial prediction models. Methods in Ecology and Evolution 12, 1620–1633. https://doi.org/10.1111/2041-210X.13650
Mitchell, B., McCowan, D., Nicholson, I.A., 1976. Annual cycles of body weight and condition in Scottish Red deer, Cervus elaphus. Journal of Zoology 180, 107–127. https://doi.org/10.1111/j.1469-7998.1976.tb04667.x
Mitchell, B., Staines, B.W., Welch, D., 1977. Ecology of Red Deer: A research review relevant to their management in Scotland. Institute of Terrestrial Ecology, Cambridge.
Mohr, C.O., 1947. Table of Equivalent Populations of North American Small Mammals. The American Midland Naturalist 37, 223–249. https://doi.org/10.2307/2421652

Muff, S., Signer, J., Fieberg, J., 2020. Accounting for individual-specific variation in habitat-selection studies: Efficient estimation of mixed-effects models using Bayesian or frequentist computation. Journal of Animal Ecology 89, 80–92. https://doi.org/10.1111/1365-2656.13087
Mysterud, A., Vike, B.K., Meisingset, E.L., Rivrud, I.M., 2017. The role of landscape characteristics for forage maturation and nutritional benefits of migration in red deer. Ecology and Evolution 7, 4448–4455. https://doi.org/10.1002/ece3.3006
Naegeli, K., Damm, A., Huss, M., Schaepman, M., Hoelzle, M., 2015. Imaging spectroscopy to assess the composition of ice surface materials and their impact on glacier mass balance. Remote Sensing of Environment 168, 388–402. https://doi.org/10.1016/j.rse.2015.07.006
Naegeli, K., Damm, A., Huss, M., Wulf, H., Schaepman, M., Hoelzle, M., 2017. Cross-Comparison of Albedo Products for Glacier Surfaces Derived from Airborne and Satellite (Sentinel-2 and Landsat 8) Optical Data. Remote Sensing 9, 110. https://doi.org/10.3390/rs9020110
NASA, n.d. EO-1 Hyperion [WWW Document]. URL https://cmr.earthdata.nasa.gov/search/concepts/C1220567951-USGS_LTA.html (accessed 2.23.26).
Neneman, M., Wagner, S., Bourg, L., Blanot, L., Bouvet, M., Adriaensen, S., Nieke, J., 2020. Use of Moon Observations for Characterization of Sentinel-3B Ocean and Land Color Instrument. Remote Sensing 12. https://doi.org/10.3390/rs12162543
Nickel, B.A., Suraci, J.P., Nisi, A.C., Wilmers, C.C., 2021. Energetics and fear of humans constrain the spatial ecology of pumas. Proc. Natl. Acad. Sci. U.S.A. 118, e2004592118. https://doi.org/10.1073/pnas.2004592118
Oftedal, O.T., 1985. Pregnancy and Lactation, in: Bioenergetics Of Wild Herbivores. CRC Press, p. 24.
Olaya, V., 2009. Chapter 6 Basic Land-Surface Parameters, in: Developments in Soil Science. Elsevier, pp. 141–169. https://doi.org/10.1016/S0166-2481(08)00006-8
Paterson, J.E., 2023. Estimating home range overlap in R [WWW Document]. URL https://jamesepaterson.github.io/jamespatersonblog/2023-09-24_homerangeoverlap.html (accessed 2.4.26).
Phillips, S.J., Dudík, M., Elith, J., Graham, C.H., Lehmann, A., Leathwick, J., Ferrier, S., 2009. Sample selection bias and presence-only distribution models: implications for background and pseudo-absence data. Ecological Applications 19, 181–197. https://doi.org/10.1890/07-2153.1
Piedallu, C., Gégout, J.-C., 2005. Effects of Forest Environment and Survey Protocol on GPS Accuracy. Photogrammetric Engineering & Remote Sensing 71, 1071–1078. https://doi.org/10.14358/PERS.71.9.1071
Pinna, D., Basso, E., Pornaro, C., Pullanagari, R., Macolino, S., Pezzuolo, A., Marinello, F., 2025. Optimising grassland Above-Ground biomass Estimation for managed grasslands: A Gaussian process regression approach for Sentinel-2 and Planet Scope in Northern Italy. Precision Agric 26, 98. https://doi.org/10.1007/s11119-025-10298-2
Poggiato, G., Andréoletti, J., Pollock, L.J., Thuiller, W., 2025. Integrating food webs in species distribution models can improve ecological niche estimation and predictions. Ecography 2025, e07546. https://doi.org/10.1111/ecog.07546
Pottier, J., Malenovský, Z., Psomas, A., Homolová, L., Schaepman, M.E., Choler, P., Thuiller, W., Guisan, A., Zimmermann, N.E., 2014. Modelling plant species distribution in alpine grasslands using airborne imaging spectroscopy. Biol. Lett. 10, 20140347. https://doi.org/10.1098/rsbl.2014.0347
Putman, R.J., Wratten, S.D., 1984. The Concept of the Niche, in: Putman, R.J., Wratten, S.D. (Eds.), Principles of Ecology. Springer, Dordrecht, pp. 105–126. https://doi.org/10.1007/978-94-011-6948-6_6
Quaglia, E., Ravetto Enri, S., Perotti, E., Probo, M., Lombardi, G., Lonati, M., 2020. Alpine tundra species phenology is mostly driven by climate-related variables rather than by photoperiod. J. Mt. Sci. 17, 2081–2096. https://doi.org/10.1007/s11629-020-6079-2
Rapiya, M., Ramoelo, A., Truter, W., 2025. Seasonal monitoring of forage C:N:ADF ratio in natural rangeland using remote sensing data. Environ Monit Assess 197, 137. https://doi.org/10.1007/s10661-024-13579-x
Rauschkolb, R., Herben, T., Kattge, J., Knickmann, B., Linstädter, A., Menzel, A., Mora, K., Nordt, B., Vitasse, Y., Weigelt, P., Römermann, C., 2025. The performance of growing degree day models

to predict spring phenology of herbaceous species depends on the species' temporal niche. Functional Ecology 00, 1–14. https://doi.org/10.1111/1365-2435.70020
Rempfler, T., n.d. GPS Positionen der Hirsche (Projekt Ingio Via).
Rempfler, T., Peters, W., Signer, C., Filli, F., Jenny, H., Hackländer, K., Buchmann, S., Anderwald, P., 2025. Contrasting Daytime Habitat Selection in Wild Red Deer Within and Outside Hunting Ban Areas Emphasises Importance of Small-Scale Refuges From Humans. Ecol Evol 15, e71407. https://doi.org/10.1002/ece3.71407
Rempfler, T., Rossi, C., Schweizer, J., Peters, W., Signer, C., Filli, F., Jenny, H., Hackländer, K., Buchmann, S., Anderwald, P., 2024. Remote sensing reveals the role of forage quality and quantity for summer habitat use in red deer. Movement Ecology 12, 80. https://doi.org/10.1186/s40462-024-00521-6
Richard, E., Said, S., Hamann, J.-L., Gaillard, J.-M., 2011. Toward an Identification of Resources Influencing Habitat Use in a Multi-Specific Context. PLOS ONE 6, e29048. https://doi.org/10.1371/journal.pone.0029048
Richter, R., Schläpfer, D., 2002. Geo-atmospheric processing of airborne imaging spectrometry data. Part 2: Atmospheric/topographic correction. International Journal of Remote Sensing 23, 2631–2649. https://doi.org/10.1080/01431160110115834
Rivrud, I.M., Heurich, M., Krupczynski, P., Müller, J., Mysterud, A., 2016. Green wave tracking by large herbivores: an experimental approach. Ecology 97, 3547–3553. https://doi.org/10.1002/ecy.1596
Rivrud, I.M., Loe, L.E., Mysterud, A., 2010. How does local weather predict red deer home range size at different temporal scales? Journal of Animal Ecology 79, 1280–1295. https://doi.org/10.1111/j.1365-2656.2010.01731.x
Rouse, J.W., Haas, R.H., Deering, D.W., Schell, J.A., Harlan, J.C., 1974. Monitoring the Vernal Advancement and Retrogradation (Green Wave Effect) of Natural Vegetation (No. E75-10354).
Schaepman, M.E., Jehle, M., Hueni, A., D'Odorico, P., Damm, A., Weyermann, J., Schneider, F.D., Laurent, V., Popp, C., Seidel, F.C., Lenhard, K., Gege, P., Küchler, C., Brazile, J., Kohler, P., De Vos, L., Meuleman, K., Meynart, R., Schläpfer, D., Kneubühler, M., Itten, K.I., 2015. Advanced radiometry measurements and Earth science applications with the Airborne Prism Experiment (APEX). Remote Sensing of Environment 158, 207–219. https://doi.org/10.1016/j.rse.2014.11.014
Schläpfer, D., Richter, R., 2002. Geo-atmospheric processing of airborne imaging spectrometry data. Part 1: Parametric orthorectification. International Journal of Remote Sensing 23, 2609–2630. https://doi.org/10.1080/01431160110115825
Schütz, M., Risch, A.C., Achermann, G., Thiel-Egenter, C., Page-Dumroese, D.S., Jurgensen, M.F., Edwards, P.J., 2006. Phosphorus Translocation by Red Deer on a Subalpine Grassland in the Central European Alps. Ecosystems 9, 624–633. https://doi.org/10.1007/s10021-006-0091-4
Schweiger, A.K., Risch, A.C., Damm, A., Kneubühler, M., Haller, R., Schaepman, M.E., Schütz, M., 2015a. Using imaging spectroscopy to predict above-ground plant biomass in alpine grasslands grazed by large ungulates. Journal of Vegetation Science 26, 175–190. https://doi.org/10.1111/jvs.12214
Schweiger, A.K., Schütz, M., Anderwald, P., Schaepman, M.E., Kneubühler, M., Haller, R., Risch, A.C., 2015b. Foraging ecology of three sympatric ungulate species – Behavioural and resource maps indicate differences between chamois, ibex and red deer. Mov Ecol 3. https://doi.org/10.1186/s40462-015-0033-x
Schweizerischer Nationalpark, n.d. . Willkommen im Schweizerischen Nationalpark. URL https://nationalpark.ch/ (accessed 10.22.25).
Serbin, S.P., 2024. spectra-trait_reseco_lma_plsr_example.R. plantphys / spectratrait.
Sibbald, A.M., Hooper, R.J., McLeod, J.E., Gordon, I.J., 2011. Responses of red deer (Cervus elaphus) to regular disturbance by hill walkers. Eur J Wildl Res 57, 817–825. https://doi.org/10.1007/s10344-011-0493-2
Signer, J., Fieberg, J., Avgar, T., 2019. Animal movement tools (amt): R package for managing tracking data and conducting habitat selection analyses. Ecology and Evolution 9, 880–890. https://doi.org/10.1002/ece3.4823
Signer, J., Fieberg, J.R., 2021. A fresh look at an old concept: home-range estimation in a tidy world. PeerJ 9, e11031. https://doi.org/10.7717/peerj.11031

Sigrist, B., Signer, C., Wellig, S.D., Ozgul, A., Filli, F., Jenny, H., Thiel, D., Wirthner, S., Graf, R.F., 2022. Green-up selection by red deer in heterogeneous, human-dominated landscapes of Central Europe. Ecology and Evolution 12, 1–13. https://doi.org/10.1002/ece3.9048
Silva, I., Fleming, C.H., Noonan, M.J., Alston, J., Folta, C., Fagan, W.F., Calabrese, J.M., 2022. Autocorrelation-informed home range estimation: A review and practical guide. Methods in Ecology and Evolution 13, 534–544. https://doi.org/10.1111/2041-210X.13786
Smolko, P., Garaj, P., Lebocký, T., Bútora, Ľ., Pataky, T., Jaňáková, Z., Babic, M., Veselovská, A., Kubala, J., Kropil, R., 2022. Soil nutrients and deer density affect antler size of the Carpathian red deer. Mamm Biol 102, 119–130. https://doi.org/10.1007/s42991-021-00203-5
SNP, WSL, RSL, n.d. APEX rawdata.
Soley-Guardia, M., Alvarado-Serrano, D.F., Anderson, R.P., 2024. Top ten hazards to avoid when modeling species distributions: a didactic guide of assumptions, problems, and recommendations. Ecography 2024, e06852. https://doi.org/10.1111/ecog.06852
Spalinger, D.E., Robbins, C.T., Hanley, T.A., 1986. The assessment of handling time in ruminants: the effect of plant chemical and physical structure on the rate of breakdown of plant particles in the rumen of mule deer and elk. Can. J. Zool. 64, 312–321. https://doi.org/10.1139/z86-051
Studer, S., Appenzeller, C., Defila, C., 2005. Inter-Annual Variability and Decadal Trends in Alpine Spring Phenology: A Multivariate Analysis Approach. Climatic Change 73, 395–414. https://doi.org/10.1007/s10584-005-6886-z
Suter, W., Suter, U., Kriisi, B., Schütz, M., 2004. Spatial variation of summer diet of red deer Cervus elaphus in the eastern Swiss Alps. wbio 10, 43–50. https://doi.org/10.2981/wlb.2004.008
Swisstopo, n.d. SwissALTI3D 2m DEM - DHM – MNT.
Tansock, J., Bancroft, D., Butler, J., Cao, C., Datla, R., Hansen, S., Helder, D., Kacker, R., Latvakoski, H., Mylnczak, M., Murdock, T., Peterson, J., Pollock, D., Russell, R., Scott, D., Seamons, J., Stone, T., Thurgood, A., Williams, R., Xiong, X., Yoon, H., 2015. Guidelines for Radiometric Calibration of Electro-Optical Instruments for Remote Sensing. Space Dynamics Laboratory Publications. https://doi.org/10.6028/NIST.HB.157
The Pennsylvania State University, n.d. 7.7 - Polynomial Regression | STAT 462 [WWW Document]. URL https://online.stat.psu.edu/stat462/node/158/ (accessed 3.12.26).
Thiel-Egenter, C., Risch, A., Jurgensen, M., Page-Dumroese, D., Krüsi, B., Schütz, M., 2007. Response of a subalpine grassland to simulated grazing: aboveground productivity along soil phosphorus gradients. Community Ecology 8, 111–117. https://doi.org/10.1556/ComEc.8.2007.1.13
Thompson, D.R., Gao, B.-C., Green, R.O., Roberts, D.A., Dennison, P.E., Lundeen, S.R., 2015. Atmospheric correction for global mapping spectroscopy: ATREM advances for the HyspIRI preparatory campaign. Remote Sensing of Environment, Special Issue on the Hyperspectral Infrared Imager (HyspIRI) 167, 64–77. https://doi.org/10.1016/j.rse.2015.02.010
Thulin, S., Hill, M.J., Held, A., Jones, S., Woodgate, P., 2012. Hyperspectral determination of feed quality constituents in temperate pastures: Effect of processing methods on predictive relationships from partial least squares regression. International Journal of Applied Earth Observation and Geoinformation 19, 322–334. https://doi.org/10.1016/j.jag.2012.06.006
Trepel, J., le Roux, E., Abraham, A.J., Buitenwerf, R., Kamp, J., Kristensen, J.A., Tietje, M., Lundgren, E.J., Svenning, J.-C., 2024. Meta-analysis shows that wild large herbivores shape ecosystem properties and promote spatial heterogeneity. Nat Ecol Evol 8, 705–716. https://doi.org/10.1038/s41559-024-02327-6
Ustin, S.L., Roberts, D.A., Gamon, J.A., Asner, G.P., Green, R.O., 2004. Using Imaging Spectroscopy to Study Ecosystem Processes and Properties. BioScience 54, 523–534. https://doi.org/10.1641/0006-3568(2004)054%255B0523:UISTSE%255D2.0.CO;2
van der Graaf, S., Stahl, J., Klimkowska, A., Bakker, J.P., Drent, R.H., 2006. Surfing on a green wave – how plant growth drives spring migration in the Barnacle Goose Branta leucopsis. Ardea 94, 567–577.
Van Soest, P.J., 1994. Nutritional Ecology of the Ruminant, 2nd ed. Cornell University Press.
Van Winkle, W., 1975. Comparison of Several Probabilistic Home-Range Models. The Journal of Wildlife Management 39, 118–123. https://doi.org/10.2307/3800474

VanDerWal, J., Shoo, L.P., Graham, C., Williams, S.E., 2009. Selecting pseudo-absence data for presence-only distribution modeling: How far should you stray from what you know? Ecological Modelling 220, 589–594. https://doi.org/10.1016/j.ecolmodel.2008.11.010
VECTRONIC Aerospace GmbH, 2016. VERTEX Plus Collar.
Volodin, I., Volodina, E., Frey, R., Carranza, J., Torres-Porras, J., 2013. Spectrographic analysis points to source–filter coupling in rutting roars of Iberian red deer. acta ethol 16, 57–63. https://doi.org/10.1007/s10211-012-0133-1
Vorkauf, M., Kahmen, A., Körner, C., Hiltbrunner, E., 2021. Flowering phenology in alpine grassland strongly responds to shifts in snowmelt but weakly to summer drought. Alp Botany 131, 73–88. https://doi.org/10.1007/s00035-021-00252-z
Wang, J., 1995. The models of niche and their application. Ecological Modelling 80, 279–291. https://doi.org/10.1016/0304-3800(94)00067-R
Wang, N., Xue, J., Peng, J., Biswas, A., He, Y., Shi, Z., 2020. Integrating Remote Sensing and Landscape Characteristics to Estimate Soil Salinity Using Machine Learning Methods: A Case Study from Southern Xinjiang, China. Remote Sensing 12, 4118. https://doi.org/10.3390/rs12244118
Warner, T.A., Nellis, M.D., Foody, G.M., 2009. Remote Sensing Scale and Data Selection Issues, in: The SAGE Handbook of Remote Sensing. SAGE Publications, pp. 1–17.
Weyermann, J., Damm, A., Kneubühler, M., Schaepman, M.E., 2014. Correction of Reflectance Anisotropy Effects of Vegetation on Airborne Spectroscopy Data and Derived Products. IEEE Transactions on Geoscience and Remote Sensing 52, 616–627. https://doi.org/10.1109/TGRS.2013.2242898
Widén, A., Cromsigt, J.P.G.M., Felton, A.M., Widemo, F., Graf, L., Ericsson, G., Singh, N.J., 2025. Temperature mediated habitat selection in sympatric deer species with varying body size: thermal cover and forage availability as potential drivers. Mov Ecol 13, 52. https://doi.org/10.1186/s40462-025-00581-2
Wijesingha, J., Astor, T., Schulze-Brüninghoff, D., Wengert, M., Wachendorf, M., 2020. Predicting Forage Quality of Grasslands Using UAV-Borne Imaging Spectroscopy. Remote Sensing 12, 126. https://doi.org/10.3390/rs12010126
Willis, S.G., Foden, W., Baker, D.J., Belle, E., Burgess, N.D., Carr, J.A., Doswald, N., Garcia, R.A., Hartley, A., Hof, C., Newbold, T., Rahbek, C., Smith, R.J., Visconti, P., Young, B.E., Butchart, S.H.M., 2015. Integrating climate change vulnerability assessments from species distribution models and trait-based approaches. Biological Conservation 190, 167–178. https://doi.org/10.1016/j.biocon.2015.05.001
Willisch, C.S., Willisch, K.B., Boldt, A., Magun, B., Marreros, N., Struch, M., Tschan, M., Pisano, S.R., 2024. Novel insights into red deer (Cervus elaphus) habitat use and suitability in human-dominated versus near-natural landscapes. Mammalia 88, 465–478. https://doi.org/10.1515/mammalia-2023-0176
Wold, S., Sjöström, M., Eriksson, L., 2001. PLS-regression: a basic tool of chemometrics. Chemometrics and Intelligent Laboratory Systems, PLS Methods 58, 109–130. https://doi.org/10.1016/S0169-7439(01)00155-1
Worton, B.J., 1989. Kernel Methods for Estimating the Utilization Distribution in Home-Range Studies. Ecology 70, 164–168. https://doi.org/10.2307/1938423
Zanaga, D., Van De Kerchove, R., Daems, D., De Keersmaecker, W., Brockmann, C., Kirches, G., Wevers, J., Cartus, O., Santoro, M., Fritz, S., Lesiv, M., Herold, M., Tsendbazar, N.-E., Xu, P., Ramoino, F., Arino, O., 2022. ESA WorldCover 10 m 2021 v200. https://doi.org/10.5281/ZENODO.7254221
Zaniewski, A.E., Lehmann, A., Overton, J.M., 2002. Predicting species spatial distributions using presence-only data: a case study of native New Zealand ferns. Ecological Modelling 157, 261–280. https://doi.org/10.1016/S0304-3800(02)00199-0
Zhang, S., Zhao, B., Jian, X., Fu, J., Chen, Y., Fei, T., 2025. Improving the prediction of vegetation carbon, phosphorus, and C:P ratio of alpine grassland in the Three-River Headwater Region by combining the field and laboratory reflectance spectroscopy. Soil and Tillage Research 251, 106563. https://doi.org/10.1016/j.still.2025.106563
Zurell, D., Franklin, J., König, C., Bouchet, P.J., Dormann, C.F., Elith, J., Fandos, G., Feng, X., Guillera-Arroita, G., Guisan, A., Lahoz-Monfort, J.J., Leitão, P.J., Park, D.S., Peterson, A.T.,

Rapacciuolo, G., Schmatz, D.R., Schröder, B., Serra-Diaz, J.M., Thuiller, W., Yates, K.L., Zimmermann, N.E., Merow, C., 2020. A standard protocol for reporting species distribution models. Ecography 43, 1261–1277. https://doi.org/10.1111/ecog.04960

Zweifel-Schielly, B., Leuenberger, Y., Kreuzer, M., Suter, W., 2012. A herbivore's food landscape: seasonal dynamics and nutritional implications of diet selection by a red deer population in contrasting Alpine habitats. Journal of Zoology 286, 68–80. https://doi.org/10.1111/j.1469-7998.2011.00853.x

8.1 Data used in maps created in ArcGIS Pro

ASTRA, n.d. hauptstrassennetz_dl.
BAFU / Netzwerk Schweizer Pärke, n.d. swiss_parks.
Swisstopo, n.d. tlm_fliessgewaesser.
Swisstopo, n.d. tlmregio_building.
Swisstopo, n.d. tlmregio_lake.
Swisstopo / SCNAT, n.d. tlm_landesgebiet.

8.2 Software

BioRender: https://www.biorender.com/

Esri. (2023). *ArcGIS Pro* (Version 3.6.0) [Computer software]. Esri, Inc. Accessed March 26, 2026. https://www.esri.com

R Core Team (2025). R: A Language and Environment for Statistical Computing. R Foundation for Statistical Computing, Vienna, Austria. https://www.r-project.org/. R version: 4.5.1 (13.06.2025)

9 Appendix

9.1 Supplementary figures and tables

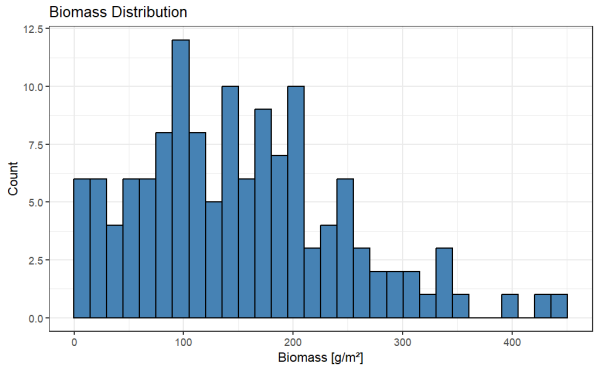

Supplementary Figure 1: Distribution of in-situ biomass values in g/m² collected in 2010 and 2013. Distribution is slightly left skewed.

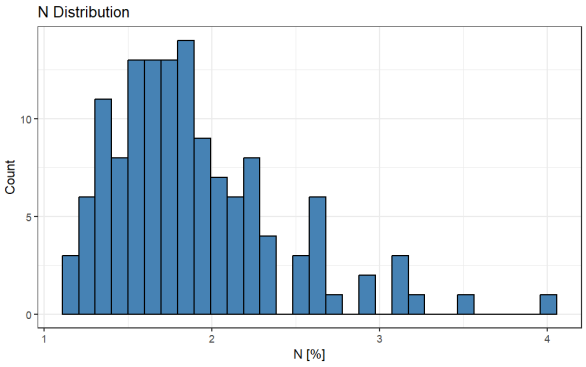

Supplementary Figure 2: Distribution of in-situ nitrogen values in % collected in 2010 and 2013. Distribution has a slightly long tail.

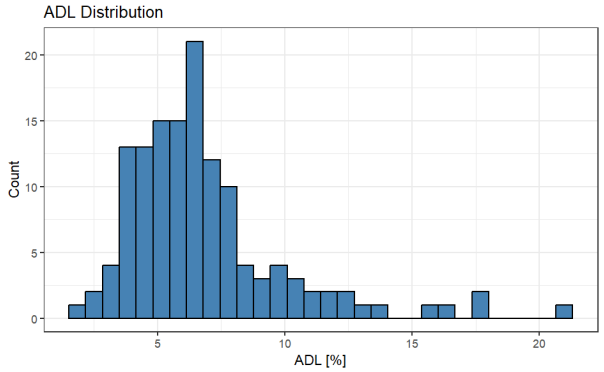

Supplementary Figure 3: Distribution of in-situ ADL values in % collected in 2010 and 2013. Distribution has a slightly long tail.

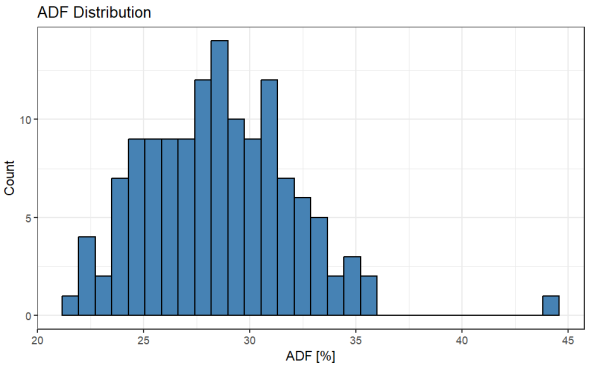

Supplementary Figure 4: Distribution of in-situ ADF values in % collected in 2010 and 2013. Distribution has one outlier.

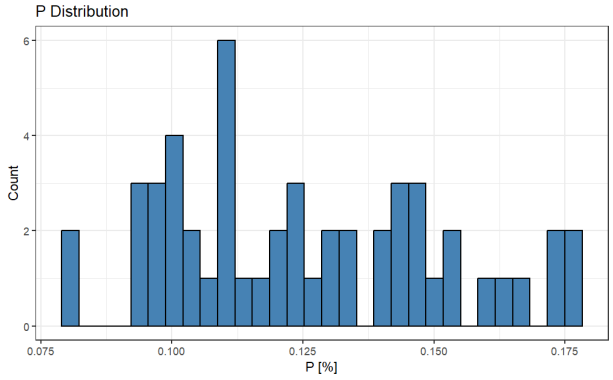

Supplementary Figure 5: Distribution of in-situ phosphorus values in % collected in 2010.

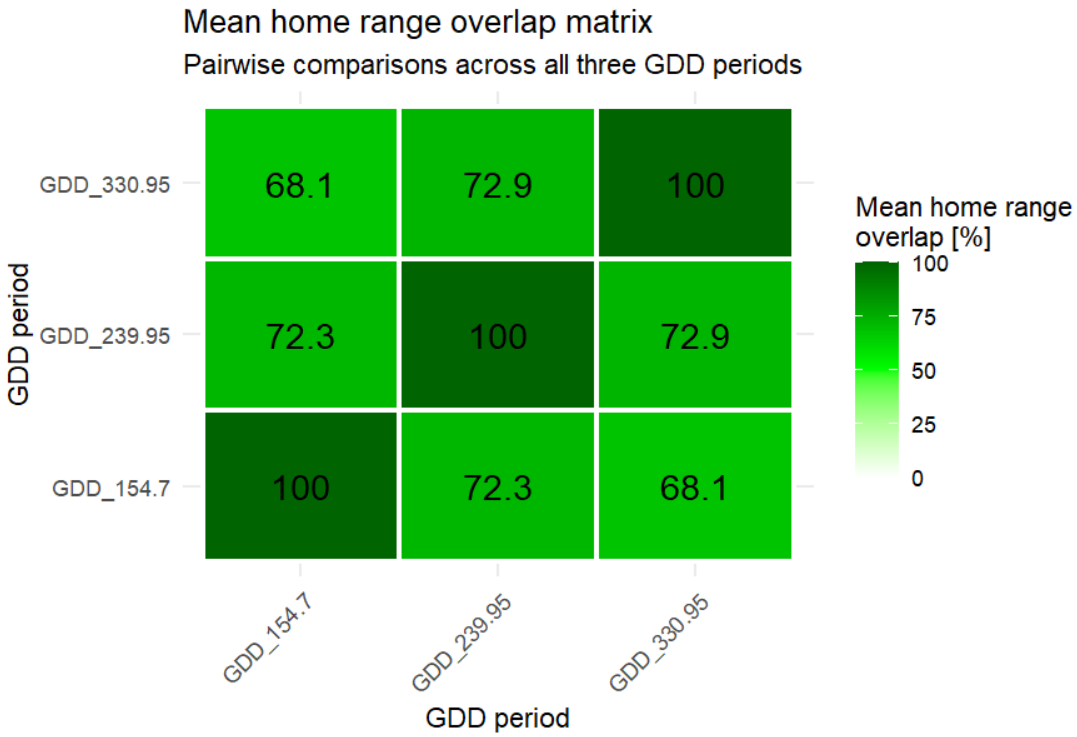

Supplementary Figure 6: Home range overlap matrix across the three GDD periods.

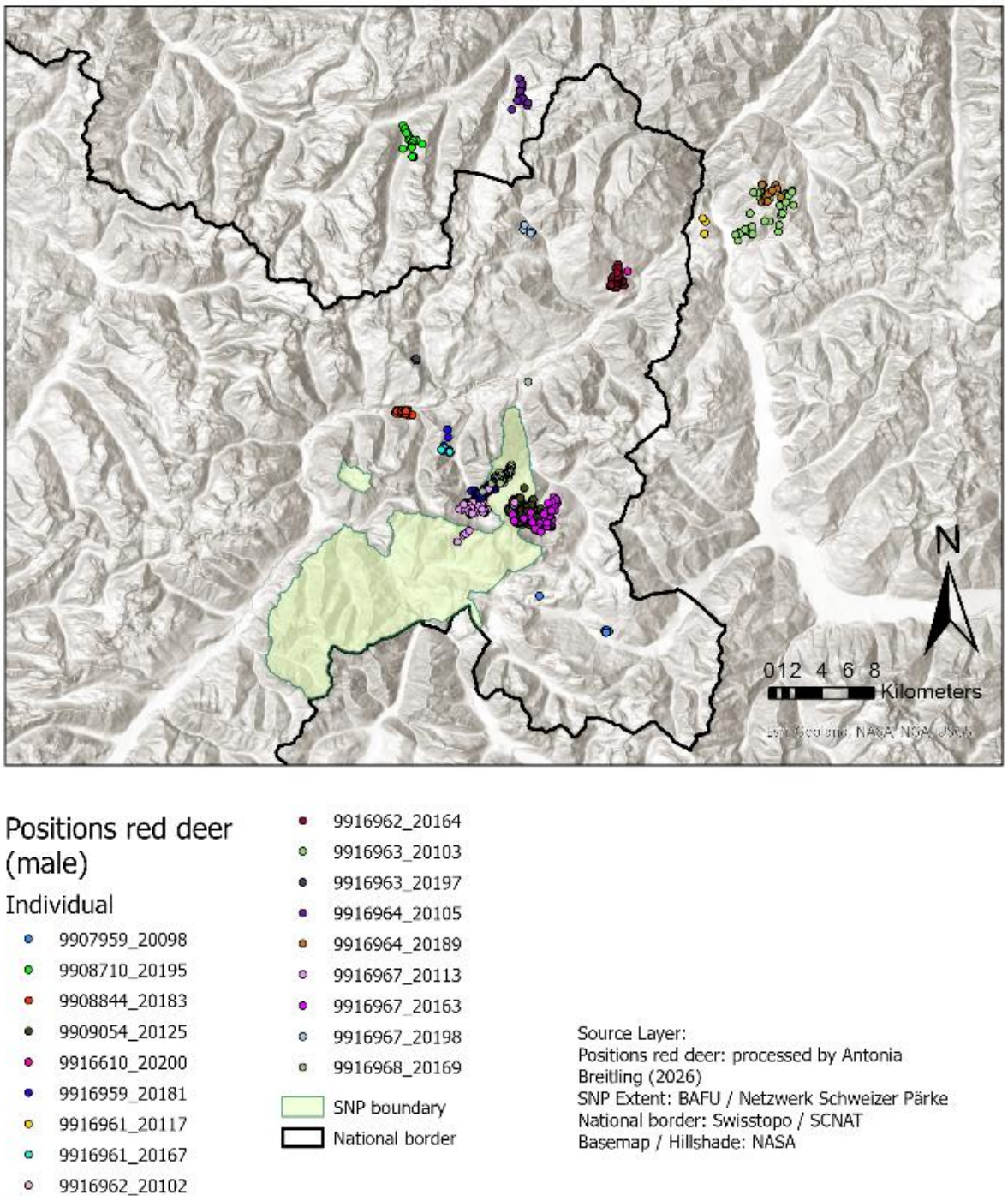

Supplementary Figure 7: Recorded male red deer positions in and around the SNP. Different colours indicate different individuals, in green is the SNP.

```
> summary(m7_slope_ADF)
 Family: binomial  ( logit )
Formula:          presence ~ elevation + I(elevation^2) + slope + aspect_cos +
    aspect_sin + Biomass_dry * ADF_perc * Nitrogen_perc + (1 |
    deployment) + (0 + ADF_perc | deployment)
Data: feeding_final_scaled
Weights: w

      AIC       BIC    logLik -2*log(L)  df.resid
  48792.2   48906.9  -24382.1   48764.2     26782

Random effects:

Conditional model:
 Groups       Name        Variance Std.Dev.
 deployment   (Intercept) 1.00e+06 1000.000
 deployment.1 ADF_perc    2.55e+00    1.597
Number of obs: 26796, groups:  deployment, 28

Conditional model:
                                  Estimate Std. Error z value Pr(>|z|)
(Intercept)                     -0.001296 188.937100   0.000  0.99999
elevation                        0.189024   0.068582   2.756  0.00585 **
I(elevation^2)                  -0.746289   0.093466  -7.985 1.41e-15 ***
slope                           -0.526695   0.058761  -8.963  < 2e-16 ***
aspect_cos                      -0.661966   0.051871 -12.762  < 2e-16 ***
aspect_sin                       0.675940   0.047035  14.371  < 2e-16 ***
Biomass_dry                      1.117913   0.054821  20.392  < 2e-16 ***
ADF_perc                        -1.450714   0.324859  -4.466 7.98e-06 ***
Nitrogen_perc                    0.530699   0.066453   7.986 1.39e-15 ***
Biomass_dry:ADF_perc             0.970184   0.088652  10.944  < 2e-16 ***
Biomass_dry:Nitrogen_perc        0.960306   0.100537   9.552  < 2e-16 ***
ADF_perc:Nitrogen_perc           0.857635   0.124121   6.910 4.86e-12 ***
Biomass_dry:ADF_perc:Nitrogen_perc   0.215935   0.183287   1.178  0.23875
---
Signif. codes:  0 ‘***’ 0.001 ‘**’ 0.01 ‘*’ 0.05 ‘.’ 0.1 ‘ ’ 1
```

Supplementary Figure 8: Summary output of the overall best model (M7d) with random slopes for ADF. All estimates are in the log odds scale.

```
> summary(m7_slope_ADF_f)
 Family: binomial  ( logit )
Formula:          presence ~ elevation + I(elevation^2) + slope + aspect_cos +
    aspect_sin + Biomass_dry * ADF_perc * Nitrogen_perc + (1 |
    deployment) + (0 + ADF_perc | deployment)
Data: female_filtered
Weights: w

      AIC       BIC    logLik -2*log(L)  df.resid
  27302.1   27408.7  -13637.0   27274.1     15010

Random effects:

Conditional model:
 Groups       Name        Variance  Std.Dev.
 deployment   (Intercept) 1.000e+06 1000.000
 deployment.1 ADF_perc    4.027e+00    2.007
Number of obs: 15024, groups:  deployment, 23

Conditional model:
                                  Estimate Std. Error z value Pr(>|z|)
(Intercept)                     -0.001115 208.510946   0.000 0.999996
elevation                       -1.159290   0.113882 -10.180  < 2e-16 ***
I(elevation^2)                  -1.385964   0.131934 -10.505  < 2e-16 ***
slope                           -0.402372   0.079191  -5.081 3.75e-07 ***
aspect_cos                      -0.687248   0.066250 -10.374  < 2e-16 ***
aspect_sin                       0.836062   0.061811  13.526  < 2e-16 ***
Biomass_dry                      0.533948   0.088716   6.019 1.76e-09 ***
ADF_perc                        -1.619644   0.446980  -3.624 0.000291 ***
Nitrogen_perc                    0.081675   0.101690   0.803 0.421874
Biomass_dry:ADF_perc             0.386377   0.135301   2.856 0.004295 **
Biomass_dry:Nitrogen_perc        0.670713   0.162862   4.118 3.82e-05 ***
ADF_perc:Nitrogen_perc           1.103241   0.183756   6.004 1.93e-09 ***
Biomass_dry:ADF_perc:Nitrogen_perc -0.113805   0.280164  -0.406 0.684589
---
Signif. codes:  0 ‘***’ 0.001 ‘**’ 0.01 ‘*’ 0.05 ‘.’ 0.1 ‘ ’ 1
```

Supplementary Figure 9: Summary output of the best model (M7d) explaining female red deer presence in the SNP with random slopes for ADF. All estimates are in the log odds scale.

Supplementary Table 1: Overview of the model performance for stags in the SNP characterised by the AIC value. Best model per category is highlighted in green. The overall best model is highlighted in blue

Model	**Degree of Freedom**	**AIC**
M0: random effects only	1	22165.37
M1: topographic variables	6	21680.61
M2: topographic variables + Biomass (random intercept only)	7	21413.18
M2: topographic variables + Biomass (random slopes)	8	21391.06
M3: topographic variables + Biomass * N (random intercept only)	9	21181.70
M3: topographic variables + Biomass * N (random slope for Biomass)	10	21137.52
M3: topographic variables + Biomass * N (random slope for Nitrogen)	10	21181.56
M4: topographic variables + Biomass * P (random intercept only)	9	21191.35
M4: topographic variables + Biomass * P (random slopes for Biomass)	10	21158.67
M4: topographic variables + Biomass * P (random slopes for P)	10	21184.74
M5: topographic variables + Biomass * ADL (random intercept only)	9	21408.56
M5: topographic variables + Biomass * ADL (random slopes for Biomass)	10	21388.34
M5: topographic variables + Biomass * ADL (random slopes for ADL)	10	21407.67
M6: topographic variables + Biomass * ADF (random intercept only)	9	21264.64
M6: topographic variables + Biomass * ADF (random slopes for Biomass)	10	21248.26
M6: topographic variables + Biomass * ADF (random slopes for ADF)	10	21251.83
M7: topographic variables + Biomass * ADF * N (random intercept only)	13	21053.46
M7: topographic variables + Biomass * ADF * N (random slopes for Biomass)	14	21030.04
M7: topographic variables + Biomass * ADF * N (random slopes for Nitrogen)	14	21053.52
M7: topographic variables + Biomass * ADF * N (random slopes for ADF)	14	21047.98
M8: topographic variables + Biomass * ADF * P (random intercept only)	13	21031.86
M8: topographic variables + Biomass * ADF * P (random slopes for Biomass)	14	21007.33
M8: topographic variables + Biomass * ADF * P (random slopes for Phosphorus)	14	21030.14
M8: topographic variables + Biomass * ADF * P (random slopes for ADF)	14	21021.04

```
> summary(m8_slope_B_m)
 Family: binomial  ( logit )
Formula:          presence ~ elevation + I(elevation^2) + slope + aspect_cos +
    aspect_sin + Biomass_dry * ADF_perc * P_perc + (1 | deployment) +
    (0 + Biomass_dry | deployment)
Data: male_filtered
Weights: w

      AIC       BIC    logLik -2*log(L)  df.resid
  21007.3   21110.6  -10489.7   20979.3     11758

Random effects:

Conditional model:
 Groups       Name        Variance  Std.Dev.
 deployment   (Intercept) 1.000e+06 1000.0000
 deployment.1 Biomass_dry 2.741e-01    0.5235
Number of obs: 11772, groups:  deployment, 5

Conditional model:
                              Estimate Std. Error z value Pr(>|z|)
(Intercept)                 -1.092e-04  4.473e+02   0.000  1.00000
elevation                    2.082e+00  1.478e-01  14.084  < 2e-16 ***
I(elevation^2)              -2.315e+00  2.372e-01  -9.759  < 2e-16 ***
slope                       -7.763e-01  8.618e-02  -9.008  < 2e-16 ***
aspect_cos                  -5.779e-01  8.437e-02  -6.850 7.40e-12 ***
aspect_sin                   4.306e-01  7.330e-02   5.874 4.24e-09 ***
Biomass_dry                  1.407e+00  2.488e-01   5.655 1.56e-08 ***
ADF_perc                    -9.058e-01  8.708e-02 -10.402  < 2e-16 ***
P_perc                       8.641e-01  8.899e-02   9.710  < 2e-16 ***
Biomass_dry:ADF_perc         3.756e-01  1.322e-01   2.840  0.00451 **
Biomass_dry:P_perc           1.223e+00  1.438e-01   8.505  < 2e-16 ***
ADF_perc:P_perc             -2.793e-01  1.702e-01  -1.641  0.10074
Biomass_dry:ADF_perc:P_perc -5.595e-01  2.743e-01  -2.040  0.04138 *
---
Signif. codes:  0 ‘***’ 0.001 ‘**’ 0.01 ‘*’ 0.05 ‘.’ 0.1 ‘ ’ 1
```

Supplementary Figure 10: Summary output of the best model (M8b) explaining male red deer presence in the SNP with random slopes for ADF. All estimates are in the log odds scale.

Supplementary Table 2: Home range area statistic for hinds in the SNP.

Female red deer home range statistics 95 % kernel density estimates across phenological stages					
Phenological stage	N	Mean Area [ha]	SD Area [ha]	Mean Radius [m]	SD Radius [m]
GDD 154.7 (early)	53	275.1	121.6	914	203
GDD 239.95 (mid)	53	279.0	107.8	925	180
GDD 330.95 (late)	53	271.4	112.9	909	196

Supplementary Table 3: Home range area statistic for stags in the SNP.

Male red deer home range statistics 95 % kernel density estimates across phenological stages					
Phenological stage	N	Mean Area [ha]	SD Area [ha]	Mean Radius [m]	SD Radius [m]
GDD 154.7 (early)	17	423.6	247.3	1,115	336
GDD 239.95 (mid)	17	421.1	206.5	1,125	282
GDD 330.95 (late)	17	284.1	141.5	926	222

Supplementary Table 4: ODMAP Protocol following Zurell et al. (2020)

ODMAP section	ODMAP subsection	ODMAP elements
Overview	Authorship	Antonia Breitling, antonia.breitling@uzh.ch
	Model objective	Explaining red deer feeding habitat selection in the Swiss National Park (in general and sex-specific)
	Taxon	Red deer (Cervus elaphus)
	Location	Swiss National Park (SNP)
	Scale of analysis	- Spatial extent: 2800000 – 2825000 Easting, 1185000 – 1160000 Northing (LV95) - Spatial resolution: 2 x 2 m - Temporal extent: GPS data collected from 2011 – 2019, filtered for GDD 239.95 ± 10 days - Extent boundary: SNP
	Biodiversity data overview	- Observation type: GPS locations of red deer (telemetry) - Response data type: binary
	Type of predictors	- Topography (elevation, slope, aspect) - forage quantity (biomass) - forage quality (nitrogen, phosphorus, lignin, fibres)
	Conceptual model / hypotheses	Which combination of topography, forage quality proxies (N, P, ADL and ADF) and forage quantity (biomass) best explains red deer feeding habitat selection? - Topography alone? - Topography and food quantity (biomass)? - Topography together with food quantity (biomass) and quality (N, P, ADL, ADF)?
	Assumptions	- Species are in equilibrium with their environment - Species don't move too far and are rather stable within their niche - No sampling bias of red deer data (recorded by GPS, accuracy of 11.3 ± 4.7 m)
	SDM algorithms	Resource selection function (RSF) used as special case of SDM for accounting for variations between individuals. Implemented as generalised linear mixed model (GLMM) framework because the independence assumption was violated due to multiple datapoints per individual. Best model was identified via AIC. No model averaging used.
	Model workflow	The presence data were the feeding locations. Additionally, the data were

		filtered for only the GDD period 239.95 ± 10 days, independent of the year and only positions within the grassland mask and the mosaic were kept. Pseudo-absence points were generated via a buffer. Data were centred and scaled prior to model fitting to a mean = 0 and SD = 0.5 Models were fitted with random intercepts and random slopes in the model to avoid biased and overconfident results when modelling RSFs. Intercept variance was fixed at a large value (10^6) to avoid shrinkage and bias and weights were given to the datapoints (presence = 1, available = 1000). The number of positions recorded for each individual were checked. Out of 41 individuals, 11 had less than 10 presence points and were therefore excluded, resulting in 28 individuals (26796 points) for the analysis.
	Software, codes and data	R / R studio
Data	Biodiversity data	Red deer (Cervus elaphus) in the SNP, Switzerland. Presence data measured by GPS (accuracy of 11.3 ± 4.7 m) and together with data from accelerometer, actual feeding locations determined by a machine learning approach were identified. Temporal matching of accelerometer and GPS data within a ± 20-minute window Filtered for GDD period 239.95 ± 10 days. Only individuals with more than 10 GPS positions kept for RSF / SDM. Absence data: Buffer of 1km around each presence location, 10 absence points per presence location defined (first 30 random points generated, then subsampled to 10 points)
	Predictor variables	- Topography: values extracted from DEM (Swisstopo, n.d.) - Forage quantity and forage quality: variables are the output of a PLSR model, trained with in-situ and imaging spectroscopy data collected within the SNP - Both in LV95, 2 x 2 m resolution
Model	Multicollinearity	Pearson correlation checked for $r > 0.7$. Nitrogen and phosphorus not included in the same model due to $r = 0.8$
	Model settings / model complexity	- Random intercepts and slopes per individual - Intercept variance fixed at 10^6

		- Weights: presence = 1, available = 1000
	Model estimates	- Model coefficients reported in log odds scale - 95 % confidence interval reported - Fixed and random effects reported
	Model selection / model averaging / ensembles	- Model selection via AIC - Single best model identified (in general, for females and males) - Models compared within three hypothesis categories
	Non-independence correction/analyses-	- Moran's I tested on model residuals for spatial autocorrelation - GPS data (presence data) tested beforehand for temporal autocorrelation with ctmm (SVF), IID model identified as best model
Assessment	Performance statistics	- No independent test data used - Model performance assessed via AIC and ΔAIC. - No independent performance statistics calculated.
	Plausibility Check	Results compared to other studies conducted within the SNP

9.2 Personal declaration

I hereby declare that the submitted thesis is the result of my own, independent work. All external sources are explicitly acknowledged in the thesis.

9.3 Statement on AI use

I used Claude and DeepL as AI-tools in this thesis as supportive tools in the following purposes:

1. To translate words and to check grammar and spelling in text passages and the reading flow:
   "Please check this passage in terms of grammar and spelling errors and the flow but do not change the content, only paraphrase it"

2. Code explanation of found online tutorials:
   "What does this line do in this code section?"

3. Error debugging:
   "I have the following error, what and where could be the problem?"

4. Speeding up the R code (making it more efficient):
   "How can I make this R code more efficient? How can I do that in a loop?"

Date, Place

23.04.2026
Feuerthalen

Signature